



THE UNIVERSITY OF
WAIKATO
Te Whare Wānanga o Waikato

Research Commons

<https://researchcommons.waikato.ac.nz/>

Research Commons at the University of Waikato

Copyright Statement:

The digital copy of this thesis is protected by the Copyright Act 1994 (New Zealand).

The thesis may be consulted by you, provided you comply with the provisions of the Act and the following conditions of use:

- Any use you make of these documents or images must be for research or private study purposes only, and you may not make them available to any other person.
- Authors control the copyright of their thesis. You will recognise the author's right to be identified as the author of the thesis, and due acknowledgement will be made to the author where appropriate.
- You will obtain the author's permission before publishing any material from the thesis.

Importance of stream-wetland refuges for kōaro populations

Are wetlands overlooked climate refugia for kōaro (*Galaxias brevipinnis*) due to underestimation of their ecological flexibility?

A thesis

submitted in partial fulfilment

of the requirements for the degree

of

Master of Science (Research) in Ecology and Biodiversity

at

The University of Waikato

by

Josette Kahotea



THE UNIVERSITY OF
WAIKATO
Te Whare Wānanga o Waikato

2026

Abstract

Wetlands are widely valued in conservation and restoration, yet their ecological role when connected to lakes is often misunderstood in the management of freshwater fish. Rather than functioning simply as hydrological buffers for lake catchments, wetlands may serve as critical refugia for native fishes under increasing pressure from climatic variability and invasive predators.

I investigated whether the spring-fed Millar Road Wetland (MRW), located on the margin of Lake Ōkāreka (Rotorua Te Arawa Lakes, Aotearoa), supports a persistent population of kōaro (*Galaxias brevipinnis* Günther, 1866). A key objective of my research was to examine the mechanisms underpinning the potential refuge function of the wetland. By integrating year-round population monitoring, mark–recapture analysis, environmental modelling, and stable isotope analysis, I assessed demographic stability, predator limitation, and trophic structure of kōaro in this habitat.

The MRW supported a resident, multi-cohort kōaro population exhibiting seasonal recruitment, positive allometric growth, and stable body condition across years. Mark-recapture data indicated close site fidelity and continued individual growth, while interannual comparisons demonstrated stable adult size structure despite evidence for variable juvenile recruitment. Other notable members of the MRW community included common bullies (*Gobiomorphus cotidianus* McDowall, 1975) and kōura (*Paranephrops planifrons* White, 1842). Although juvenile rainbow trout (*Oncorhynchus mykiss* Walbaum, 1792) appear to enter the wetland periodically, their occurrence was spatially restricted to upstream areas and may be strongly mediated by hydrological connectivity. Episodic dissolved oxygen minima and shallow, structurally complex habitat likely constrain trout residency and growth, while kōaro were able to persist in the wetland across seasons. Stable isotope analysis revealed strong trophic differentiation: kōaro were supported predominantly by allochthonous carbon, largely via detritivorous aquatic insects, whereas common bullies relied on autochthonous benthic production. I hypothesised that this energy-channel partitioning of the food web reduces exploitative competition and helps explain the coexistence of these two native fish species at relatively high densities.

Together, these findings suggest that the role of the MRW as a refuge emerges not from absolute predator exclusion, but from a locally-dependent balance between hydrological connectivity, environmental filtering, habitat structure, and trophic organisation. Connectivity in the wetland is both essential and risky: it sustains demographic exchange with the lake whilst periodically permitting an invasive, non-native predator access, yet environmental harshness limits sustained trout establishment, and asymmetric tolerances allow kōaro to persist.

In a climate-sensitive species such as kōaro, the persistence of a robust wetland population highlights the potential importance of small, groundwater-fed systems as dynamic refugia within invaded landscapes. Protecting and restoring similar wetlands may therefore play a critical role in safeguarding native freshwater biodiversity under ongoing climatic and hydrological change in Aotearoa.

Acknowledgements

This thesis represents far more than a research project. It reflects a journey shaped by people, place, and purpose. At its heart, this work is about wai, the living waters of Aotearoa and the responsibility we carry to protect, restore, and understand them for those who will come after us. I begin by acknowledging the Tangata Whenua (Tūhourangi and Ngāti Tarawhai) of Akakahia-Ōkareka and the wider Te Arawa Lakes rohe. Thank you to those who continue to show kaitiakitanga over these waters and who have shared their mātauranga with generosity and humility. I stand on the knowledge of those who have come before me, and I carry deep respect for the whakapapa of this whenua and its tāonga.

This study would not have been possible without the devotion, kindness, and collective effort of many people:

To my primary supervisor, Dr Frank Burdon - E kore rawa te mihi e mutu ki a koe. You guided and supported me just as much as you challenged me to be a better scientist. You listened to my ideas, helped shape them into something sharper, and patiently worked through draft after draft with me. Your generosity, perseverance, and steady belief in this project and me made the difficult moments manageable and the breakthroughs deeply rewarding. I feel incredibly fortunate to have had such a thoughtful and invested supervisor.

To Ian Kusabs, you have been a mentor and inspiration from the very beginning of my journey. Your mātauranga, manaakitanga, and mana are shared with humility and with a genuine desire to understand and protect our taonga while uplifting others in environmental science. You are a beacon for Māori entering freshwater science, and I am deeply grateful for your guidance, your support, and your unwavering commitment to the lakes and to our people.

To Mike Goodwin and Brian Law — thank you for sinking into the mud with me month after month without complaint. Your love for the wetland and the tāonga that reside there, and your dedication to restoring this whenua, is grounded in aroha. The hours of trapping, planting, pest control, and retrievals are countless, and you do it not for recognition, but because you care. That kind of commitment is inspiring. To you both

and to all restoration champions of Te Arawa, your dedication is woven through every page of this thesis.

To Kristina Thompson and girls, Milly Farquhar, Zak Browne, Steve Goodwin, Melissa Boardman, Jody Richardson, the Tūwharetoa lads and all those who joined me in the field, thank you for braving rain, mud, and the occasional wet wader. You measured thousands of bullies, scribed endlessly, carried gear, flew drones, and most importantly, helped care for and appreciate our taonga. Your energy and support carried me forward in ways you may not even realise.

I thank Sarah Bury and her team at the Earth Sciences New Zealand Environmental and Ecological Stable Isotope Analysis Laboratory in Wellington for expediting the processing and analysis of my isotope samples. Their expertise and assistance was indispensable.

To Erica Williams, Earth Sciences NZ, Whakahohetia Ngā Wai Kāinga and Toitū Ngā Taonga Waimāori programme for the wider project framework and funding that made this study possible as well as the mahi you do.

To Soweeta, Will and the team at Te Arawa Lakes Trust, thank you for your ongoing tautoko and for bringing home the kaupapa to Te Arawa Lakes Trust.

To Te Arawa Lakes Trust, Earth Sciences NZ, The University of Waikato and Lake Ōkareka Community Association for the financial support that allowed me to undertake and complete this study, I am profoundly grateful. The opportunity to pursue this work with financial backing eased burdens and allowed me to focus fully on the kaupapa.

To MAI ki Waikato, especially Reina Daji, thank you for the writing retreats. You created a space where I was fed, cared for, and able to focus deeply. Those weeks of quiet dedication were so important in me completing my writing on time and relatively stress free. I felt privileged to be held in such a supportive environment and held by other mana-wahine.

To the New Zealand Freshwater Sciences Society and Te Wai Māori Rōpū, thank you for awarding me the NZFSS He Manawā ā Whenua Scholarship 2025. I am honoured to stand alongside those working to uplift Māori in freshwater science and to help pave

the way for those coming next. Your contribution will guide and support me for years to come.

To the research scientists across Aotearoa who have dedicated their lives to understanding and protecting our taonga — Whakawhetai ki a koe. Your work paved the way for mine. Every dataset, paper, and report I drew upon represents years of commitment and care for our country.

To my whānau — thank you for supporting me as a mature student returning to study after many years away. Your encouragement carried me through the steep learning curves and the long nights.

To my parents — Dad, thank you for introducing me to the water and instilling in me a lifelong love of freshwater and marine environments. Mum, you taught me that I can do anything. I miss you deeply. I wish you were here to celebrate this moment, to cheer me on in this new chapter. This achievement carries your strength within it.

And finally, to my husband and my tamariki — Ka nui taku aroha ki a koutou. You have sacrificed time with me so that I could finish this. You supported the long field days, the late nights, the emotional rollercoaster that comes with postgraduate study and you gave me hours of back rubs. You are my reason for doing this mahi. This work is for you, for your generation, and for the future of our wai.

May this thesis contribute, in some small way, to protecting and restoring the mauri of our freshwater systems, and to sharing knowledge that empowers the next generation to carry this responsibility forward.

Ngā mihi mahana ki a koe. Nōku te reka i tō tautoko.

Table of Contents

Abstract	2
Acknowledgements	4
Introduction	21
1.1 Freshwater fish in Aotearoa	22
1.2 Diadromy	24
1.3 Kōaro	26
1.4 The ecology of kōaro	28
1.5 Ecosystem connectivity and resource subsidies	31
1.6 Habitat preferences	33
1.7 Climate change	35
1.8 Te Arawa Lakes	36
1.9 Research aims and hypotheses	39
1.9.1 H1: Demographic function of the wetland	40
1.9.2 H2: Environmental filtering and trout limitation	40
1.9.3 H3: Trophic structure and resource use	40
1.9.4 H4: Coexistence with common bully	41
Methods	42
2.1 Study site and sampling design	42
2.2 Environmental conditions	44
2.3 Kōaro trapping	44
2.4 eDNA sampling	47
2.5 Tagging and fin clipping	48
2.5.1 Recapture	49
2.6 Stable isotope analysis	50
2.6.1 Collection	50
2.6.2 Processing	51
2.6.3 Analysis	52
2.7 Data analysis	52

2.7.1	CPUE, biomass and size structure	53
2.7.2	Habitat associations	53
2.7.3	Recapture analyses.....	53
2.7.4	Length-weight relationships and body condition	54
2.7.5	Hydrology and environmental drivers	55
2.7.6	Comparison of March 2019 and March 2025	56
2.7.7	Analysis of stable isotope data	56
Results		58
3.1	Physical environment	58
3.1.1	Habitat.....	58
3.1.2	Hydrology.....	60
3.1.3	Physiochemical.....	60
3.2	Community overview	62
3.3	Kōaro in the Millar Road Wetland (MRW).....	64
3.3.1	Kōaro catch per unit effort (CPUE).....	64
3.3.2	Kōaro body length	65
3.3.3	Kōaro body mass.....	67
3.3.4	Kōaro mass-length relationship	69
3.3.5	Kōaro condition.....	70
3.3.6	Kōaro biomass	72
3.3.7	Kōaro recruitment	73
3.3.8	Kōaro-habitat associations	75
3.3.9	Influence of hydrology on kōaro.....	76
3.4	Kōaro comparison (2019 and 2025)	77
3.5	Kōaro mark-recapture.....	82
3.5.1	PIT-tagged kōaro movement and site fidelity	82
3.5.2	Individual growth post tagging	84
3.5.3	Population estimate	86
3.5.4	Monthly spatial variation in kōaro CPUE	87
3.6	Common bullies in MRW.....	90
3.6.1	Size structure	90
3.6.2	Seasonal abundance patterns	91
3.6.3	Co-occurrence with kōaro.....	92
3.6.4	Relative dominance and seasonal contrasts	94
3.6.5	Common bully recruitment	96

3.7	Kōura in MRW	97
3.7.1	Seasonal abundance	97
3.7.2	Size structure	99
3.7.3	Recruitment patterns	100
3.8	Rainbow trout in MRW.....	101
3.8.1	Occurrence and frequency.....	101
3.8.2	Spatial distribution.....	104
3.8.3	Relationship with kōaro	105
3.8.4	Environmental drivers	105
3.9	Stable isotope analysis	106
<i>Discussion.....</i>		114
4.1	H1: Demographic function of the wetland.....	114
4.2	H2: Environmental filtering and trout limitation	118
4.3	H3: Trophic structure and resource use.....	121
4.4	H4: Coexistence with common bully	123
<i>Summary.....</i>		126
5.1	Synopsis.....	126
5.2	Implications and limitations	127
5.3	Future research directions.....	129
5.4	Conclusion.....	132
<i>References</i>		133
<i>Appendix</i>		144
6.1	Appendix A All Traps	144
6.2	Appendix B Habitat	147
6.3	Appendix C Environmental DNA (eDNA).....	150
6.4	Appendix D Stable Isotope Analysis	152

Figures

- Figure 1: Conceptual life cycle of landlocked kōaro (*Galaxias brevipinnis*) in Lake Ōkareka, adapted from Kusabs (1989) and Rowe et al. (2008). Adult kōaro occupy littoral and benthic lake habitats and migrate upstream into tributary streams during summer–autumn to spawn. Eggs are deposited in stream gravels and incubate in flowing water. Upon hatching, larvae drift downstream into the lake and occur primarily in the pelagic mid-water zone; larval diet remains uncertain. Juveniles rear in littoral lake habitats (0–10 m), forming near-surface schools and feeding predominantly on zooplankton. Adults utilise deeper benthic habitats (>15 m) where they feed on benthic invertebrates before undertaking seasonal upstream migration to spawning habitats. 30
- Figure 2: Location of the Millar Road Wetland within the Lake Ōkareka catchment (Rotorua Lakes district, New Zealand) and spatial arrangement of trapping sites. The main panel shows Lake Ōkareka and surrounding topography, with the Millar Road Wetland on the lake margin indicated by the red polygon; the dashed leader line links to the inset. The inset (high-resolution aerial imagery) maps the full trap network ($n = 20$), with individual traps labelled (T1–T17, TA–TC) and positioned along the stream-wetland ecotone to capture spatial variation in kōaro activity across the wetland mosaic. 43
- Figure 3: Deployment of dissolved oxygen and temperature loggers within the wetland study reach. (Left) Loggers secured to a stake prior to installation at one of two sites. (Right) Placement of a logger at a monitoring site (T6) within the wetland system. Loggers recorded dissolved oxygen (mg L^{-1}) and temperature ($^{\circ}\text{C}$) at hourly intervals. 44
- Figure 4: Gee’s minnow trap deployment at a sampling site (T8) within the Millar Road Wetland from February 2025 to January 2026. Traps were positioned parallel to flow and secured to the bank. Each trap was left in situ for 24 hours during monthly sampling. 45
- Figure 5: (Left) Total catch from a Gee’s minnow trap at one site in Millar Road Wetland between February 2025 and January 2026. (Right) Individual kōaro length was measured to the nearest mm using a stainless-steel measuring board. 46
- Figure 6: Kōura (*Paranephrops planifrons*) orbit–carapace length (OCL) measurement used at Millar Road Wetland, Reproduced from NIWA (n.d.). OCL is defined as the linear distance from the posterior margin of the orbital cavity to the posterior margin of the carapace and is commonly used as a standard size metric in freshwater crayfish studies. 47
- Figure 7: Field processing setup for passive integrated transponder (PIT) tagging and fin-clip collection at Millar Road Wetland in September 2025 ($n = 27$). Following 2-Phenoxyethanol sedation, kōaro were transferred to a sterile tray. Individuals were PIT-tagged and a small fin clip was removed using sterile instruments. Each fin clip was placed into a uniquely labelled microcentrifuge tube for stable isotope analysis. 49
- Figure 8: Identification of individuals for passive integrated transponder (PIT) tagged kōaro at Millar Road Wetland between October 2025 and January 2026. On each sampling occasion, individuals were

visually inspected for fin clips (Right) and scanned using a handheld PIT tag reader (V8BT RT100, SwissPlus ID Pty Ltd, Vienna, Austria). Detected tag numbers were recorded for growth and movement analyses (Left). Individuals exhibiting a fin clip, but no detectable PIT tag were noted separately. 50

Figure 9: Principal Component Analysis (PCA) of habitat characteristics measured at the initial trap locations ($n = 20$; traps 1–17 and A–C). (a) Trap scores plotted along the first two principal components. (b) Variable loadings showing the direction and relative contribution of habitat predictors to each principal component. PC1 explained 52.1 % of total habitat variation and represented a gradient from macrophyte-dominated habitats (raupō and aquatic vegetation) to more shaded habitats. PC2 explained 26.5 % of variation and described a gradient from aquatic vegetation-dominated sites to grass-dominated habitats. Together, the first two components accounted for 78.5 % of total variation in habitat structure. 58

Figure 10: Spatial distribution of raupō (*Typha orientalis*) cover across the 12 initial Gee’s minnow trap locations in the Millar Road Wetland. Points represent trap locations in NZTM2000 coordinates. Colour indicates raupō cover class (0–3), where 0 = absent and 3 = dense cover. Raupō was absent from most upstream and mid-wetland traps and was concentrated in the downstream section, indicating strong spatial heterogeneity in emergent vegetation structure. 59

Figure 11: Temporal variation in dissolved oxygen concentration and water temperature recorded at two monitoring sites in the Millar Road wetland between April 2025 and January 2026. Panels (a) and (c) show dissolved oxygen (O_2 , $mg L^{-1}$) time series for Logger One and Logger Two, respectively, while panels (b) and (d) show corresponding water temperature ($^{\circ}C$) time series. Grey points represent individual logger measurements, and blue lines indicate smoothed trends (LOESS). Both sites exhibited strong seasonal patterns, with higher temperatures and dissolved oxygen concentrations during spring and summer and lower values during winter. Overall thermal conditions were similar between sites, although Logger One recorded higher episodic temperature maxima, while Logger Two experienced more pronounced low dissolved oxygen events. 61

Figure 12: Relationship between water temperature ($^{\circ}C$) and dissolved oxygen concentration (O_2 , $mg L^{-1}$) at two monitoring sites in the Millar Road wetland. Panel (a) shows Logger One and panel (b) shows Logger Two. Grey points represent individual paired temperature and dissolved oxygen observations, and blue lines indicate fitted linear regressions. At both sites, dissolved oxygen declined with increasing temperature, reflecting the expected inverse relationship between temperature and oxygen solubility. Logger Two exhibited greater variability in dissolved oxygen across the observed temperature range, including more frequent low-oxygen conditions. 62

Figure 13: Monthly variation in mean kōaro (*Galaxias brevipinnis*) catch per unit effort (CPUE; mean kōaro per trap, per sampling occasion) in the Millar Road wetland. Data were derived from the initial 12 Gee’s minnow traps sampled monthly from February 2025 to January 2026. Error bars indicate the 95 % confidence interval (CI). 65

Figure 14: Monthly variation in mean kōaro (*Galaxias brevipinnis*) length (mm) in the Millar Road wetland. Data comes from the initial 12 Gee’s minnow traps which were set monthly from February 2025 to January 2026. The errors bars indicate the 95 % confidence interval (CI). 66

Figure 15: Seasonal size-frequency distributions of kōaro (*Galaxias brevipinnis*) captured in the Millar Road wetland. Data are from the initial 12 Gee’s minnow traps deployed monthly from February 2025 to January 2026 and show the frequency of individual total lengths (mm) recorded each month, illustrating temporal variation in size structure across the sampling period. 67

Figure 16: Monthly variation in mean kōaro (*Galaxias brevipinnis*) mass (g) in the Millar Road wetland. Data are from the initial 12 Gee’s minnow traps which were set monthly from February 2025 to January 2026. Error bars indicate the 95 % confidence interval (CI). 68

Figure 17: Seasonal mass-frequency distribution of kōaro (*Galaxias brevipinnis*) captured in the Millar Road wetland. Data are from the initial 12 Gee’s minnow traps deployed monthly from February 2025 to January 2026. The figure shows the frequency of individual body masses recorded each month, illustrating temporal variation in mass distribution across the sampling period. 69

Figure 18: Log–log relationship between total length (mm) and wet mass (g) for kōaro (*Galaxias brevipinnis*) captured at the Millar Road wetland between February 2025 and January 2026 (n = 419). Points represent individual fish. The solid blue line shows the fitted linear regression of $\log_{10}(\text{wet mass})$ on $\log_{10}(\text{total length})$. The regression equation and coefficient of determination (R^2) are displayed on the plot ($p < 0.001$). 70

Figure 19: Monthly distribution of kōaro (*Galaxias brevipinnis*) condition relative to the national length–weight relationship (Jellyman et al., 2013). Condition is expressed as the \log_{10} residual between observed weight and expected weight derived from the national equation. Values greater than zero indicate individuals heavier than predicted for their length, while values below zero indicate individuals lighter than predicted. Ridgelines represent kernel density distributions for each month, and the dashed vertical line indicates the national expectation (residual = 0). Monitoring began in February 2025 and continued monthly until January 2026. 71

Figure 20: Monthly variation in relative weight (W_r) of kōaro (*Galaxias brevipinnis*) at the Millar Road wetland between February 2025 and January 2026. Relative weight was calculated as $100 \times (\text{observed mass} / \text{expected mass})$ using the national length–weight relationship for kōaro (Jellyman et al., 2013). Points represent individual fish, lines show monthly means, and error bars indicate $\pm 95\%$ confidence intervals. The dashed horizontal line represents $W_r = 100$, corresponding to the national expected mass for a given length. 72

Figure 21: Monthly variation in mean kōaro (*Galaxias brevipinnis*) biomass per unit effort (BPUE; g kōaro per trap) in the Millar Road wetland. Data were derived from the initial 12 Gee’s minnow traps sampled monthly from February 2025 to January 2026. Bars and points represent monthly mean BPUE values, and error bars indicate the 95 % confidence interval (CI). 73

- Figure 22: Proportion of adult and juvenile kōaro (*Galaxias brevipinnis*) in the Millar Road wetland. Data were derived from the initial 12 Gee’s minnow traps sampled monthly from February 2025 to January 2026. Juveniles were defined as individuals <70 mm total length. 74
- Figure 23: Model-predicted probability of kōaro (*Galaxias brevipinnis*) being juvenile (< 70 mm total length) by month, estimated using a binomial generalised linear model. Data were derived from the initial 12 Gee’s minnow traps sampled monthly from February 2025 to January 2026. Points show predicted probabilities and error bars indicate 95 % confidence interval. 75
- Figure 24: Comparison of kōaro (*Galaxias brevipinnis*) mean catch per unit effort (CPUE; individuals per trap) in the Millar Road wetland. Data were derived from the initial 12 Gee’s minnow traps sampled during March 2019 and March 2025. Bars and represent monthly mean CPUE values, and error bars indicate the 95 % confidence interval (CI). 78
- Figure 25: Comparison of kōaro (*Galaxias brevipinnis*) Catch Per Unit Effort (CPUE; individuals per trap) in the Millar Road wetland. Data were derived from 12 Gee’s minnow traps sampled during March 2019 and March 2025. 78
- Figure 26: Comparison of kōaro (*Galaxias brevipinnis*) total length (mm) between March 2019 and March 2025 sampling events at the 12 monitored traps in the Millar Road wetland. Histograms show length-frequency distributions for each year respectively (March 2019: n = 36; March 2025: n = 26). The dashed blue vertical line in each panel indicates the median total length for that corresponding year. 79
- Figure 27: Comparison of kōaro (*Galaxias brevipinnis*) Mass (g) between March 2019 and March 2025 sampling events at the 12 monitored traps in the Millar Road wetland. Histograms show mass-frequency distributions for each year (March 2019: n = 36; March 2025: n = 26). The dashed vertical line in each panel indicates the median total mass for that year. 80
- Figure 28: Comparison of adult and juvenile kōaro (*Galaxias brevipinnis*) between March 2019 and March 2025 sampling events at the 12 monitored traps in the Millar Road wetland. Individuals were classified as juveniles (<70 mm total length) or adults (≥70 mm) to assess differences in size-class composition between sampling years. Values show total counts and the proportion of juveniles within each year. 81
- Figure 29: Capture histories of PIT-tagged kōaro (*Galaxias brevipinnis*) in the Millar Road wetland following release. Individuals were PIT-tagged and released in September 2025, and subsequent recaptures were recorded during monthly sampling from October 2025 to January 2026. The y-axis shows individual PIT tag IDs, ordered by the month of first recapture, with individuals not recaptured during the study period shown at the bottom. The x-axis shows sampling month. Large, filled symbols indicate months in which an individual was recaptured, while small open symbols indicate months in which the individual was not recaptured. December shows no recaptures due to technical problems recording individual tag data. 83
- Figure 30: Movement of PIT-tagged kōaro (*Galaxias brevipinnis*) between successive recapture events at Millar Road wetland between September 2025 and January 2026. Boxes show the median and

interquartile range, whiskers indicate the range, and points represent individual movements. Only individuals captured more than once were included. 84

Figure 31: Change in individual kōaro (*Galaxias brevipinnis*) total length (Δ length, mm) relative to initial tagging in September 2025, excluding December. Boxes show the median and interquartile range, whiskers indicate the range, and points represent individual fish. Positive values indicate growth. 86

Figure 32: Spatial distribution of kōaro (*Galaxias brevipinnis*) catch per unit effort (CPUE) across the 12 initial traps in the Millar Road Wetland over the February–January sampling period. Panels represent monthly sampling occasions, with trap locations fixed across panels to facilitate temporal comparison. CPUE values were classified into Low (0–1 kōaro), Medium (2–3 kōaro), and High (≥ 4 kōaro) categories using global quantiles calculated across all trap–month observations (0%, 33%, 66%, 100% = 0, 1, 3, 12) to allow direct comparison among months. Axes are shown in NZTM2000 coordinates (EPSG:2193), with tick labels expressed in kilometres to indicate spatial scale. Visual inspection suggests a seasonal concentration effect, with February–April and November–January characterised by a greater frequency of high CPUE classifications, indicating temporally clustered use of particular wetland areas. 88

Figure 33: Overall spatial distribution of kōaro (*Galaxias brevipinnis*) CPUE across the 12 initial traps, summarised as the median CPUE per trap over the 12-month sampling period. Symbol size and colour are scaled proportionally to median CPUE, providing redundant visual encoding to emphasise differences among traps. Median values were used due to strong zero inflation and right-skewed catch distributions, providing a robust estimate of typical trap performance across months. Axes are shown in NZTM2000 coordinates (EPSG:2193), with labels expressed in kilometres. Traps exhibiting consistently higher median CPUE indicate areas of sustained kōaro use within the wetland and may represent spatially stable core-use areas under prevailing hydrological conditions. 89

Figure 34: Length-frequency distribution of common bullies (*Gobiomorphus cotidianus*) at Millar Road wetland. Data comes from all 20 Gee’s minnow traps which were set monthly from February 2025 to January 2026. The histogram summarises the size structure of individuals recorded across the sampling period ($n = 1,392$), with the dashed vertical line indicating the median total length. The distribution is right-skewed, reflecting a predominance of smaller-bodied individuals. 90

Figure 35: Mass frequency distributions of common bullies (*Gobiomorphus cotidianus*) at Millar Road wetland. Data comes from all 20 Gee’s minnow traps which were set monthly from February 2025 to January 2026. The histogram summarises body mass variation among individuals recorded during the study ($n = 1,392$), with the dashed vertical line indicating the median body mass. The strongly right-skewed distribution reflects a high proportion of low-mass individuals and a small number of larger fish. 91

Figure 36: Monthly variation in size of common bullies (*Gobiomorphus cotidianus*) at Millar Road wetland. Data comes from all 20 Gee’s minnow traps which were set monthly from February 2025 to January

2026. Bars represent the total number of individuals recorded across all traps in each month, illustrating seasonal variation in relative abundance.	92
Figure 37: Monthly mean common bully (<i>Gobiomorphus cotidianus</i>) catch per unit effort (CPUE; individuals per trap per 24-hour sampling occasion) from February 2025 to January 2026. Bars and points show mean CPUE across traps, with error bars indicating 95 % confidence intervals.	93
Figure 38: Relationship between kōaro (<i>Galaxias brevipinnis</i>) and common bully (<i>Gobiomorphus cotidianus</i>) catch per unit effort (CPUE) at the trap-month scale at Millar Road wetland. Each point represents one trap deployment in one month. CPUE values are expressed as per month. Data comes from all 20 Gee’s minnow traps which were set monthly from February 2025 to January 2026.	94
Figure 39: Monthly total counts of kōaro (<i>Galaxias brevipinnis</i>) and common bully (<i>Gobiomorphus cotidianus</i>) at Millar Road wetland. Data comes from all 20 Gee’s minnow traps which were set monthly from February 2025 to January 2026. Bars are stacked to illustrate seasonal variation in absolute abundance and relative numerical dominance between species.	95
Figure 40: Monthly ratio of common bully (<i>Gobiomorphus cotidianus</i>) to kōaro (<i>Galaxias brevipinnis</i>) at Millar Road wetland. Data comes from all 20 Gee’s minnow traps which were set monthly from February 2025 to January 2026. Values represent the total number of common bullies divided by the total number of kōaro recorded across all traps within each month. The dashed horizontal line indicates a ratio of 1, representing equal numerical abundance of the two species.	96
Figure 41: Monthly proportion of juvenile to adult common bullies (<i>Gobiomorphus cotidianus</i>) captured at the Millar Road wetland from February 2025 to January 2026. Juveniles were defined as individuals ≤ 32 mm total length. Bars represent the proportion of juveniles to adults within total monthly captures, illustrating seasonal variation in recruitment.	97
Figure 42: Monthly counts of kōura (<i>Paranephrops planifrons</i>) at Millar Road wetland. Data comes from all 20 Gee’s minnow traps which were set monthly from February 2025 to January 2026. Bars represent the total number of individuals recorded on each monthly sampling occasion, illustrating seasonal variation in kōura abundance.	98
Figure 43: Distribution of orbit carapace length (OCL, mm) of kōura (<i>Paranephrops planifrons</i>) at Millar Road wetland. Data were obtained from all 20 Gee’s minnow traps set monthly between February 2025 and January 2026 ($n = 162$). The histogram displays the frequency of individuals within successive OCL size classes, illustrating the size structure of the population across the sampled reach. The dashed blue vertical line indicates the mean OCL of the sampled population, providing a measure of central tendency relative to the observed size distribution.	99
Figure 44: Distribution of wet mass for kōura (<i>Paranephrops planifrons</i>) at Millar Road wetland. Data comes from all 20 Gee’s minnow traps which were set monthly from February 2025 to January 2026. Mass values were estimated from orbit-carapace length (OCL) and illustrate seasonal variation in individual body size.	100

- Figure 45: Monthly size-class composition of kōura (*Paranephrops planifrons*) at Millar Road wetland. Data comes from all 20 Gee's minnow traps which were set monthly from February 2025 to January 2026. Stacked bars show the relative contributions of juvenile (OCL \leq 10 mm) and adult (OCL $>$ 10 mm) individuals to total monthly captures. 101
- Figure 46: Frequency of rainbow trout (*Oncorhynchus mykiss*) detections at Millar Road wetland. Data comes from all 20 Gee's minnow traps which were set monthly from February 2025 to January 2026. Bars indicate sampling months in which trout were recorded. 102
- Figure 47: Length-frequency distribution of rainbow trout (*Oncorhynchus mykiss*) at Millar Road wetland. Data comes from all 20 Gee's minnow traps which were set monthly from February 2025 to January 2026. The histogram summarises the size structure of individuals recorded across the sampling period ($n = 28$), with the dashed vertical line indicating the median total length. The distribution shows a narrow size range. 103
- Figure 48: Mass-frequency distribution of rainbow trout (*Oncorhynchus mykiss*) at Millar Road wetland. Data were collected from Gee's minnow traps set monthly from February 2025 to January 2026. The histogram summarises the mass structure of individuals recorded across the sampling period ($n = 28$), with the dashed vertical line indicating the median mass. The distribution is slightly right skewed, reflecting a dominance of lighter individuals. 104
- Figure 49: Spatial distribution and relative intensity of rainbow trout (*Oncorhynchus mykiss*) across the Millar Road wetland during 3 months in which trout were detected in the 20 Gee's Minnow Traps between February 2025 and January 2026. Point size represents the number of trout captured per trap per month, with larger symbols indicating higher capture counts. Trap numbers are ordered spatially along the wetland from downstream to upstream. 105
- Figure 50: Stable isotope biplot of $\delta^{13}\text{C}$ and $\delta^{15}\text{N}$ (‰) describing the Millar Road Wetland food web on the margins of Lake Ōkāreka. Error bars (± 1 standard deviation) are shown to indicate variation in stable isotope ratios for selected food web components. Symbols indicate functional groups (including invertebrate functional feeding groups), colours indicate broad trophic groups (basal resources, invertebrates, fish). Kōaro, *Galaxias brevipinnis*; Bully, *Gobiomorphus cotidianus*; Kōura, *Paranephrops planifrons*; Caddisfly, including *Leptoceridae* and *Oeconesidae*; Moth, including *Oecophoridae* and *Noctuidae*; FBOM, fine benthic organic matter; CPOM, coarse particulate organic matter. 108
- Figure 51: Stable isotope biplot of $\delta^{13}\text{C}$ and $\delta^{15}\text{N}$ (‰) describing the individual variation in fish (Kōaro, *Galaxias brevipinnis*; Bully, *Gobiomorphus cotidianus*) in the Millar Road Wetland food web. Each point represents an individual fish. Standard ellipses indicate the 95 % confidence interval. .. 109
- Figure 52: Boxplot describing the variation in the Bayesian Standard Ellipse Area (‰²) for individual kōaro (*Galaxias brevipinnis*; and common bully, *Gobiomorphus cotidianus*) in the Millar Road Wetland food web. Boxes indicate the 50 %, 95 % and 99 % credible intervals. The black dot indicates the mode for the estimated values of Bayesian Standard Ellipse Area (‰²). The red dot indicates the

<p>maximum-likelihood (ML) estimated Standard Ellipse Area (%²) corrected for sample size (SEA-c).....</p>	110
<p>Figure 53: Stable isotope biplot of $\delta^{13}\text{C}$ and $\delta^{15}\text{N}$ (‰) describing putative prey and carbon sources used by fish (Kōaro, <i>Galaxias brevipinnis</i>; Bully, <i>Gobiomorphus cotidianus</i>) in the Millar Road Wetland food web. These sources were used in Bayesian mixing models. Error bars (± 1 standard deviation) are shown to indicate variation in stable isotope ratios for selected food web components. Symbols indicate functional groups (including invertebrate functional feeding groups), colours indicate broad trophic groups (basal resource, invertebrates, fish). Mud snail, <i>Potamopyrgus antipodarum</i>; Midge larvae, Chironomidae, Simuliidae, Dixidae, and Limoniidae; Caddisfly, including adult Leptoceridae and Oeconesidae; Moth, including Oecophoridae and Noctuidae; Autochthonous, organic matter including biofilms, filamentous algae (Chlorophyta), and Potamogeton cheesemanii; Allochthonous, organic matter including fine benthic organic matter (FBOM) and coarse particulate organic matter (CPOM).....</p>	111
<p>Figure 54: Dietary contribution (mean ± 1 standard deviation) of different prey sources to kōaro (<i>Galaxias brevipinnis</i>) and common bully (<i>Gobiomorphus cotidianus</i>) in the Millar Road Wetland food web estimated by a Bayesian mixing model. See Appendix 6.4 for credible intervals from the mixing model.</p>	112
<p>Figure 55: Dietary contribution (mean ± 1 standard deviation) of different carbon sources to kōaro (<i>Galaxias brevipinnis</i>) and common bully (<i>Gobiomorphus cotidianus</i>) in the Millar Road Wetland food web estimated by a Bayesian mixing model. See Appendix 6.4 for credible intervals from the mixing model.</p>	113
<p>Figure 56: Conceptual model of the Millar Road Wetland (MRW) as a hydrologically mediated refuge for kōaro. Coloured groupings represent interacting drivers identified in this study: climate and hydrology (blue tones) regulate surface-water connectivity; environmental filtering processes (green tones), including shallow depth, macrophyte structure, and episodic low dissolved oxygen, asymmetrically constrain trout residency and growth; biotic interactions (orange tones) reflect trophic partitioning and habitat-mediated space use; and predator dynamics (red tones) illustrate episodic trout access and limited piscivory. Together, these interacting processes support persistent kōaro occupancy while restricting sustained predator pressure. Refuge function emerges not from absolute predator exclusion, but from a context-dependent balance between necessary hydrological connectivity for demographic exchange and environmental constraints that limit trout establishment.</p>	131
<p>Figure 57: Monthly variation in mean kōaro (<i>Galaxias brevipinnis</i>) length (mm) in the Millar Road wetland. Data comes from all 20 Gee's minnow traps which were set monthly from February 2025 to January 2026. The errors bars indicate the 95 % confidence interval (CI).....</p>	144
<p>Figure 58: Monthly variation in mean kōaro (<i>Galaxias brevipinnis</i>) catch per unit effort (CPUE; mean kōaro per trap, per sampling occasion) in the Millar Road wetland. Data were derived from all 20 Gee's</p>	

minnow traps sampled monthly from February 2025 to January 2026. Error bars indicate the 95 % confidence interval (CI).	145
Figure 59: Monthly variation in mean kōaro (<i>Galaxias brevipinnis</i>) mass (g) in the Millar Road wetland. Data are from all 20 Gee’s minnow traps which were set monthly from February 2025 to January 2026. Error bars indicate the 95 % confidence interval (CI).	146
Figure 60: Trap locations (Trap 1–Trap 17 and Trap A–C) within the Millar Road wetland. Images show representative local habitat conditions used for qualitative and semi-quantitative habitat assessment in January 2026.	149
Figure 61: Environmental DNA (eDNA), collected at site T4 on 21 February 2025 in the Millar Road wetland using six replicate 1.2 µm cellulose acetate filters following Wilderlab protocols (Wilkinson et al., 2024). DNA was extracted, amplified, and sequenced using high-throughput metabarcoding targeting the 16S gene region for fish and the CO1 region for aquatic invertebrates. Panels (a) and (b) show read counts per 100 mL for kōaro (<i>Galaxias brevipinnis</i>) and common bully (“Toitoi”; <i>Gobiomorphus cotidianus</i>), respectively, across the six filter replicates. The dashed horizontal line indicates mean read count across replicates. Panel (c) shows proportional read composition of detected fish taxa per filter, including kōaro, common bully, and rainbow trout (<i>Oncorhynchus mykiss</i>).	151

Tables

- Table 1: Species composition at Millar Road wetland, Lake Ōkāreka. Data were derived from the initial 12 sites sampled monthly from February 2025 to January 2026 using Gee’s minnow traps. Values summarise total captures, proportional contribution to total catch (%), Occupancy (percentage of sampling occasions in which a species was detected) and mean catch per unit effort (CPUE; individuals per trap-month \pm one standard deviation, SD). Median CPUE and interquartile range (IQR) are presented to account for zero-inflated and skewed catch distributions. 63*
- Table 2: Species composition at Millar Road wetland, Lake Ōkāreka. Data were derived from all 20 sites sampled monthly from February 2025 to January 2026 using Gee’s minnow traps. Values summarise total captures, proportional contribution to total catch (%), Occupancy (percentage of sampling occasions in which a species was detected) and mean catch per unit effort (CPUE; individuals per trap-month \pm one standard deviation, SD). Median CPUE and interquartile range (IQR) are presented to account for zero-inflated and skewed catch distributions. 63*
- Table 3: Results of a generalized linear model examining the effects of habitat variables and co-occurring species on kōaro (*Galaxias brevipinnis*) presence in the Millar Road wetland. Estimates (β) are logit-scale coefficients, with associated standard errors (SE), z-values, and p-values. Habitat predictors included ordinal cover scores (0–3) for shade, raupō, and aquatic vegetation, and presence/abundance measures of grasses, trout, common bully, and kōura. Negative coefficients indicate a decrease in the probability of kōaro presence with increasing predictor values, whereas positive coefficients indicate an increase. 76*
- Table 4: Summary statistics for kōaro (*Galaxias brevipinnis*) total length (mm) recorded in Millar Road wetland. Data were derived from the initial 12 Gee’s minnow traps sampled during March 2019 and March 2025 and pooled across all monthly sampling occasions in 2025/2026. Values shown include sample size (n), mean length, median length and standard deviation (SD). 77*
- Table 5: Comparison of kōaro (*Galaxias brevipinnis*) length-class composition between 2019 and 2025. Individuals were classified as juveniles (<70 mm total length) or adults (\geq 70 mm) to assess the relative contribution of juvenile fish in each sampling year. Values show total counts and the proportion of juveniles within each year’s sample. 80*
- Table 6: Monthly recapture of PIT-tagged kōaro (*Galaxias brevipinnis*) following tagging in September 2025 at the Millar Road wetland. Values show the number and proportion of tagged individuals detected in each subsequent sampling month (n = 27 tagged individuals). *Fin-clipped individuals counted only due to technical issues with the tag reader. 82*
- Table 7: Paired comparisons of individual kōaro (*Galaxias brevipinnis*) growth between the initial tagging event in September 2025 and subsequent recapture surveys, excluding December. Mean absolute and proportional changes in total length and body mass are shown for each interval. Statistical significance was assessed using paired t-tests on log-transformed data. 85*

Table 8. Lincoln–Petersen mark–recapture estimates of kōaro abundance by month at all sites in the Millar Road wetland between September 2025 and January 2026. M represents the number of individuals marked during the initial tagging event, C the total number of individuals captured during the recapture survey, and R the number of marked individuals recaptured. Estimated population size (N) represents short-term closed population estimates between marking and recapture events and should be interpreted as indices of relative abundance rather than absolute population size. 87

Table 1: Summary statistics for the Bayesian mixing model testing the contribution of four putative prey sources to the diet of kōaro (Galaxias brevipinnis) and common bully (Gobiomorphus cotidianus) in Millar Road Wetland. Statistics include mean, standard deviation (SD), median (50 %), and the 50 %, 90 % and 95 % credible intervals. 152

Table 2: Summary statistics for the Bayesian mixing model testing the contribution of autochthonous and allochthonous carbon to the diet of kōaro (Galaxias brevipinnis) and common bully (Gobiomorphus cotidianus) in Millar Road Wetland. Statistics include mean, standard deviation (SD), median (50 %), and the 50 %, 90 % and 95 % credible intervals. 152

Introduction

Freshwater ecosystems, although occupying less than one percent of the Earth's surface, support a disproportionately high level of global biodiversity and maintain a wide range of ecological and societal functions (Dudgeon et al., 2006). However, freshwater ecosystem health is undergoing sustained and often rapid decline, with rates of biodiversity loss exceeding those reported for terrestrial or marine environments (Strayer & Dudgeon, 2010). Over the past five decades, cumulative pressures including overexploitation, pollution, flow alteration, habitat degradation, and the introduction of non-native species have contributed to significant reductions in the abundance, distribution, and functional diversity of freshwater biota (Dudgeon et al., 2006; Strayer & Dudgeon, 2010). These long-standing threats have been further exacerbated by climate change, urban development, and widespread modification of hydrological regimes (Reid et al., 2019; Cazzolla Gatti, 2016).

Together, these drivers have created what is now widely regarded as a global freshwater biodiversity crisis (Harrison et al., 2018; Albert et al., 2021). Indicators of population trend consistently show declines that surpass those of any other major biome and extinction risks continue to rise across most freshwater taxonomic groups. Although advances in ecological understanding and conservation practice have been made, progress remains constrained by fragmented implementation and the continued marginalisation of freshwater systems within wider biodiversity policies (Strayer & Dudgeon, 2010; Tickner et al., 2020). In response, international initiatives have called for coordinated recovery efforts centred on protecting free-flowing rivers, restoring longitudinal and lateral connectivity, improving water allocation and quality, and reducing pollution to halt further losses (Tickner et al., 2020; Dudgeon & Strayer, 2025).

This global context frames the situation in Aotearoa New Zealand (Aotearoa hereafter), where many of the same pressures are evident. The degradation of Aotearoa's freshwater ecosystems is well recognised, and all regions throughout the country have experienced declines in water quality and freshwater ecosystem health, with lowland lakes and rivers typically the most degraded (Larned et al. 2016). Over 70% of Aotearoa's indigenous freshwater fish are threatened or at risk of extinction,

with 22 species listed as 'threatened', 25 'at risk', and one species (upokororo/grayling, *Prototroctes oxyrhynchus*) already extinct (Dunn et al. 2023). Key threats include agricultural intensification, wetland drainage, and in-stream structures like culverts that block migration for species such as whitebait (īnanga) and eels (tuna). These pressures have severely restricted the distribution and abundance of many native species. Understanding these broader trends is essential for interpreting the status and vulnerability of Aotearoa's distinctive freshwater fish fauna, which has evolved under prolonged isolation and marked geological and climatic variability.

1.1 Freshwater fish in Aotearoa

Aotearoa's freshwater fish fauna has evolved in unique conditions involving geographical isolation, geological dynamism, and climatic fluctuations (Stevens et al., 1988), situated in the southwest Pacific and separated from other landmasses for more than 80 million years (Goldberg et al., 2008). According to Joy & Death (2013), Aotearoa has developed a small, very distinctive and highly (92%) endemic assemblage of freshwater fish fauna with some yet to be formally described. They recognised the fauna to be categorised by nine families: Geotriidae, Anguillidae, Retropinnidae, Prototroctidae, Galaxiidae, Cheimarrhichthyidae, Eleotridae, Mugilidae, and Pleuronectidae. In Aotearoa, diadromy is obligatory in 13 of these species and facultative in six (Ling, 2010). Most species are small, benthic, riverine, and cryptic, with unusual life histories such as spending extended periods within the substrate, reflecting both their ecological specialisation and evolutionary isolation (McDowall, 1990; McEwan & Joy, 2011). This fauna is dominated by the Galaxiidae, a family with Gondwanan origins that exemplifies adaptive persistence in an island environment (McDowall, 2006).

Of the approximately 32 galaxiid species currently recognised in Aotearoa, including five *Neochanna* spp., all but two (*Galaxias brevipinnis* and *G. maculatus*) are endemic. Five species, kōaro (*G. brevipinnis*), īnanga (*G. maculatus*), banded kōkopu (*G. fasciatus*), giant kōkopu (*G. postvectis*), and shortjaw kōkopu (*G. argenteus*), are typically diadromous and collectively comprise the species targeted in the annual whitebait fishery, migrating between marine and freshwater habitats at different life stages (McDowall, 1990; Joy & Death, 2013). However, diadromy in galaxiids is not

universally expressed across all populations, a flexibility that has contributed significantly to their diversification within Aotearoa. Earlier sources suggested that nearly half were diadromous, but advances in taxonomy and molecular phylogenetics have revealed that many populations previously considered migratory are not, particularly within the *G. vulgaris* complex (Waters & Wallis, 2001; Waters et al., 2010). This revision highlights how our understanding of galaxiid life histories and speciation has evolved as scientific methods have become more precise. Non-diadromous species, particularly those in the *G. vulgaris* complex, exhibit high population subdivision, deep genetic divergence, and strong geographic restriction (Allibone & Wallis, 1993; McDowall & Chadderton, 1999; Waters & Wallis, 2001). This combination of migratory flexibility in some taxa and long-term isolation in others highlights both the evolutionary resilience of the group and its ongoing diversification, with new cryptic lineages still being identified through molecular and morphological analyses.

Galaxiids show extensive morphological plasticity and intraspecific morphological differentiation, allowing populations to adapt rapidly to contrasting environments. This plasticity helps explain how multiple non-migratory galaxiids were able to diversify repeatedly within New Zealand's fragmented landscapes, once they became isolated from the ancestral diadromous lineage (Waters & Wallis, 2001). Morphological (McDowall 1970) and isozyme evidence (Allibone & Wallis 1993) suggest that the migratory kōaro and the non-migratory *G. vulgaris* complex share a single evolutionary origin, a relationship later confirmed by Waters & Wallis (2001), who showed that the *G. vulgaris* complex forms a monophyletic lineage derived from a diadromous ancestor. Wallis (2021) further demonstrated that galaxiids possess exceptional morphological plasticity and fine-scale ecological differentiation, helping explain how these freshwater-restricted descendants repeatedly diversified across New Zealand's geologically fragmented landscapes once isolated from their migratory ancestor. Together, these studies show that much of New Zealand's galaxiid diversity represents a rapid inland radiation following the loss of diadromy in a single ancestral lineage.

1.2 Diadromy

Diadromy, whether amphidromous, catadromous, or anadromous, has provided species in Aotearoa with a mechanism to maintain connectivity in a fragmented landscape. By linking marine and freshwater environments, diadromous species have been able to colonise and recolonise catchments following disturbances such as glaciation, volcanism, and river capture events, which have repeatedly reshaped drainage networks and isolated populations (McDowall, 1998; Jellyman et al., 1996; Waters et al., 2020). According to Ling (2010), the nine native families making up Aotearoa's indigenous freshwater fish fauna have diadromous representatives occurring in every one of them. Without this ability, many lineages would likely have been extirpated during periods of geological instability. The persistence of diadromy among the Galaxiidae therefore reflects both evolutionary inheritance and ecological necessity in a geologically active island nation.

Diadromy, as defined by McDowall (1992), refers to regular, predictable, and physiologically mediated movements between freshwater and marine environments that are an inherent part of a species' life cycle. Unlike dispersal or opportunistic habitat shifts, diadromy is obligatory, bidirectional, and linked to specific life stages. Anadromy involves fish spawning in freshwater, with juveniles migrating to the sea to feed and grow before returning to reproduce (e.g., *Geotria australis*). Catadromy is the reverse, with species spawning in the sea and migrating into freshwater for juvenile growth before returning to spawn in the marine environment (e.g., Anguillidae). Amphidromy involves migrations between freshwater and marine habitats that are not directly tied to reproduction or feeding, typically occurring early in life; larvae may drift to the sea or a lentic habitat before returning to the natal environment to complete pre-reproductive growth (e.g., Galaxiidae). This developmental-driven behaviour, rather than resource- or reproduction-driven, distinguishes amphidromy from anadromy and catadromy.

McDowall (1998) posed a seminal framework that highlighted the prevalence of diadromy in Aotearoa's freshwater fish fauna. Recent studies have recognised the flexibility and ecological contingency of diadromy in the Galaxiidae, indicating that this life-history behaviour is not as fixed as previously thought. Delgado et al. (2020) show

that diadromy can be facultative, with populations shifting between migratory and resident tactics depending on ecological and energetic conditions, and that it has evolved multiple times across lineages. Ramírez-Álvarez et al. (2022) further demonstrate that amphidromy is environmentally contingent rather than obligatory, while Hicks et al. (2017) showed that *G. brevipinnis* populations can be entirely freshwater-recruited even where sea access exists, with upstream populations supply-limited and genetically distinct, emphasizing the role of local recruitment and metapopulation dynamics. Together, these studies support McDowall's physiological and ecological definitions of diadromy while underscoring its facultative expression, plasticity, and evolutionary lability, particularly in amphidromous species. In this context, Waters et al. (2020) show that river-capture events and drainage rearrangements have generated isolated galaxiid lineages in New Zealand, demonstrating that connectivity across freshwater–marine interfaces is critical for dispersal, recolonisation, and gene flow. Diadromy, by linking marine and freshwater habitats, therefore provides a key adaptive mechanism that allows galaxiids to persist, maintain population connectivity, and respond to dynamic geological landscapes, reinforcing both the evolutionary and ecological significance of this life-history strategy in Aotearoa.

Given the Gondwanan distribution of the galaxiids, diadromy is likely a life-history feature that has persisted for millions of years. Fossil evidence from the Miocene period in southern Aotearoa supports the deep antiquity of this life history strategy. Kaulfuss et al. (2020) documented fossilised galaxiids exhibiting both diadromous and stream resident morphologies in the Lake Manuherikia deposits, including ancestral forms closely resembling modern kōaro (*G. brevipinnis*). These findings demonstrate that transitions between migratory and non-migratory lifestyles have occurred repeatedly through evolutionary time. Lakes likely acted as refugia during periods of climatic and tectonic upheaval, providing stable habitats that encouraged local adaptation and speciation. Repeated secondary landlocking of diadromous ancestors thus fostered the proliferation of non-migratory lineages, contributing to Aotearoa's unusually high level of freshwater endemism (McDowall, 1998; Kaulfuss et al., 2020). From an ecological standpoint, diadromy has been central to structuring Aotearoa's freshwater communities. Jowett and Richardson (1996) demonstrated that medium to large rivers supporting diadromous recruitment tend to exhibit higher fish densities and

species richness than those without marine connectivity. These patterns often outweigh influences from local catchment factors such as substrate composition, flow regime, or land use. Elevation also mediates community structure where diadromous taxa dominate lowland and transitional reaches, while non-diadromous species prevail in upland systems where physical barriers restrict access to the sea (Leathwick et al., 2005). Such ecological partitioning demonstrates the profound role of migratory life histories in shaping freshwater biodiversity in Aotearoa.

At a population level, diadromy maintains genetic connectivity by promoting long distance dispersal of larvae or juveniles, thereby reducing genetic drift and sustaining cohesive gene pools across catchments. This contrasts sharply with the evolutionary outcomes of landlocking, in which isolation produces strong genetic subdivision and local adaptation. Comparative analyses show that diadromous species exhibit low inter catchment genetic differentiation, while non-diadromous taxa display marked genetic divergence and fixed allelic differences shaped by prolonged isolation (Allibone & Wallis, 1993; Waters et al., 2020). Consequently, diadromy acts both as a stabilising force, maintaining connectivity and resilience, and as a diversifying mechanism, as its loss repeatedly generates locally adapted, endemic lineages.

The ecological benefits of diadromy extend beyond population genetics. By migrating between marine and freshwater environments, diadromous fish function as biological bridges, transferring energy and nutrients across ecosystem boundaries (Gende et al., 2002). The larvae of amphidromous species can contribute to lacustrine and marine planktonic food webs (McDowall et al., 1975; David et al., 2022), while returning juveniles and adults subsidise freshwater communities (Stewart et al., 2022). Such trophic connectivity can enhance ecosystem productivity and stability, with ecological theory predicting that such subsidies help facilitate rapid recovery following disturbances such as floods and sedimentation (Takimoto et al., 2002).

1.3 Kōaro

Within this evolutionary and ecological framework, the tāonga species kōaro (*G. brevipinnis*) exemplifies the adaptive potential of the diadromous Galaxiidae. Kōaro are an amphidromous species where larvae of river-sea and river-lake populations

drift to the marine environment or large lakes shortly after hatching, develop in pelagic habitats, and later return to lotic systems as juveniles. This strategy allows them to exploit a wide range of habitats and persist under varying environmental conditions (Hicks et al., 2021; Toorchi et al., 2025). Their remarkable climbing ability, aided by a muscular ventral surface and adhesive pectoral fins, enables colonisation of steep headwater streams beyond the reach of many predators, including native competitors and introduced species such as trout (Kusabs, 1989; Jowett & Richardson, 1996).

Kōaro populations exhibit life history plasticity. While many populations remain diadromous, others have become landlocked in lakes, functioning as ecologically diadromous analogues within entirely freshwater systems. These landlocked populations often retain physiological traits of their migratory ancestors such as osmoregulatory flexibility and extended spawning periods, reflecting evolutionary continuity despite ecological isolation (King et al., 2003; Darestani, 2023). Genetic studies show that landlocked kōaro are only slightly differentiated from coastal counterparts, consistent with relatively recent isolation events. However, continued separation can lead to genetic drift and reduced diversity, heightening vulnerability to environmental change (Allibone & Wallis, 1993).

For instance, kōaro have adapted to lacustrine rearing conditions in three South Island lakes (Takapō, Pukaki and Ōhau), with larvae developing within each lake's pelagic zone before migrating upstream to adult fluvial habitats (Toorchi et al., 2025). Lake populations of kōaro have been recorded in Lakes Taupō and Rotoaira on the volcanic plateau of Aotearoa's North Island (Kusabs, 1989; Rowe et al., 2002). It is highly likely that kōaro populations in Lake Ōkāreka (Rotorua, Te Arawa Lakes Rohe) exhibit similar flexibility. Although such populations benefit from reduced predation and competition, particularly where barriers exclude non-native trout, they also face demographic constraints and limited gene flow (Jolly et al., 2024). This dynamic represents an evolutionary trade-off in which isolation can promote local adaptation and enable short-term persistence, simultaneously diminishing long-term resilience typically conferred by migratory connectivity. The restriction of larvae dispersal would effectively reduce population sizes, potentially limiting genetic diversity and the capacity to respond to future environmental change.

Previously, I described how the evolutionary history of Aotearoa's galaxiids has been shaped by diadromy and landlocking, leading to diversification ranging from marine-linked migrants to highly localised freshwater residents by driving colonisation, isolation, and divergence across geological time. Kōaro exemplify this continuum, with populations demonstrating both ancestral oceanic migratory strategies and adaptation to lacustrine environments attesting to their persistence in a dynamic archipelago. Flexible diadromy, coupled with an extraordinary ability to penetrate far inland, defines the ecological role of kōaro.

1.4 The ecology of kōaro

By epitomising the prevalence of diadromy, and related evolutionary and ecological consequences for Aotearoa's galaxiids, kōaro demonstrate how adaptability and limitation interact within the ever-changing conditions of freshwater ecosystems. As an amphidromous species capable of facultative landlocking, kōaro occupies a broad ecological niche encompassing both lotic and lentic ecosystems. However, kōaro are widely described as preferring steep, shaded, cool, fast-flowing forest streams, where their climbing ability allows them to occupy headwater habitats above barriers to passage for other fish species (McDowall 1990). This preference is reiterated in McDowall (2000), who emphasised their association with swift, oligotrophic streams, yet also noted that kōaro are among the most lake adapted galaxiids, readily forming natural landlocked populations. The latter point is indicative of their habitat flexibility. Historical evidence and mātauranga Māori from Lake Taupō demonstrate the significance of lake populations where kōaro were once a dominant pelagic fish, sustaining important Māori fisheries (Phillips, 1940). Their decline after the introduction of trout and smelt indicate that kōaro evolved to have a greater dispersal capacity over competitive abilities. However, the behavioural plasticity, habitat versatility, and generalist feeding strategies of kōaro have enabled its ecological success, but these traits may not confer resilience to novel threats including climate change, invasive species, and widespread habitat modification. Further understanding kōaro ecology therefore offers critical insight into the processes governing persistence and decline among Aotearoa's native freshwater fauna.

In rivers connected to the sea, kōaro is an amphidromous species. Adults live and breed in small streams, and larvae and juveniles rear at sea until their annual migration back into rivers during spring (McDowall, 1990). Kusabs (1989) studied stream populations of adult kōaro in several inlet streams of Lake Taupō. Juveniles reared from larvae in the lake migrated into the streams from August until February, with a peak in December (Figure 1). Fish grew from 50 mm (when they first entered streams) to 130 mm in four years. Gravid female kōaro were caught in spring and mean fecundity was 5,500 (range 3,613-19,830). Gonadosomatic indices (reflecting gonadal size) were highest over the summer/autumn months, indicating that spawning occurs during these months. O'Conner & Koehn (1998) reported *G. brevipinnis* eggs from cobbles at the margins of a hard-bottomed Australian stream. Allibone & Caskey (2000) recorded a kōaro nest in cobbles 0-2 cm deep at the margins of a hard-bottomed stream. This suggests that lacustrine populations of kōaro spawn in the cobbly margins of lake inlet streams (Figure 1). Larval kōaro are presumed to hatch when rising floodwaters raise stream levels and inundate eggs (McDowall & Suren 1995; O'Conner & Koehn 1998). Larval fish are weak swimmers, meaning it is likely that they are carried downstream by the current to the lake where they rear into juveniles. There is ontogenetic habitat partitioning where juveniles (36-49 mm long) have limnetic, schooling habit, whereas adults are benthic and can be found down to depths of 80 m (Rowe et al. 2002). Rearing larvae in a productive pelagic environment may enable kōaro to produce many small offspring that contribute disproportionately to recruitment and allow higher juvenile abundance to support adult populations (Closs et al., 2013).

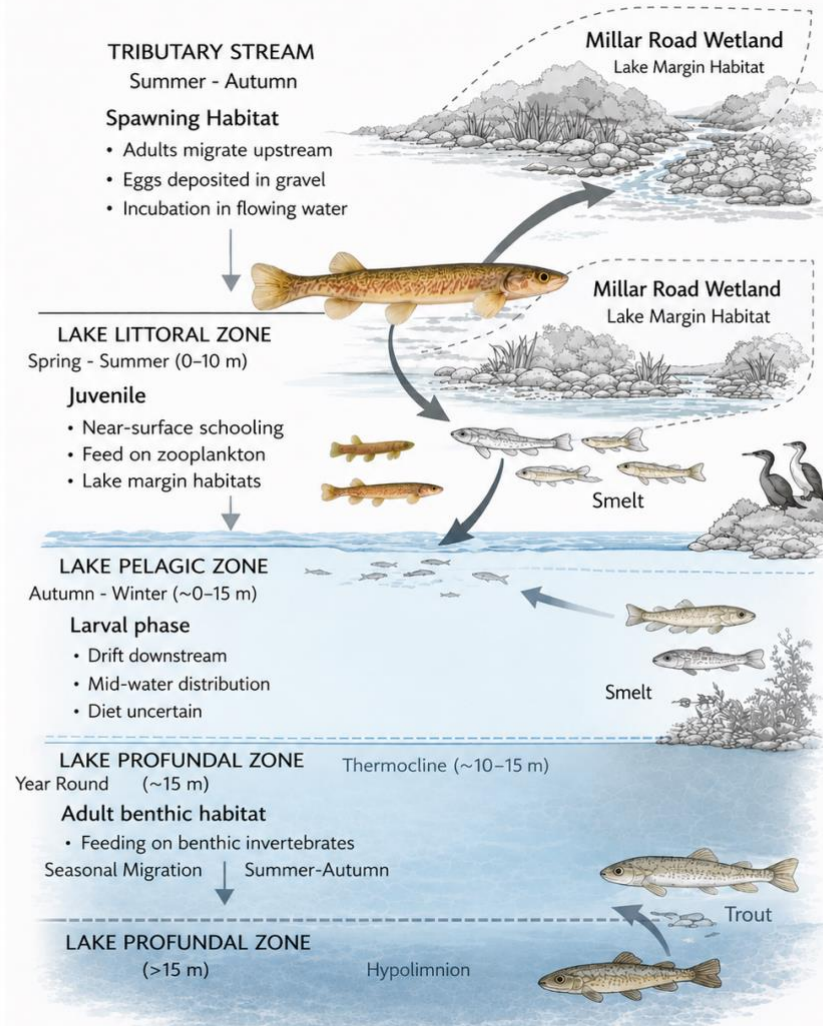


Figure 1: Conceptual life cycle of landlocked kōaro (*Galaxias brevipinnis*) in Lake Ōkareka, adapted from Kusabs (1989) and Rowe et al. (2008). Adult kōaro occupy littoral and benthic lake habitats and migrate upstream into tributary streams during summer–autumn to spawn. Eggs are deposited in stream gravels and incubate in flowing water. Upon hatching, larvae drift downstream into the lake and occur primarily in the pelagic mid-water zone; larval diet remains uncertain. Juveniles rear in littoral lake habitats (0–10 m), forming near-surface schools and feeding predominantly on zooplankton. Adults utilise deeper benthic habitats (>15 m) where they feed on benthic invertebrates before undertaking seasonal upstream migration to spawning habitats.

Kōaro diet varies predictably with both life stage and habitat type. In swift riffle-dominated streams, kōaro predominantly consume benthic macroinvertebrates in accordance with substrate focused foraging, whereas lake resident individuals selectively target benthic prey within littoral zones (Stuart, 2021). Ontogenetic shifts in foraging mode allows kōaro to exploit distinct prey fields across their amphidromous life cycle while minimising direct competition with sympatric species. Juveniles

inhabiting pelagic marine or lacustrine environments feed predominantly on zooplankton and drifting invertebrates, taking advantage of high densities of small, mobile prey. In Lake Rotoaira, the diet of lake-dwelling kōaro was dominated by purse caddis larvae (*Paroxythira* sp.), but small fish (<70 mm) also fed on *Daphnia*, whereas larger individuals (>90 mm) fed on Odonata larvae, snails, and common bullies (Rowe et al., 2002). As individuals migrate upstream into freshwater streams, their diet shifts toward benthic macroinvertebrates, including Trichoptera, Diptera, and Ephemeroptera larvae, alongside occasional consumption of fish eggs, small fish, and terrestrial invertebrates that enter the water column (Main, 1988; Kusabs, 1989; Kusabs & Swales, 1991). Although terrestrial insects can contribute to their diet in forested stream reaches, these subsidies are generally less important than for other galaxiids such as banded kōkopu (Main & Winterbourn, 1987). However, observations by Hayes (1996) challenge the assumption that kōaro are strictly benthic feeders. In a trout-free South Island stream, large kōaro were seen drift-feeding mid water and at the surface, demonstrating previously underappreciated behavioural flexibility. This capacity to switch between benthic and pelagic feeding modes reinforces kōaro's broad trophic niche and may provide resilience under fluctuating prey availability.

1.5 Ecosystem connectivity and resource subsidies

Freshwater fish populations rarely function as continuous populations because river networks are spatially structured and dispersal is constrained by barriers, habitat transitions, and species interactions. Instead, populations typically operate as metapopulations, in which local subpopulations occupy discrete habitat patches linked by dispersal (Hanski, 1999). Within these networks, some habitats act as demographic sources where reproduction exceeds mortality, while others function as sinks where populations persist only through immigration.

Connectivity within these systems is therefore fundamental to population persistence, as it enables dispersal between local subpopulation sources and sinks, thereby facilitating demographic rescue (Brown & Kodric-Brown, 1977). Introduced predators can strongly restructure these dynamics. In New Zealand streams, trout suppress recruitment of native galaxiids, converting otherwise suitable habitats into demographic sinks rather than eliminating populations outright (Woodford & McIntosh, 2010). Although individuals may persist in predator occupied reaches, these

populations are maintained primarily by immigration from predator-free refugia where successful recruitment occurs. Persistence across the landscape then depends less on local habitat quality than on connectivity to refuge habitats capable of sustaining recruitment.

This connectivity also has broader ecosystem level consequences, because dispersal not only moves individuals but also links energy and nutrient pathways across habitats. In spatially structured freshwater systems, mobile consumers connect benthic, pelagic, and marginal habitats by transferring biomass and nutrients across ecosystem boundaries. As a result, connectivity simultaneously supports metapopulation stability and trophic integration.

For amphidromous species such as kōaro, which move among tributaries, lakes, and potentially wetlands during their life cycle, connectivity is especially critical (Lee et al. 2023). Their persistence depends not only on access to recruitment habitats but also on the maintenance of pathways linking these habitats across the catchment (Hicks et al., 2017). Within this framework, isolated or structurally complex environments such as headwater streams, wetlands, or spring-fed tributaries, may function as demographic sources that sustain populations in more predator accessible environments. Identifying whether non typical habitats, including wetlands, perform this role is therefore essential for understanding kōaro persistence in modified catchments. However, ground-fed wetlands, particularly those with periodic low dissolved oxygen and restricted connectivity, are rarely considered core habitat for kōaro and are more often assumed to function as marginal or sink environments.

Beyond their demographic role, galaxiids are ecologically significant because their feeding plasticity positions them as connectors of multiple food webs (Crichton et al., 2026). As trophic generalists, kōaro exploit benthic and pelagic prey across habitats, allowing them to integrate production from spatially distinct energy channels. This cross habitat coupling reflects general ecological mechanisms described by Rooney et al. (2006), in which mobile generalist consumers stabilise food webs by linking otherwise disconnected resource pathways.

As an amphidromous species, kōaro also have the potential to transport resource subsidies across ecosystem boundaries. Juveniles returning from lacustrine or marine influenced environments import nutrients derived from offshore food webs into

freshwater systems upon settlement. Although this process has not been quantified directly for kōaro, analogous galaxiid species demonstrate similar dynamics. Stewart et al. (2022), for example, showed that upstream migrating īnanga (*Galaxias maculatus*) deliver substantial marine derived energy subsidies to freshwater predators, with longfin eels deriving 60–80% of their diet from these returning fish. Given the shared migratory strategy within the Galaxiidae, kōaro likely perform a comparable function, linking marine, lacustrine, and headwater food webs through juvenile recruitment.

Together, kōaro's metapopulation dynamics, migratory life history, and flexible feeding ecology highlight the dual role of connectivity in maintaining population persistence and coupling freshwater food webs. Consequently, habitats that sustain persistent kōaro populations may influence ecosystem processes far beyond their spatial extent, highlighting the functional importance of protecting connected refuge habitats within freshwater landscapes.

1.6 Habitat preferences

Koaro display distinct habitat preferences shaped by hydrology, temperature, and structural complexity. They thrive in cold, clear, well oxygenated streams with coarse gravel or cobble substrates and shaded riparian zones that maintain stable microclimates (Jowett & Richardson, 1996; Bell, 2001). Their remarkable climbing ability enables access to steep, headwater streams, often beyond the reach of trout (Eikaas, 2004). Consequently, upland, forested tributaries and pool rich streams represent vital strongholds for diadromous and resident kōaro populations, not necessarily because these habitats are intrinsically optimal, but because they remain among the few environments that are sufficiently complex and trout-free to function as ecological refuges.

Patterns of kōaro habitat use are strongly shaped not only by physical habitat structure but also by interactions with other native galaxiids and introduced species. In small upland streams where kōaro co-occur with shortjaw kokopu (*G. postvectis*), McEwan & Joy (2014a) showed that kōaro consistently occupied faster, deeper, and more turbulent flow habitats with larger substrates and extensive interstitial refuge space, regardless of time of day. These microhabitats correspond to areas less frequently

used by shortjaw kōkopu, suggesting that biotic interactions, likely behavioural avoidance or competitive displacement, contribute to kōaro concentrating in high-velocity channel habitats. Shortjaw kōkopu, by contrast, used larger-substrate, high cover habitat by day but shifted to slower pool habitats at night, a pattern that differs from kōaro's stable flow-channel association. McEwan & Joy (2014a) concluded that competition from shortjaw kōkopu may have influenced kōaro habitat selection, narrowing the range of microhabitats effectively available to them. This is consistent with broader patterns observed in the presence of trout and competitive species such as smelt, where kōaro persist primarily in habitats that function as ecological refuges, often steep, turbulent, or structurally complex reaches that exclude or reduce the foraging efficiency of other species.

In lakes, kōaro exploit deeper benthic zones and connected tributaries, which provide spawning and larval rearing habitats (Rowe, 1993; Stuart, 2021; Toorchi et al., 2025). Landlocked populations, such as those in the Rotorua and Taupō catchments, depend on hydrological connectivity between lake and tributary systems for recruitment and feeding. Where this connectivity is disrupted by barriers, fluctuating water levels, or sediment infilling, populations become fragmented and genetically isolated (Allibone et al., 2010; Darestani, 2023).

Habitat degradation from deforestation, agriculture, and sedimentation has reduced freshwater habitats with cool, well-oxygenated water and complex structure (Eikaas, 2004). Deposited sediments fill interstitial spaces among cobbles and boulders, limiting refuge and preferred spawning sites for small benthic fish like kōaro and redfin bully (NIWA, 2023; McEwan & Joy, 2014b). While short-term suspended sediment has limited effects on feeding or survival, chronic sediment deposition indirectly reduces growth and population resilience. McEwan & Joy (2014b) observed that kōaro actively select deeper, more complex microhabitats with larger substrates during the day, highlighting the importance of structural habitat as refuges. Sedimentation also decreases benthic invertebrate abundance, limiting food resources, while nutrient enrichment promotes algal growth that alters benthic communities.

1.7 Climate change

Climate change represents a multifaceted and escalating threat to kōaro, affecting both diadromous and landlocked populations across Aotearoa. National scale analyses indicate that galaxiid distributions are strongly influenced by diadromy and elevation, while catchment condition indirectly affects water quality and flow, shaping habitat suitability (Jowett & Richardson, 1996). In landlocked systems, sediment dynamics and hydrological variability may be even more critical for population viability than forest cover alone. Rising temperatures, altered flow regimes, and increasing eutrophication are expected to reduce the availability of cool, well-oxygenated habitats essential for spawning, larval development, and adult survival, compounding pressures from invasive species, habitat fragmentation, and other anthropogenic impacts (McDowall, 2006; Morrongiello et al., 2011; Canning et al., 2025).

Temperature increases are particularly consequential for kōaro, which tolerate maximum temperatures around 28 °C, slightly lower than other native galaxiids such as banded kōkopu (~30 °C) (Main, 1988). Warming waters can affect metabolism, reproductive success, and larval development, potentially forcing kōaro to seek thermal refugia within lakes, streams, or wetlands. Similarly, altered hydrology, including droughts, extreme floods, and artificial water level fluctuations, can disrupt spawning cues, wash out eggs, strand juveniles, and reduce habitat availability of ecological refuges (Stuart, 2021; Koehn et al., 2011). Hydrological stress may further influence connectivity between tributaries and lake margins, affecting recruitment, larval dispersal, and overall population stability (Koehn et al., 2011; Toorchi et al., 2025).

The ecological consequences of climate change propagate through food webs. Kōaro are benthic generalist feeders, relying on stream insects (e.g., Trichoptera, Ephemeroptera), whose abundance and distribution are influenced by turbidity, sedimentation, and macrophyte cover (Rowe et al., 2003). Climate driven sedimentation, altered flows, or eutrophication may reduce prey availability, while warming can drive shifts in invertebrate community composition, indirectly affecting kōaro nutrition, growth, and recruitment. Predator-prey dynamics are also affected. Warming waters and changing hydrology may expand the ranges or feeding intensity of introduced species such as trout and smelt, increasing predation on juveniles and

altering competitive interactions with other small fish (Rowe et al., 2003; Hicks et al., 2021; Canning et al., 2025). Habitat complexity and turbidity can mitigate predation risk, but climate driven degradation of these features may exacerbate vulnerability.

Extreme events further magnify risks. Under high emission scenarios (RCP 8.5), habitat-restricted galaxiids could lose more than 99% of their suitable range, risking local extirpations (Canning et al., 2025). Whilst kōaro are less threatened at the national-scale, sensitive populations at the local and regional-scales, such as Lake Ōkāreka and the Arawa lakes, may be particularly susceptible to climate-related pressures. Droughts, severe floods, or artificial water level changes can temporarily isolate wetlands from lakes or streams, limiting dispersal and gene flow. Even moderate hydrological variability may challenge populations if refugia are limited or degraded. These effects are compounded in small, landlocked populations, which face reduced genetic diversity, potential Allee effects, and heightened sensitivity to stochastic events (Morrongiello et al., 2011; Koehn et al., 2011).

1.8 Te Arawa Lakes

The Rotorua Te Arawa Lakes form a geothermally and volcanically active lake district in Aotearoa's central North Island. This network of fourteen crater and caldera lakes, including Rotorua, Tarawera, Rotoiti and Ōkāreka, originated around 140,000 years ago following a series of eruptions and caldera collapse events (Te Arawa Lakes Trust, 2023; Rotorua Lakes Council, 2024). These eruptions created deep depressions and dammed valleys that later filled with groundwater and rainfall, forming the interconnected hydrological system observed today. The region remains geothermally active, and some lakes, such as Rotorua and Rotoehu, receive geothermal inflows enriched with phosphorus, silica, and trace metals, naturally influencing water chemistry and productivity.

Subsequent land-use change including deforestation, pastoral farming, and urban development, has accelerated nutrient and sediment loading in several of the lakes, promoting eutrophication. Consequently, trophic states now range from oligotrophic systems to highly eutrophic systems, while thermal mixing regimes vary from monomictic to polymictic depending on depth and altitude (Bay of Plenty Regional Council, 2023). This variability provides a natural laboratory for understanding how

volcanic lake ecosystems respond to climatic, geological, and anthropogenic pressures. Projected increases in lake stratification under climate change may intensify nutrient cycling, metal mobilisation, and oxygen depletion, with implications for ecosystem health.

Within this system, Lake Ōkāreka occupies the western margin of the Ōkātina Caldera, between Lakes Rotorua and Tarawera. The lake covers approximately 3.4 km², has a mean depth of 20 m, and reaches 34 m at its deepest point (Rotorua Lakes Council, 2024). Its 19.6 km² catchment is roughly half forested, three-quarters of which is indigenous vegetation, while the remainder consists of pasture, exotic or invasive species, and residential land concentrated on the southern shore. Hydrologically, the lake is sustained by groundwater inflow, rainfall, and minor surface tributaries, and drains through a regulated outlet at Waitangi Springs to Lake Tarawera.

Historic nutrient enrichment from agriculture, sedimentation, and septic tank effluent led to declining water quality, prompting the development of the Lake Ōkāreka Catchment Management Plan in 2004 and subsequent restoration actions under the Arawa Lakes Programme (Bay of Plenty Regional Council, 2004; 2024). Measures such as wastewater reticulation to the Rotorua city treatment plant, farm nutrient management, and alum dosing have reduced phosphorus inputs and stabilised lake conditions. Ōkāreka remains mesotrophic, with a Trophic Level Index (TLI) of around 3.3, slightly above the target value of 3.0.

Culturally, Lake Ōkāreka is a tāonga (treasured) lake and is managed under kaitiakitanga (guardianship) principles. It supports diverse native fauna, including kōaro, kōura (*Paranephrops planifrons*; freshwater crayfish), kākahi (*Echyridella menziesii*; freshwater mussels), aquatic plants, and waterfowl. The surrounding forests and riparian zones strengthen ecological connectivity between terrestrial and aquatic habitats, while walking tracks and reserves highlight the lake's recreational and aesthetic value (RotoruaNZ, 2024; Rotorua Lakes Council, 2024).

Of particular ecological significance is the Millar Road Wetland (MRW) on the southern margin of the lake, a transitional ecosystem linking terrestrial vegetation with the lakes littoral zone (Department of Conservation, 2024; RotoruaNZ, 2024). This wetland complex of open water, emergent vegetation, and slow flowing stream channels

provides important habitat for invertebrates, native birds, and macrophytes, while filtering nutrients and trapping sediment before water enters the lake. In 2010, a fisheries survey that was carried out by the Bay of Plenty Regional Council (BOPRC) found a relatively abundant population of kōaro in the MRW and a second survey was completed in 2019 with similar results (Ian Kusabs & Associates, 2019). This population was found in an atypical habitat but may be important for metapopulation persistence in Lake Ōkāreka and connected systems. The MRW is an ideal location to study the ecology of this species and explore how habitat refugia, metapopulations and habitat connectivity might support freshwater biodiversity and resilience across the Arawa Lakes system.

1.9 Research aims and hypotheses

Historically, kōaro were abundant throughout the Arawa Lakes and formed an important component of customary māhinga kai for Te Arawa hapū. Over the twentieth century their numbers declined markedly, driven primarily by catchment modification (deforestation, agricultural intensification and sedimentation), hydrological alteration, and the introduction of fish species not traditionally found in the Te Arawa Lakes, notably introduced rainbow trout (*Oncorhynchus mykiss*) and the native smelt (*Retropinna retropinna*). These stressors have degraded spawning and rearing habitats, increased predation and competition, and fragmented formerly continuous migratory pathways. As a result, kōaro in the Arawa system now persist mainly as small, remnant populations confined to landlocked lakes and refugial habitats (Rowe, Smith & Grayling, 2008).

Kōaro are typically associated with cool, well oxygenated, forested streams and are widely regarded as sensitive to habitat degradation and salmonid predation. Ground-fed wetlands characterised by shallow vegetated margins, periodic low dissolved oxygen, and restricted hydrological connectivity would not traditionally be considered core habitat for this species. Such systems would be expected to support low densities of kōaro or function primarily as demographic sinks rather than key recruitment areas.

However, monitoring at the Millar Road wetland adjacent to Lake Ōkāreka identified a kōaro population in 2010 that remained relatively abundant when resurveyed in 2019. This persistence challenges assumptions regarding habitat suitability, predator limitation, and trophic structure for kōaro. Understanding how this population persists in a seemingly sub-optimal environment provides an opportunity to evaluate whether such wetlands may function as overlooked refugia within fragmented lake-stream networks under increasing climatic and biological pressures.

This study was conducted as part of Whakahohetia Ngā Wai Kāinga, a focus study within the Toitū Ngā Taonga Waimāori programme, which supports Te Arawa iwi and hapū in developing place-based adaptation strategies to enhance the resilience of culturally significant freshwater species under climate change. Within this context, the present research aimed to:

1. Characterise the population structure and seasonal demography of kōaro within the Millar Road wetland system;
2. Investigate trophic ecology and food-web dynamics to identify the key prey sources supporting this population; and
3. Evaluate the broader ecological implications of habitat flexibility for freshwater fish conservation in fragmented and climate-affected environments.

To address these aims, the following hypotheses were tested.

1.9.1 H1: Demographic function of the wetland

Isolated wetlands with restricted hydrological connectivity are commonly expected to function as demographic sinks, supporting transient individuals rather than resident populations. If the Millar Road wetland conforms to this expectation, kōaro abundance would reflect temporary occupancy, with recruitment and persistence occurring elsewhere in the lake system. Alternatively, if the wetland functions as a refuge habitat, it should support a predominantly resident adult population exhibiting seasonal persistence. Consistent with summer spawning (Young, 2002), juveniles would be expected between February and April, reflecting immigration from Lake Ōkāreka.

1.9.2 H2: Environmental filtering and trout limitation

In lake-stream systems containing trout, kōaro persistence is generally considered to be constrained by trout predation and competition, limiting their abundance in accessible habitats. If this dynamic governs the MRW system, trout presence would be expected to suppress kōaro occupancy. However, the ecological conditions of the wetland, including shallow vegetated habitat, variable dissolved oxygen and restricted hydrological connectivity, may act as an abiotic filter limiting trout establishment. If so, trout abundance should be low relative to more connected habitats, while kōaro persist within their broader tolerance range.

1.9.3 H3: Trophic structure and resource use

Fish inhabiting wetland systems are often assumed to rely predominantly on aquatic invertebrate production generated within the system. If aquatic prey resources are

abundant in the MRW, kōaro diets would be expected to reflect strong dependence on autochthonous aquatic prey. Alternatively, if aquatic prey availability is limited and kōaro exhibit trophic plasticity, individuals should rely substantially on terrestrial invertebrate inputs as a resource subsidy, demonstrating opportunistic feeding behaviour.

1.9.4 H4: Coexistence with common bully

In simplified or resource-limited habitats, sympatric benthic fish are expected to exhibit high dietary overlap, increasing the potential for interspecific competition. If such overlap occurs within MRW, kōaro and common bully would be predicted to share similar prey resources. Alternatively, competitive exclusion and limiting similarity are key tenets of coexistence theory that favor functionally dissimilar species by promoting resource partitioning (Pianka 1974, Schoener 1974). Thus, coexistence may be facilitated by trophic niche differentiation, with kōaro relying more heavily on terrestrial or other prey sources and common bully primarily exploiting aquatic benthic prey.

By testing these hypotheses, this study evaluates whether ground-fed wetlands, traditionally considered marginal habitats for galaxiids, may function as refugia under conditions of climate change and biological invasion. Demonstrating demographic persistence, environmental filtering of predators, and trophic flexibility would have important implications for culturally grounded conservation planning and restoration of freshwater ecosystems within the Arawa Lakes.

Methods

2.1 Study site and sampling design

This study was conducted in the Millar Road Wetland (MRW), a spring-fed wetland system located on the margins of Lake Ōkāreka in the Rotorua Lakes district, Aotearoa New Zealand (Figure 2). The wetland covers approximately 12.8 ha and is bounded by Millar Road to the northwest and by Lake Ōkāreka and remnant native bush to the southeast.

The wetland is currently undergoing ecological restoration. Vegetation is dominated by regenerating native wetland plants, shrubs, and ferns, alongside residual invasive woody species (*Salix* spp.). Most willows have been chemically treated, leaving standing trunks and dead branches that provide partial shade. Native understory regeneration is well underway and includes bird-dispersed shrub species such as karamū (*Coprosma robusta*) and makomako (*Aristotelia serrata*).

Previous fisheries surveys conducted by the Bay of Plenty Regional Council (BOPRC) identified kōaro within the Millar Road Wetland in 2010, with a subsequent survey in 2019 by Kusabs et al., confirming the presence of a relatively abundant population. These findings indicated that the wetland–stream system may provide important habitat for kōaro within the Lake Ōkāreka catchment.

Monthly fish sampling was conducted from February 2025 to January 2026. Sampling initially comprised 12 permanent trap sites (T1–T12) distributed throughout the stream–wetland system (Figure 2). These core sites were selected based on: (1) sufficient depth to fully submerge Gee’s minnow traps, and (2) the presence of flowing water to maximise capture probability for kōaro.

In April 2025, five additional sites (T13 - T17) were established to expand spatial coverage within the wetland. In July 2025, three further sites (TA - TC) were added in newly inundated areas associated with elevated winter water levels and suspected spring-fed inflows. These sites were selected opportunistically to capture seasonal habitat expansion during periods where the water table was high. The additional sites

improved spatial representation across the hydrologically dynamic wetland mosaic and contributed to a more comprehensive assessment of kōaro distribution and range use.

For quantitative analyses of abundance, occupancy, and habitat associations, the 12 core trap sites (T1 - T12) sampled consistently across all 12 months were used to maintain temporal comparability. Each trap deployed for a 24-hour period during a monthly sampling event was treated as a single sampling unit (hereafter referred to as a trap-month). Across the 12 core traps sampled monthly for 12 months, this resulted in 144 trap-month sampling units.

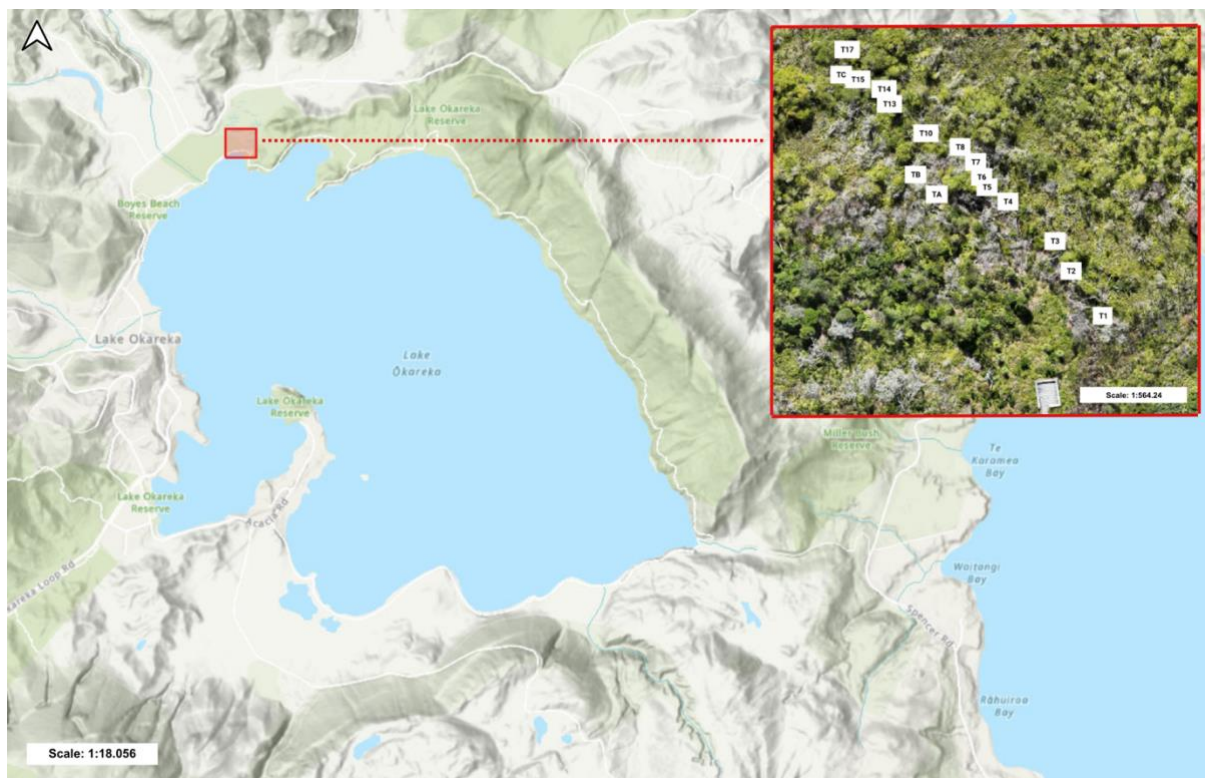


Figure 2: Location of the Millar Road Wetland within the Lake Ōkareka catchment (Rotorua Lakes district, New Zealand) and spatial arrangement of trapping sites. The main panel shows Lake Ōkareka and surrounding topography, with the Millar Road Wetland on the lake margin indicated by the red polygon; the dashed leader line links to the inset. The inset (high-resolution aerial imagery) maps the full trap network ($n = 20$), with individual traps labelled (T1–T17, TA–TC) and positioned along the stream-wetland ecotone to capture spatial variation in kōaro activity across the wetland mosaic.

2.2 Environmental conditions

I monitored dissolved oxygen (DO) and temperature continuously in the wetland. Two miniDOT loggers (PME Ltd, Vista, CA, USA) were deployed at sites T4 and T6, representing different micro-habitats within the stream-wetland system (Figure 3). These loggers recorded DO (mg/L) and temperature ($^{\circ}\text{C}$) at hourly intervals. Spot measurements of pH, conductivity (SPC), DO, and temperature were recorded using a YSI Pro2030 Dissolved Oxygen and Conductivity Meter (YSI Inc., Yellow Springs, OH, USA). pH was measured using an EC-PCTestr35 handheld probe (Eutech Instruments Pte Ltd, Paisley, UK).



Figure 3: Deployment of dissolved oxygen and temperature loggers within the wetland study reach. (Left) Loggers secured to a stake prior to installation at one of two sites. (Right) Placement of a logger at a monitoring site (T6) within the wetland system. Loggers recorded dissolved oxygen (mg L^{-1}) and temperature ($^{\circ}\text{C}$) at hourly intervals.

2.3 Kōaro trapping

At each site, one 3 mm mesh galvanised wire Gee's minnow trap was deployed overnight between the hours of 10 am to 10 am (24 hr *in situ*). The assembled traps were 42 cm long and 22.5 cm in diameter with a funnel entrance tapering to opening of 25 mm in diameter (Kusabs et al. 2019). Traps were situated parallel to the water flow (Figure 4) and attached to a tree or structure with rope. Sites were marked so that the same locations were used for monthly sampling. The traps were unbaited.



Figure 4: Gee's minnow trap deployment at a sampling site (T8) within the Millar Road Wetland from February 2025 to January 2026. Traps were positioned parallel to flow and secured to the bank. Each trap was left in situ for 24 hours during monthly sampling.

Upon retrieval, all captured organisms were identified to species level. Kōaro and common bullies were weighed using portable digital scales with an accuracy of ± 0.1 g. Standard lengths were measured to the nearest mm using a stainless-steel measuring board (Figure 5).



Figure 5: (Left) Total catch from a Gee's minnow trap at one site in Millar Road Wetland between February 2025 and January 2026. (Right) Individual kōaro length was measured to the nearest mm using a stainless-steel measuring board.

Northern Kōura (*Paranephrops planifrons*), found in Te Ika-a-Maui and the West Coast of Te Wai Pounamu, were measured using plastic callipers (± 0.1 mm) and sexed based on morphological characteristics (Figure 6). Kōura biomass was estimated using a power regression equation (Riordan, 2000) to estimate kōura wet weight where W is wet weight in g and L is OCL in mm:

$$W = 0.000648L^{3.0743}$$

Traps were retrieved one at a time and emptied into a plastic bucket with stream water. After identification and measuring, each specimen was returned to a recovery bucket with clean stream water. Once all individuals from the trap were processed, they were returned to the capture site.



Figure 6: Kōura (*Paranephrops planifrons*) orbit-carapace length (OCL) measurement used at Millar Road Wetland, Reproduced from NIWA (n.d.). OCL is defined as the linear distance from the posterior margin of the orbital cavity to the posterior margin of the carapace and is commonly used as a standard size metric in freshwater crayfish studies.

2.4 eDNA sampling

Environmental DNA (eDNA) was collected from the stream-wetland at site T4 on the 21st February 2025 using the six-replicate method recommended by Wilderlab (Wellington, NZ). Sample collection followed the detailed procedures in Wilkinson et al. (2024). A Wilderlab kit provided six 1.2 μm pore size, 30 mm diameter cellulose acetate filters, two 60 mL collection syringes, and six 3 mL syringes pre-loaded with 350 μL of DNA/RNA Shield preservation buffer (Zymo Research). Samples were obtained by drawing water into the 60 mL syringe and then pushing it through a filter up to 20 times (or a maximum of 1000 mL) until the filter clogged, with the exact volume filtered carefully recorded. After expelling excess water, the 3 mL syringe was used to add the preservative to the filter. This process was repeated for all six filters at site T4 to ensure robust replication and maximise the detection of kōaro and other species of interest.

Following collection, the filters were sent to WilderLab for DNA extraction, Polymerase Chain Reaction (PCR) amplification, sequencing, and bioinformatic processing, consistent with the methodology described in Wilkinson et al. (2024). This approach utilized DNA metabarcoding, a high-throughput sequencing (HTS) technique.

Metabarcoding involves the simultaneous taxonomic identification of multiple organisms by targeting and amplifying specific marker genes present in the environmental DNA. This process generates millions of sequences that are subsequently used to identify Operational Taxonomic Units (OTUs) or Amplicon Specific Variants (ASVs), thereby providing a comprehensive survey of the aquatic biodiversity present in the eDNA sample. Multiple assays were used, including the 16S gene region relevant to fish, and the CO1 gene region relevant to aquatic insects.

2.5 Tagging and fin clipping

I used Passive Integrated Transponder (PIT) tags to mark individual kōaro, so that I could identify them on recapture. This ability would help estimate the kōaro population size and assess seasonal movements within the stream-wetland system. PIT tags are widely used to electronically identify and track individual animals in ecological research and wildlife management, particularly for monitoring fish, but also for a wide range of other animals from birds and bats to insects (Cooke et al., 2013). A PIT tag is a tiny, glass-encapsulated microchip with a unique alphanumeric code. It is a "passive" system because the tag does not have a battery but is instead activated by a handheld scanner to identify individual fish during routine monitoring.

My methods closely followed those described in Allan et al. (2018). Captured fish on the 26th of September were first sedated using 2-Phenoxyethanol at an appropriate dose. Fish were held in the sedative until paired fin movement ceased, the ability to maintain equilibria was lost, and fish had no response to external stimuli. Each tagged fish received a Mini Bio-Glass Radio-frequency identification (RFID) tag (8.5 mm long × 1.4 mm in diameter; 0.52 g; SwissPlus ID Group Pty Ltd., Switzerland) implanted via a sterile, pre-loaded 25 mm long cannula with an outer diameter of 1.8 mm (SwissPlus ID Group Pty Ltd). The tagging procedure (Figure 7) involved a sedated fish being placed on its back onto a wetted towel whilst being gently held in position by the operator. The needle was inserted into the midpoint of the abdominal cavity to the right of the ventral midline, as per McEwan and Joy (2011), and the tag was injected towards the rear of the fish. To avoid repeated stress on individual fish, I removed a small piece of the caudal fin from each fish using sterilized dissecting scissors at the same time. The fin clip was intended for stable isotope analysis (SIA) explained in the section below. Individual fin clips were placed in a labelled 1.5 mL microtube, stored

on ice, and frozen at -20 °C upon return to the laboratory. Tagged and clipped fish were allowed to recover in an aerated bucket with clean stream water until the effects of the sedative had diminished. They were then returned to the site where they were captured. In total, 27 fish were tagged and clipped. Three kōaro that were caught were not tagged or clipped due to their small size. A sterile technique was used for tagging and clipping fish, where all surgical equipment was sterilized prior to and after the tagging of each fish. This approach is consistent with the University of Waikato's Standard Operating Procedure (SOP) for tagging fish (SOP 8).

The tagging and fin clipping was approved by the University of Waikato Animal Ethics Committee under Protocol 1241: "Monitoring of a kōaro (*Galaxias brevipinnis*) population using passive integrated transponder (PIT) tags and fin clips for further analysis".

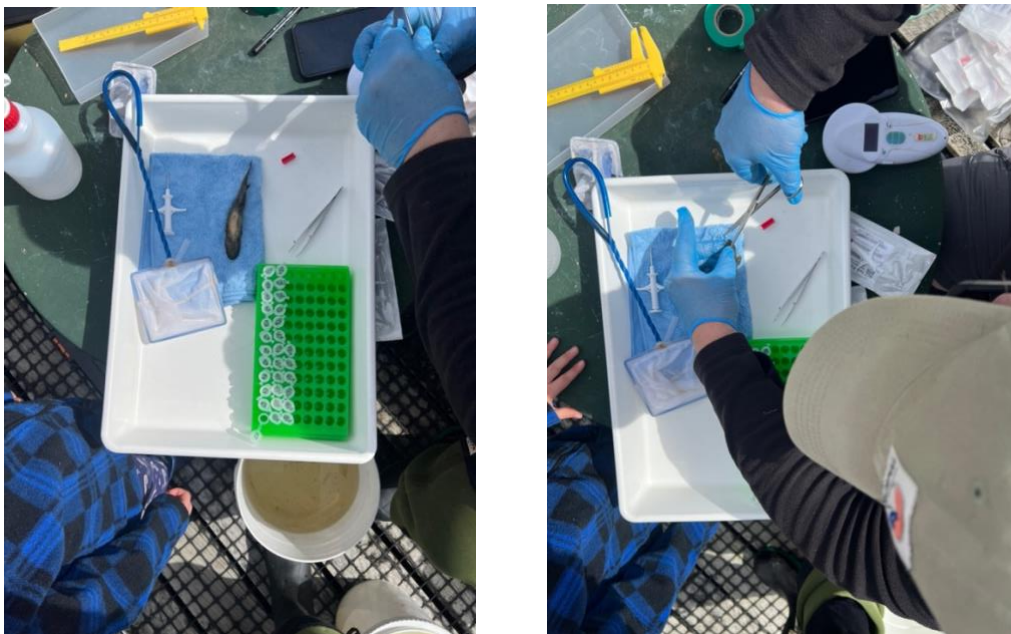


Figure 7: Field processing setup for passive integrated transponder (PIT) tagging and fin-clip collection at Millar Road Wetland in September 2025 ($n = 27$). Following 2-Phenoxyethanol sedation, kōaro were transferred to a sterile tray. Individuals were PIT-tagged and a small fin clip was removed using sterile instruments. Each fin clip was placed into a uniquely labelled microcentrifuge tube for stable isotope analysis.

2.5.1 Recapture

On subsequent sampling rounds, each kōaro was visually assessed for evidence of a fin clip during weighing and measuring (Figure 8). Each individual was scanned using a handheld reader (V8BT RT100, SwissPlus ID Pty Ltd, Vienna, Austria) to identify the

tag number. If a tag was detected, the ID was recorded next to the individual. It was also noted if a fin clip was present, but no tag was found.



Figure 8: Identification of individuals for passive integrated transponder (PIT) tagged kōaro at Millar Road Wetland between October 2025 and January 2026. On each sampling occasion, individuals were visually inspected for fin clips (Right) and scanned using a handheld PIT tag reader (V8BT RT100, SwissPlus ID Pty Ltd, Vienna, Austria). Detected tag numbers were recorded for growth and movement analyses (Left). Individuals exhibiting a fin clip, but no detectable PIT tag were noted separately.

2.6 Stable isotope analysis

2.6.1 Collection

In addition to the 27 kōaro fin clips described above, 10 kōura and 16 common bullies caught during the September sampling round were frozen and processed for stable isotope analysis.

Larval and nymphal specimens of two insect species were recovered from the minnow traps (the leptocerid caddisfly *Triplectides dolichos* and corduliid dragonfly *Hemicordulia australiae*). Semi-quantitative sampling was also used to collect putative macroinvertebrate prey. Using the National Environmental Monitoring Standards (NEMS) protocol (NEMS 2022), a single composite “kicknet” sample (500 µm mesh, 30 cm width) was collected for further processing. At the same time, basal resources were collected. These included putative food sources from autochthonous production and allochthonous inputs. All samples were placed in labelled containers or sealable plastic bags, stored on ice, and frozen at -20 °C upon return to the laboratory.

On the 25th of October, an ultra-violet (UV) light-emitting diode (LED) light trap was set overnight at Site T6 to capture putative terrestrial insects that form prey for kōaro. Two plastic white trays were filled with 1 L of ultrapure water with 5 mL of dishwashing liquid to break the surface tension. Upon each white tray a single UV LED strip was placed facing downwards, each connected to light-sensitive diode switch, which were both in turn connected to a single 12.8 V Lithium battery using a Universal Serial Bus (USB) connector fitted with alligator clips. The light trap was active from dusk to dawn, and the following morning invertebrates in the trays were sorted in the field to order or morphospecies. Samples were placed in plastic containers, stored on ice, and frozen at -20 °C upon return to the laboratory.

2.6.2 Processing

Stable isotope samples were processed following standard laboratory protocols for aquatic food-web studies. Frozen macroinvertebrates were thawed and identified to the lowest practicable levels using standard guides (Winterbourn et al., 2006). All remaining material collected in the field (including basal resources and fish) were thawed, sorted, cleaned, and transferred into individually labelled trays for drying. When individuals were too small to yield enough mass for isotope analysis (e.g. chironomids), multiple morphospecies were pooled. Each item or pooled sample was assigned a unique code (e.g., K1, BR4, CB1) as recorded in the *Temporary_location* and *Code* fields of the sample log. Each tray was dried for 24 hours at 60 °C, dried material was homogenised where appropriate and final material was transferred to microtubes and weighed to provide sample mass. Each microtube received a unique final SIA code according to its precise location in the lab trays which was recorded alongside the temporary tray label (Appendix D Stable Isotope Analysis)

Basal resources included filamentous algae, biofilm, fine benthic organic matter (FBOM), pondweed, fern tissue, and detritus. Invertebrates were separated to the lowest practical taxonomic level (Order or morphospecies). Invertebrate taxa included Diptera, Trichoptera, Hemiptera, Mollusca. Kōura were measured (occipital carapace length), tissue was collected from the tail, dried and ground for analysis. Common Bullies caudal fins were clipped, and tissue samples were also taken, dried and ground for analysis. Kōaro fin clips were taken from the caudal fin during PIT-Tagging, dried and sent for analysis. Specimens from two insect orders (Trichoptera and Lepidoptera)

that were caught in the light traps were sorted to family level or lower using taxonomic guides (Hoare et al., 2011, Winterbourn et al., 2006). All samples were dried for 24 hours at 60 °C and then ground before being placed in a 1.5 mL microtube for further analysis.

2.6.3 Analysis

Stable isotope analyses were carried out on a DELTA V Plus continuous flow stable isotope ratio mass spectrometer linked to a Flash 2000 elemental analyser using a MAS 200 R autosampler (Thermo-Fisher Scientific, Bremen, Germany) at the Earth Sciences New Zealand Environmental and Ecological Stable Isotope Facility in Wellington, New Zealand. Low N-containing samples were analysed on a DELTA Q continuous flow stable isotope ratio mass spectrometer linked to an EA-Isolink elemental analyser using a MAS PLUS autosampler (Thermo-Fisher Scientific, Bremen, Germany).

Isotope ratios, R (i.e., $^{13}\text{C}:^{12}\text{C}$ and $^{15}\text{N}:^{14}\text{N}$), were estimated relative to the ratios of their respective standards and are expressed in per mille delta notation (Eq. 1):

$$\delta^1 = \left[\frac{R_{\text{sample}}}{R_{\text{standard}}} + 1 \right] \times 1000 \quad (1)$$

where δ^1 is either ^{13}C or ^{15}N , and R is the ratio of either one to the respective lighter isotope (^{12}C or ^{14}N). Reference materials, including the international standards USGS 40 (L-glutamic acid) and IAEA N2 (ammonium sulfate), were used to determine sample isotopic values. The analytical error (i.e., 1 SD of the lab standard L-glutamic acid) associated with the $\delta^{13}\text{C}$ and $\delta^{15}\text{N}$ sample runs was estimated at 0.01‰ ($\delta^{13}\text{C}$) and 0.04‰ ($\delta^{15}\text{N}$).

2.7 Data analysis

All statistical analyses were conducted in R (R Core Team, 2022). Data manipulation and visualisation were performed using the tidyverse suite of packages.

2.7.1 CPUE, biomass and size structure

Catch per unit effort (CPUE) was calculated as the number of individuals captured per trap per 24-hour deployment (trap-month). Biomass per trap was calculated as the summed mass (g) of all individuals captured within a trap-month.

Because trap catches were zero-inflated and right-skewed, CPUE and biomass were summarised using medians and interquartile ranges (IQR), alongside monthly means with 95% confidence intervals calculated across traps ($n = 12$ traps per month).

Seasonal size structure was examined by summarising monthly length (mm) and mass (g) distributions. Occupancy was calculated as the proportion of trap-month sampling units in which a species was detected at least once (presence/absence). Where model-based comparisons were used, occupancy was analysed using binomial generalised linear mixed models with trap included as a random intercept to account for repeated sampling of fixed locations.

2.7.2 Habitat associations

Associations between kōaro presence and environmental predictors were examined using binomial generalized linear mixed models (GLMMs). The response variable was kōaro presence/absence at the trap-month level. Fixed effects included habitat variables (shade, raupō cover, aquatic vegetation cover, grass presence) and co-occurring taxa (trout, bully, kōura presence). Trap and month were included as random intercepts to account for spatial and temporal non-independence.

2.7.3 Recapture analyses

PIT-tagged kōaro recaptured during subsequent sampling events were paired by tag number. Growth was quantified as change in total length (mm) and mass (g) between capture events. Growth rates (mm day^{-1} and g day^{-1}) were calculated by dividing change in size by days at liberty.

Linear regression models were used to examine whether growth rate varied with initial size or time at liberty. Movement distances were calculated as the linear distance

between capture and recapture locations. Stepwise displacement was defined as the distance between successive recaptures for individuals captured more than twice.

To estimate the kōaro population size within the study reach, a Lincoln–Petersen mark–recapture model was applied:

$$\hat{N} = \frac{M \times C}{R}$$

where: \hat{N} = estimated population size, M = number of kōaro marked during the initial sampling event in September, C = total number of kōaro captured during the second sampling event and R = number of marked kōaro recaptured during the second sampling event.

The Lincoln–Petersen estimator assumes a closed population between sampling events, no mark loss, equal capture probability of marked and unmarked individuals, and random mixing of marked individuals within the population.

Recapture length–mass relationships were examined using a non-linear power function fitted with `nls()` and the `NLS.powerCurve` self-starting model. Model diagnostics (parameter estimates, 95% confidence intervals, and pseudo- R^2) were used to evaluate fit. Expected mass values derived from this model were used to compute individual condition indices (% expected mass), to evaluate variation in body condition among recaptured kōaro.

2.7.4 Length-weight relationships and body condition

The length-weight relationship for kōaro was modelled using the power function:

$$W = aL^b$$

where W is mass (g) and L is total length (mm). Parameters were estimated using non-linear least squares (`nls`). Model assumptions were assessed via visual inspection of residuals and Q–Q plots.

Fulton’s condition factor ($K = 100 \times W/L^3$) was not used because it assumes isometric growth ($b = 3$) and a relatively deep-bodied morphology. Kōaro (*Galaxias brevipinnis*) are elongate galaxiids that exhibit allometric growth ($b \neq 3$), meaning Fulton’s K can

bias condition estimates across size classes. Instead, body condition was assessed relative to the national length–weight relationship for kōaro reported by Jellyman et al. (2013).

Expected mass (\hat{W}) was calculated from this relationship, and condition was expressed in two complementary ways. Relative weight (Wr) was calculated as:

$$Wr = 100 \times \frac{W}{\hat{W}}$$

where W is observed mass (g) and \hat{W} is expected mass at a given total length (mm). Log-residual condition was calculated as:

$$\log(W) - \log(\hat{W})$$

which represents the deviation of an individual's mass from the expected value on a log scale. Mean relative weight was compared against 100 using one-sample t-tests and Wilcoxon signed-rank tests. Linear regression was used to examine relationships between condition and fish length, and between condition and month.

Juvenile kōaro were classified based on established size thresholds. Differences in juvenile proportion among months were assessed using binomial generalized linear models.

2.7.5 Hydrology and environmental drivers

Associations between lake level and CPUE of kōaro and trout were examined using generalized linear mixed models. Trap was included as a random effect where analyses were conducted at the trap level. January 2026 was excluded from hydrology analyses due to missing lake level data.

Spearman's rank correlation was used to examine the relationship between rainfall and lake level.

Temperature and dissolved oxygen time series were summarised using daily mean, minimum, and maximum values. Temporal trends were visualised using LOESS smoothing. Linear regression was used to examine relationships between water temperature and dissolved oxygen concentration.

2.7.6 Comparison of March 2019 and March 2025

Historic kōaro data from March 2019 (Kusabs et al., 2019) were compared with data collected in March 2025.

Total length distributions were compared using Welch's t-tests (log-transformed where necessary) and Wilcoxon rank-sum tests due to non-normal distributions.

Because the 2019 dataset contained only length measurements, mass was estimated using the 2025 fitted length-weight power function. Relative abundance between years was compared using trap-level CPUE modelled with a negative binomial generalized linear model (Count ~ Year) to account for overdispersion in count data.

2.7.7 Analysis of stable isotope data

I assessed differences in trophic niches (the 'isospace') using stable isotope analysis (SIA) to test the hypothesis that kōaro (*Galaxias brevipinnis*) are partitioning food resources to coexist with common bully (*Gobiomorphus cotidianus*) in the Millar Road Wetland (MRW).

To evaluate the trophic diversity and overlap of each fish species present in MRW I used the 'SIBER' R package (Jackson and Parnell, 2023). This approach estimated the Standard Ellipse Area (SEA) for each fish species using Bayesian inference techniques. The model used 300,000 iterations for the chain length, 200,000 iterations for the 'burn-in', thinning at the hundredth subsample, and three Markov Chain Monte Carlo (MCMC) chains to estimate the trophic diversity (SEA) for each species. The approach also included the sample size-corrected standard ellipse area (SEA-c) using maximum-likelihood estimation, an approach less susceptible to sample size and extreme values (Jackson, et al. 2011). To test whether one species ellipse was smaller or larger than the others, I calculated the probability that its posterior distribution is smaller (or larger). This was achieved by comparing each pair of posterior draws for

both species and determining which is smaller in magnitude. The proportion of draws that were smaller were the calculated as a direct proxy for the probability that one species posterior distribution (of ellipse size) was smaller than the other (Jackson and Parnell 2023). I also estimated the degree of trophic overlap in each species standard ellipses (SEA-c). This overlap is the area ($\%^{2}$) contained by the shape that lies within the overlapping region (Jackson & Parnell, 2023). I calculated a distribution of overlap based on the posterior distributions of the fitted ellipses with 100 draws and presented the mean value for the proportion of overlap (± 1 standard deviation).

I used the Bayesian mixing-model R package 'MixSIAR' to estimate resource flows to fish in the MRW food web (Stock et al. 2018, Stock and Semmens 2016). Two mixing models were used. The first model tested the dietary contribution of four prey sources to fish. The prey sources were the New Zealand mud snail (*Potamopyrgus antipodarum*), midge larvae including dipterans from the Chironomidae, Dixidae, Simuliidae and Limoniidae, adult caddisfly including representatives from the Leptoceridae and Oeconesidae, and moths including representatives from the Oecophoridae and Noctuidae. The second model use putative basal resources to track the contribution of different carbon sources (autochthonous vs allochthonous carbon). The putative food resources (e.g., midge larvae) were pooled into ecologically meaningful groups to improve model performance (Nielsen et al. 2018). Autochthonous basal resources included biofilms, filamentous algae (Chlorophyta), and the pondweed *Potamogeton cheesemanii*. Allochthonous basal resources included fine benthic organic matter (FBOM) and coarse particulate organic matter (CPOM) from a tree (*Salix* sp.), ground fern (*Blechnum novae-zelandiae*), and raupō (*Typha orientalis*). Trophic enrichment factors (TEF) values for fish were calculated from my data following Caut et al. (2009). I used mean (± 1 standard deviation) TEF values of $3.05 \pm 0.53\text{‰}$ ($\delta^{13}\text{C}$) and $2.52 \pm 0.41\text{‰}$ ($\delta^{15}\text{N}$). For each model, the 'very long' settings were used for the chain length 1,000,000 iterations), burn-in (500,000 iterations), thinning (500), and number of Markov chain Monte Carlo (MCMC) chains used (3) to estimate mean dietary contributions of resources to fish. Both models met expectations for the Gelman-Rubin (all variables < 1.05) and Gweke diagnostics ($\sim 5\%$ exceeding z-score ± 1.96) as described by Stock and Semmens (2016).

Results

3.1 Physical environment

3.1.1 Habitat

Principal Component Analysis (PCA) of four habitat variables revealed strong gradients in vegetation structure among all 20 trap locations (Figure 9). The first principal component (PC1) explained 52.1 % of total variation and described a primary gradient from macrophyte-dominated habitats (characterised by higher raupō and aquatic vegetation cover) to more shaded habitats. The second principal component (PC2) accounted for 26.5 % of variation and represented a gradient from aquatic vegetation-dominated sites to areas characterised by higher grass cover.

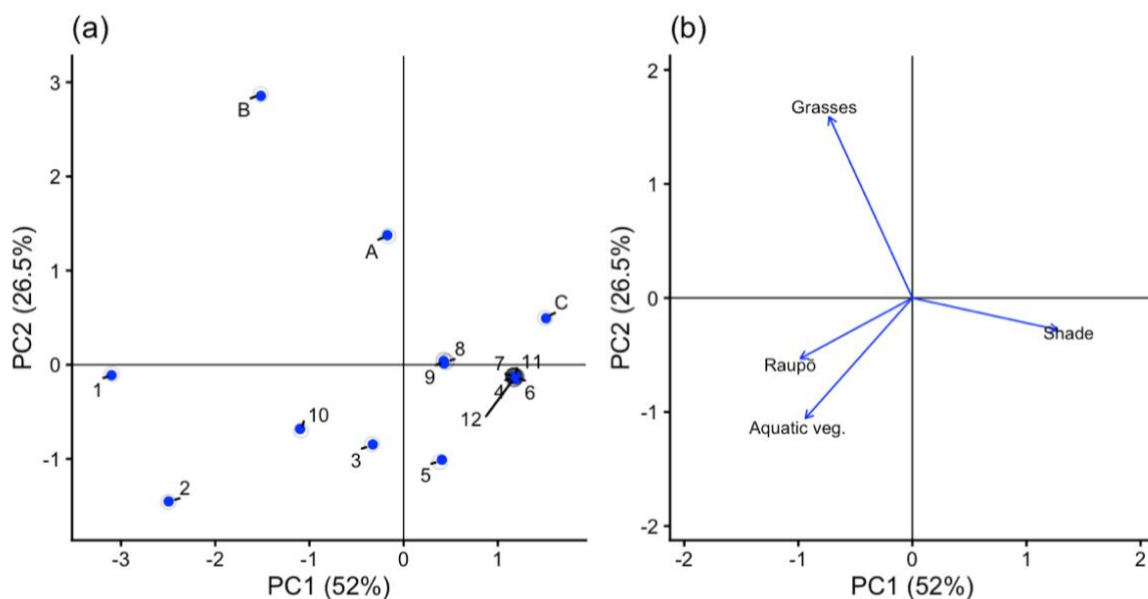


Figure 9: Principal Component Analysis (PCA) of habitat characteristics measured at the initial trap locations ($n = 20$; traps 1–17 and A–C). (a) Trap scores plotted along the first two principal components. (b) Variable loadings showing the direction and relative contribution of habitat predictors to each principal component. PC1 explained 52.1 % of total habitat variation and represented a gradient from macrophyte-dominated habitats (raupō and aquatic vegetation) to more shaded habitats. PC2 explained 26.5 % of variation and described a gradient from aquatic vegetation-dominated sites to grass-dominated habitats. Together, the first two components accounted for 78.5 % of total variation in habitat structure.

Together, PC1 and PC2 explained 78.5 % of total habitat variation, indicating that habitat structure among traps was largely captured by two dominant vegetation gradients. Some trap locations shared identical PCA scores, reflecting repeated combinations of ordinal habitat classifications across sites.

Raupō cover exhibited strong spatial structuring across the 12 initial trap locations (Figure 10). Most trap locations recorded little to no emergent raupō (class 0), whereas higher raupō classes (2–3) were concentrated at a small number of downstream locations. The highest cover values were spatially clustered, rather than evenly distributed across the wetland, indicating heterogeneity in emergent vegetation structure along the longitudinal axis of MRW.

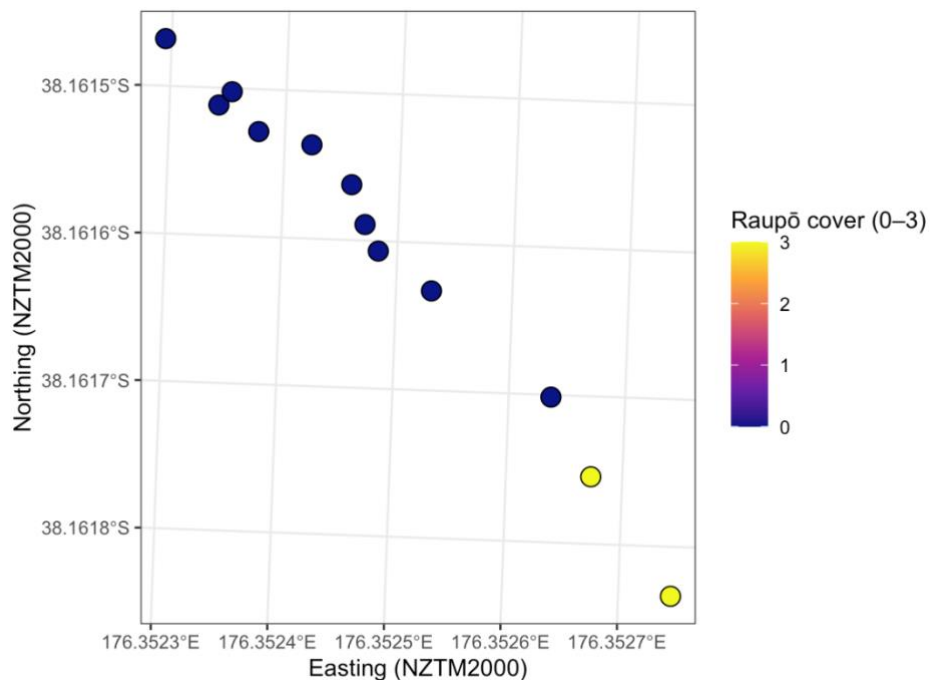


Figure 10: Spatial distribution of raupō (*Typha orientalis*) cover across the 12 initial Gee's minnow trap locations in the Millar Road Wetland. Points represent trap locations in NZTM2000 coordinates. Colour indicates raupō cover class (0–3), where 0 = absent and 3 = dense cover. Raupō was absent from most upstream and mid-wetland traps and was concentrated in the downstream section, indicating strong spatial heterogeneity in emergent vegetation structure.

3.1.2 Hydrology

Monthly rainfall showed a moderate positive association with mean lake level (Spearman $\rho = 0.48$), but this relationship was not statistically significant ($p = 0.19$).

3.1.3 Physiochemical

Logger-derived summaries shown in Figure 11 indicated similar thermal conditions at both monitoring sites (T4 and T6), with mean daily temperatures of approximately 10.9 °C at Logger One and Logger Two (overlapping 95 % confidence intervals). Temperature was relatively stable throughout the deployment period, with mean daily values ranging from ~6.1–15.4 °C; Logger One recorded higher episodic daily maxima (up to ~20.0 °C) than Logger Two (up to ~15.3 °C).

Mean daily dissolved oxygen (DO) was moderate at both loggers (Logger One: ~6.42 mg L⁻¹; Logger Two: ~6.19 mg L⁻¹), although Logger Two showed greater variability and lower daily minima, with minimum DO reaching ~2.09 mg L⁻¹ (Logger One minimum: ~2.52 mg L⁻¹). Across the monitoring period, mean pH was circumneutral (6.91) and mean specific conductivity (SPC) was 100.62 $\mu\text{S cm}^{-1}$, consistent with moderately mineralised, groundwater-influenced conditions. Overall, these data suggest broadly similar physicochemical conditions between sites, with more pronounced low-oxygen events at Logger Two.

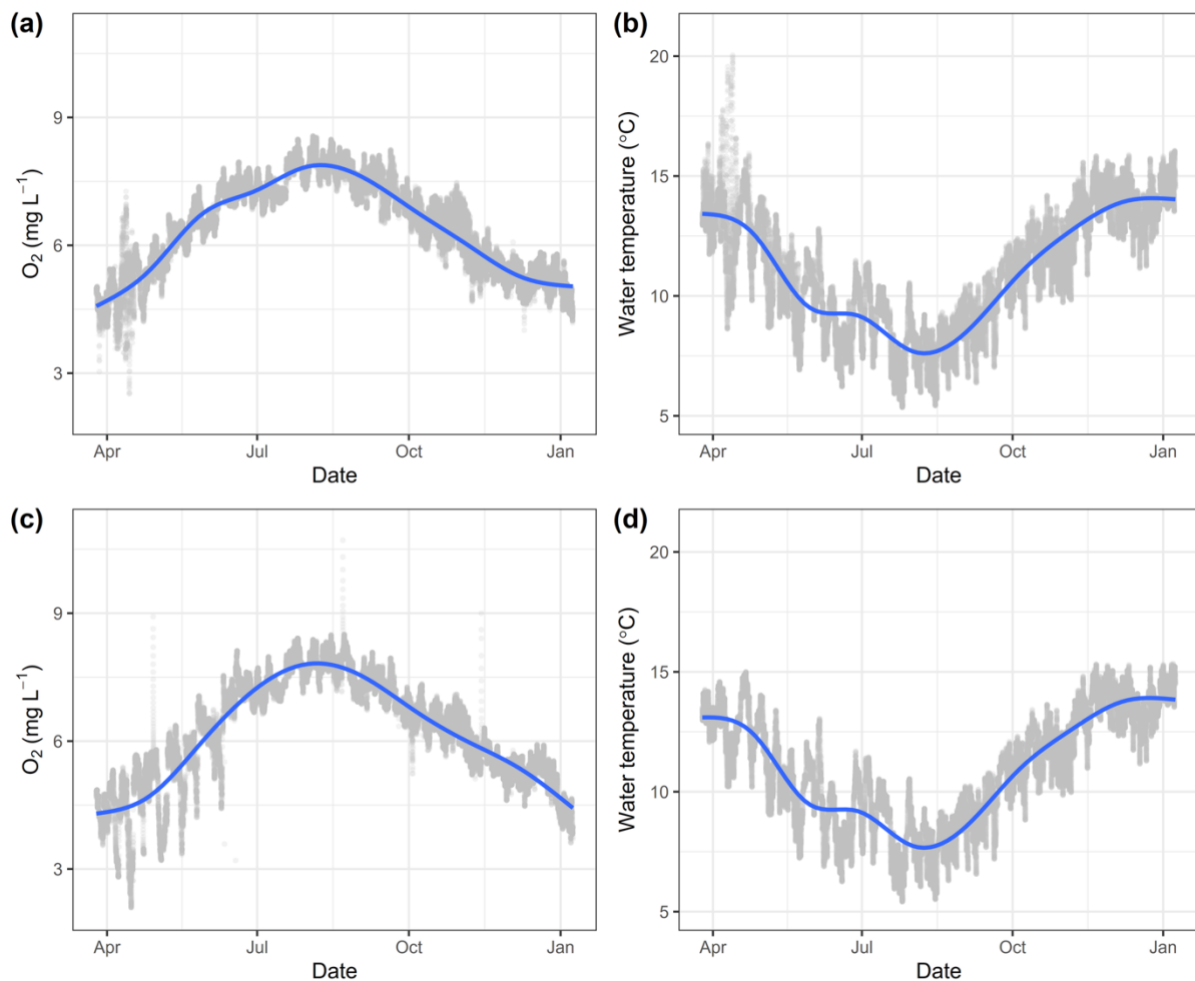


Figure 11: Temporal variation in dissolved oxygen concentration and water temperature recorded at two monitoring sites in the Millar Road wetland between April 2025 and January 2026. Panels (a) and (c) show dissolved oxygen (O_2 , $mg\ L^{-1}$) time series for Logger One and Logger Two, respectively, while panels (b) and (d) show corresponding water temperature ($^{\circ}C$) time series. Grey points represent individual logger measurements, and blue lines indicate smoothed trends (LOESS). Both sites exhibited strong seasonal patterns, with higher temperatures and dissolved oxygen concentrations during spring and summer and lower values during winter. Overall thermal conditions were similar between sites, although Logger One recorded higher episodic temperature maxima, while Logger Two experienced more pronounced low dissolved oxygen events.

Water temperature was negatively associated with dissolved oxygen concentration at both monitoring sites (Figure 12). Linear regression indicated a clear inverse relationship, with dissolved oxygen declining as temperature increased across the observed range ($\sim 6 - 16\ ^{\circ}C$). In particular, lower dissolved oxygen concentrations ($< 4\ mg\ L^{-1}$) were more frequently observed at Logger Two, whereas Logger One exhibited comparatively tighter clustering of values around the regression trend.

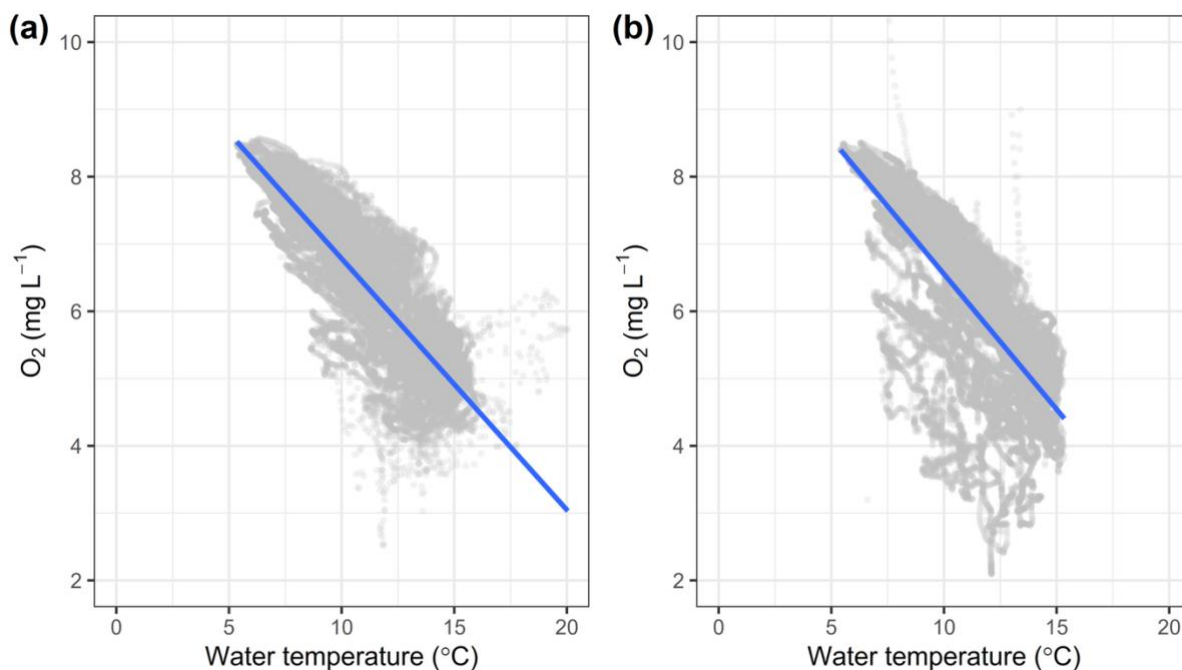


Figure 12: Relationship between water temperature ($^{\circ}\text{C}$) and dissolved oxygen concentration (O_2 , mg L^{-1}) at two monitoring sites in the Millar Road wetland. Panel (a) shows Logger One and panel (b) shows Logger Two. Grey points represent individual paired temperature and dissolved oxygen observations, and blue lines indicate fitted linear regressions. At both sites, dissolved oxygen declined with increasing temperature, reflecting the expected inverse relationship between temperature and oxygen solubility. Logger Two exhibited greater variability in dissolved oxygen across the observed temperature range, including more frequent low-oxygen conditions.

3.2 Community overview

A total of 2,007 individual kōaro (*Galaxias brevipinnis*), kōura (*Paranephrops planifrons*), common bully (toi toi, *Gobiomorphus cotidianus*) and rainbow trout (*Oncorhynchus mykiss*) were caught over 12 sampling occasions between February 2025 and January 2026 at 20 sites in the Millar Road Wetland (MRW). Over half of these individuals (1267) were caught at the initial 12 sites used for trapping.

The fish assemblage by abundance was dominated by common bullies, which accounted for the largest proportion of total catch and exhibited the highest mean Catch Per Unit Effort (CPUE) over the initial 12 traps (Table 1) and all 20 traps (Table 2).

Kōaro were widespread throughout the wetland, occurring in 72 - 74 % of trap-months, with a mean CPUE of two individuals per trap-month. Kōura were detected less frequently and at lower densities, while trout occurred in fewer than 7 % of trap-months across all traps and fewer than 3 % within the initial 12 traps (Table 2).

Median CPUE values were lower than mean CPUE for all species, reflecting zero-inflated and highly skewed catch distributions. Trout median CPUE was zero, indicating absence from most trap-months. For kōaro, median CPUE indicated that a typical trap-month yielded one to two individuals, despite occasional higher catches.

Table 1: Species composition at Millar Road wetland, Lake Ōkāreka. Data were derived from the initial 12 sites sampled monthly from February 2025 to January 2026 using Gee’s minnow traps. Values summarise total captures, proportional contribution to total catch (%), Occupancy (percentage of sampling occasions in which a species was detected) and mean catch per unit effort (CPUE; individuals per trap-month \pm one standard deviation, SD). Median CPUE and interquartile range (IQR) are presented to account for zero-inflated and skewed catch distributions.

Species	Total (n)	% of total catch	% Occupancy	Mean CPUE (\pm SD)	Median CPUE (IQR)
Kōaro	313	19.2	73.8	2.22 \pm 2.13	2 (3)
Common Bully	1,244	76.2	87.2	8.82 \pm 15.94	4 (8)
Kōura	69	4.2	33.3	0.49 \pm 0.93	0 (1)
Rainbow Trout	7	0.4	2.8	0.05 \pm 0.32	0 (0)

Table 2: Species composition at Millar Road wetland, Lake Ōkāreka. Data were derived from all 20 sites sampled monthly from February 2025 to January 2026 using Gee’s minnow traps. Values summarise total captures, proportional contribution to total catch (%), Occupancy (percentage of sampling occasions in which a species was detected) and mean catch per unit effort (CPUE; individuals per trap-month \pm one standard deviation, SD). Median CPUE and interquartile range (IQR) are presented to account for zero-inflated and skewed catch distributions.

Species	Total (n)	% of total catch	Occupancy (%)	Mean CPUE (\pm SD)	Median CPUE (IQR)
Kōaro	419	20.9	71.9	2 \pm 2.01	1.5 (3)
Common Bully	1,403	69.9	82.4	6.68 \pm 13.5	3 (5.75)
Kōura	162	8.1	42.4	0.77 \pm 1.24	0 (1)
Rainbow Trout	23	1.1	6.2	0.11 \pm 0.46	0 (0)

3.3 Kōaro in the Millar Road Wetland (MRW)

3.3.1 Kōaro catch per unit effort (CPUE)

The total observations of kōaro over 12 sampling dates was 419 with 313 observed at the initial 12 sites. Catch per unit effort (CPUE) was calculated as the mean number of kōaro captured per trap per sampling occasion ($n = 12$ traps, Figure 13).

Mean CPUE ranged from 1.17 kōaro trap⁻¹ in October (95 % CI: 0.458 – 1.87, $n = 12$ traps) to 2.92 kōaro trap⁻¹ in February (95 % CI: 0.595 – 5.24, $n = 12$ traps). Intermediate values were observed in other months, indicating temporal variation in kōaro abundance within the sampled reach.

These differences in CPUE corresponded to total monthly catches of 14 kōaro in October and 35 kōaro in February across the 12 traps respectively, providing a practical context for the observed variation in abundance.

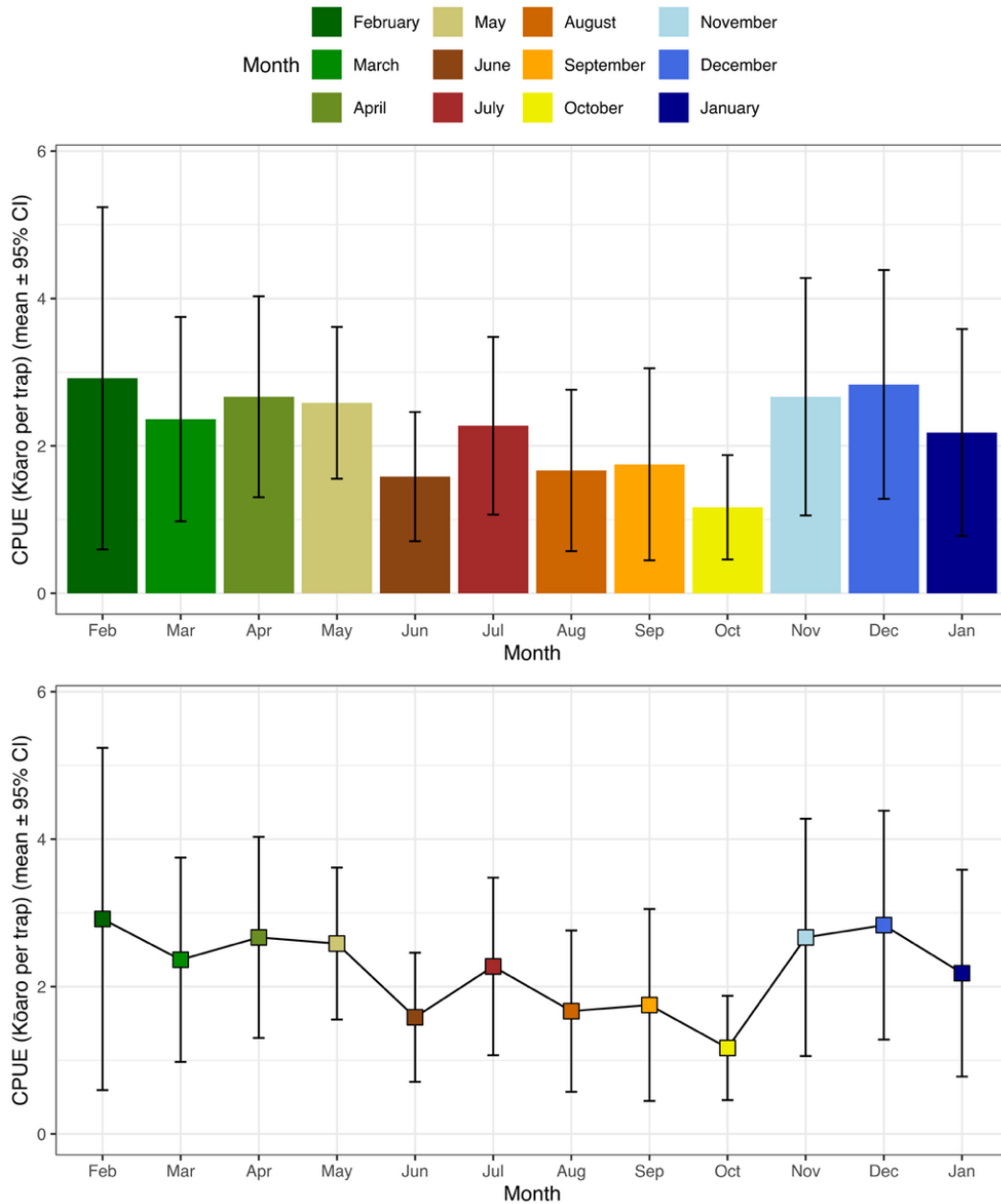


Figure 13: Monthly variation in mean kōaro (*Galaxias brevipinnis*) catch per unit effort (CPUE; mean kōaro per trap, per sampling occasion) in the Millar Road wetland. Data were derived from the initial 12 Gee’s minnow traps sampled monthly from February 2025 to January 2026. Error bars indicate the 95 % confidence interval (CI).

3.3.2 Kōaro body length

Individual kōaro lengths measured across the study ranged from 39 mm to 160 mm, indicating the presence of multiple size classes within the population (Figure 14). Overall mean length was 103.2 mm (SD = 22.0 mm), with a median length of 106 mm. The smallest individual was recorded in March, while the largest individual was captured in October.

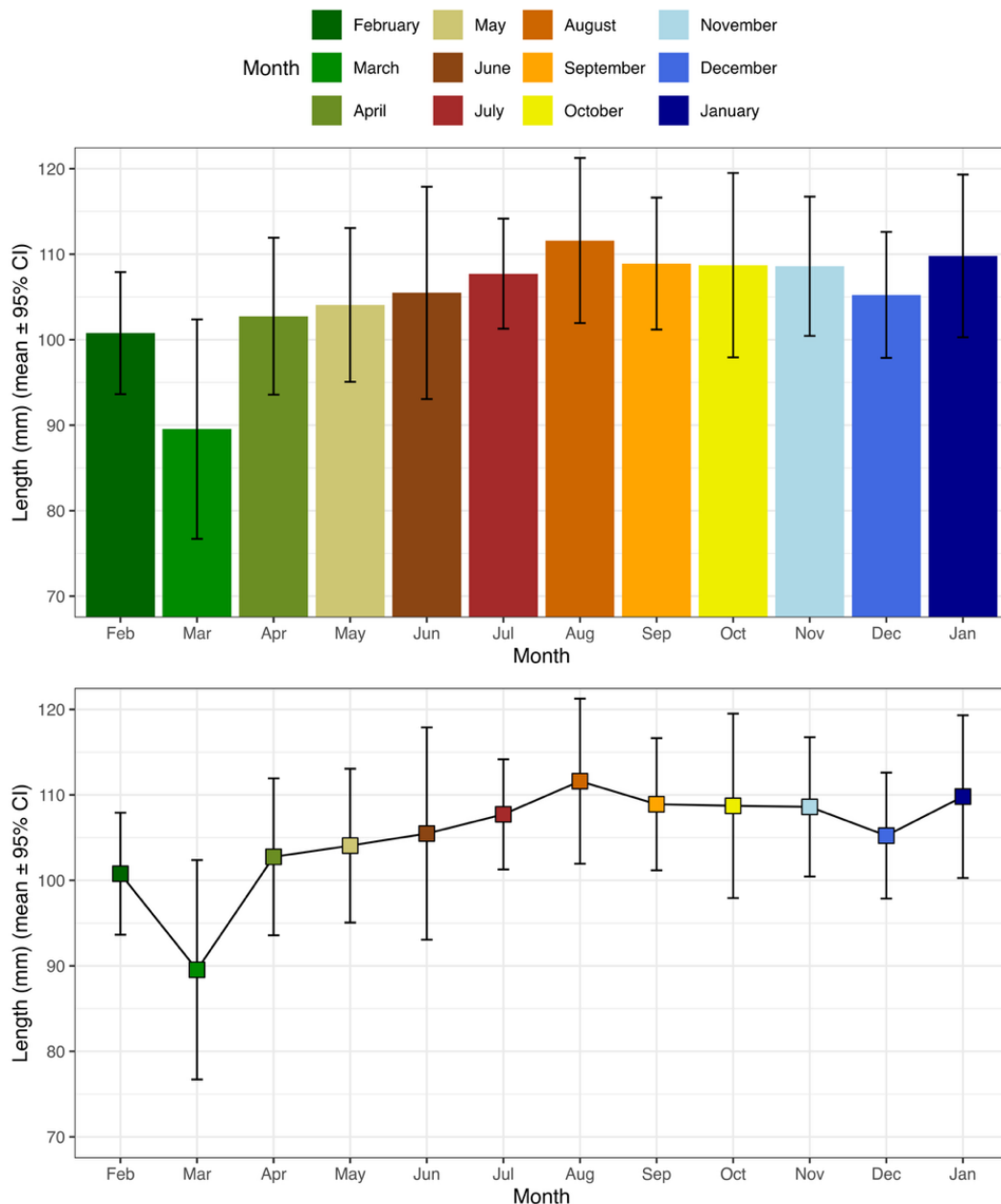


Figure 14: Monthly variation in mean kōaro (*Galaxias brevipinnis*) length (mm) in the Millar Road wetland. Data comes from the initial 12 Gee's minnow traps which were set monthly from February 2025 to January 2026. The errors bars indicate the 95 % confidence interval (CI).

Monthly median length varied through time, ranging from 102 mm in March (Interquartile range [IQR] = 55.2 mm) to 112 mm in August (IQR = 16.2 mm). Mean length also differed among months, with the lowest mean observed in March (89.5 mm, 95 % CI: 76.7–102, n = 26 fish) and the highest mean observed in August (112 mm, 95 % CI: 102–121, n = 20 fish). These patterns indicate temporal variation in size structure, with relatively smaller individuals dominating earlier in the year and larger individuals more prevalent during late winter (Figure 15).

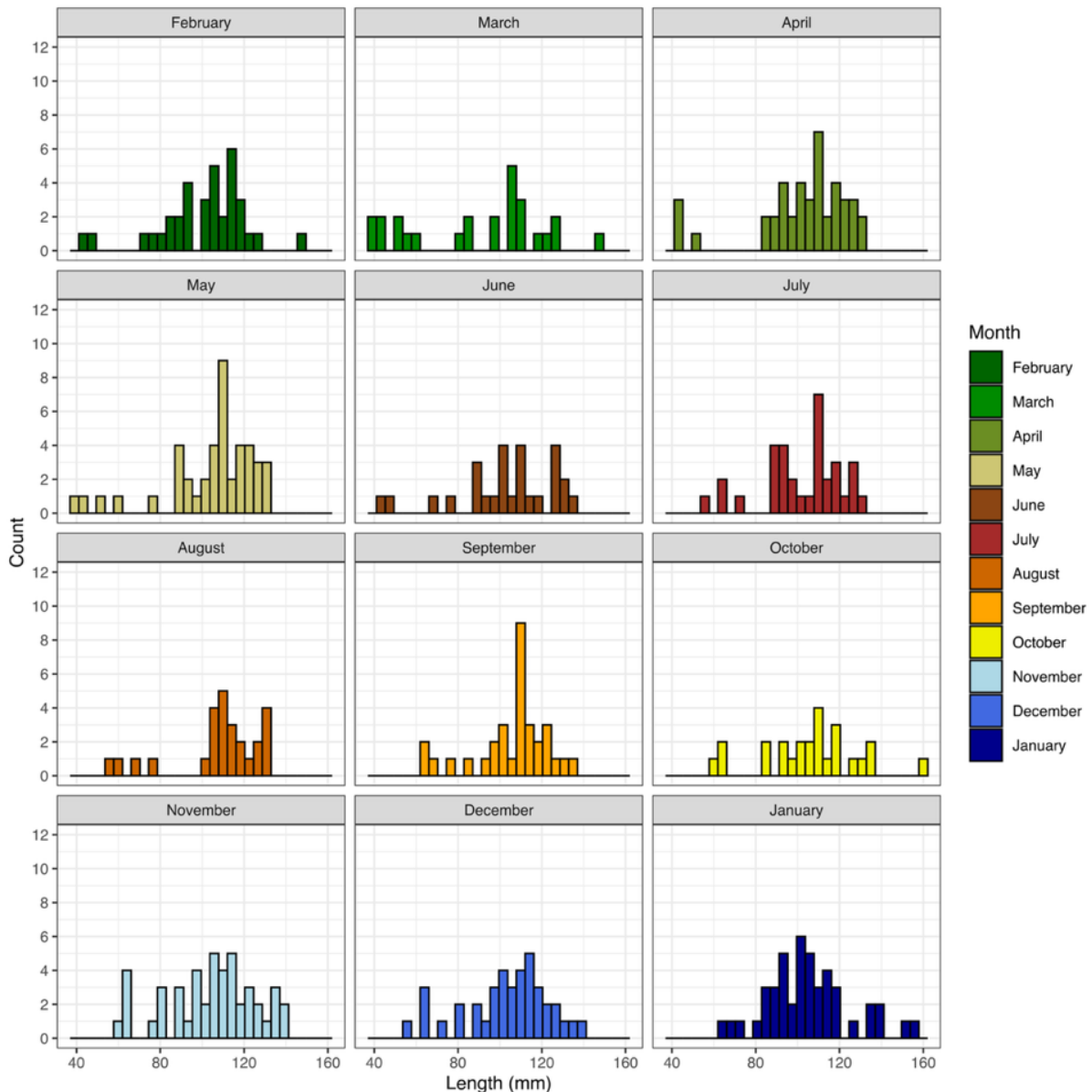


Figure 15: Seasonal size-frequency distributions of kōaro (*Galaxias brevipinnis*) captured in the Millar Road wetland. Data are from the initial 12 Gee's minnow traps deployed monthly from February 2025 to January 2026 and show the frequency of individual total lengths (mm) recorded each month, illustrating temporal variation in size structure across the sampling period.

Seasonal variation in kōaro size structure was evident with smaller individuals most common in late summer and early autumn and larger individuals present throughout the year (Figure 15).

3.3.3 Kōaro body mass

Individual kōaro mass ranged from 0.1 g to 55 g, with a mean mass of 11.6 g (SD = 7.10 g) and a median mass of 10.75 g (Figure 16). The smallest individual mass (0.1 g) was recorded in April, while the largest individual (55 g) was recorded in December.

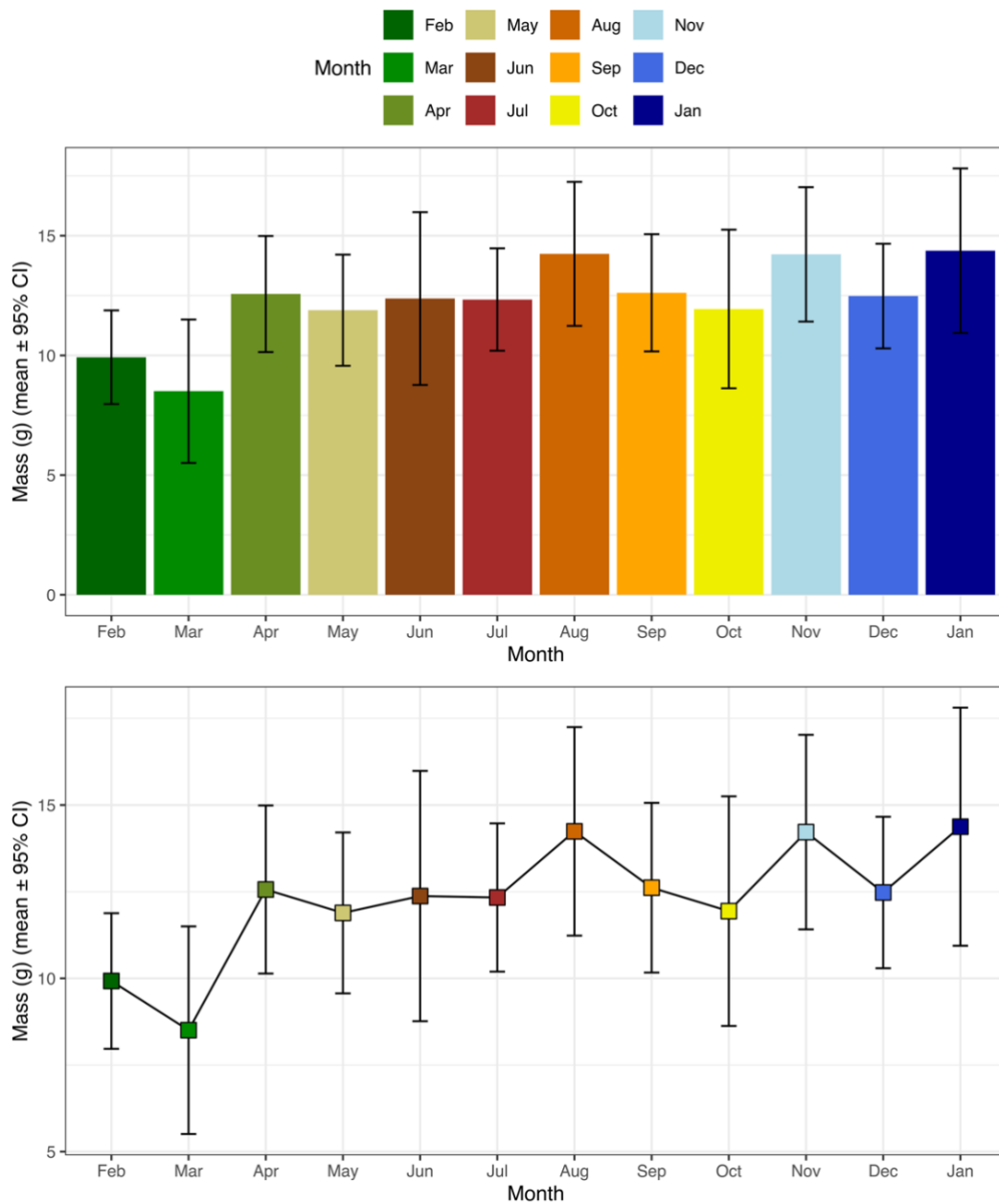


Figure 16: Monthly variation in mean kōaro (*Galaxias brevipinnis*) mass (g) in the Millar Road wetland. Data are from the initial 12 Gee's minnow traps which were set monthly from February 2025 to January 2026. Error bars indicate the 95 % confidence interval (CI).

Monthly median mass varied through time, ranging from 8.85 g in March (IQR = 10.3 g) to 12.2 g in August (IQR = 7.85 g). As with length, mass distributions showed temporal variation, with lower median masses observed in late summer and early autumn and higher median masses occurring during winter and spring.

Mass distributions were right-skewed (Figure 17), with most individuals having relatively low mass and a smaller number of larger individuals contributing disproportionately to total biomass.

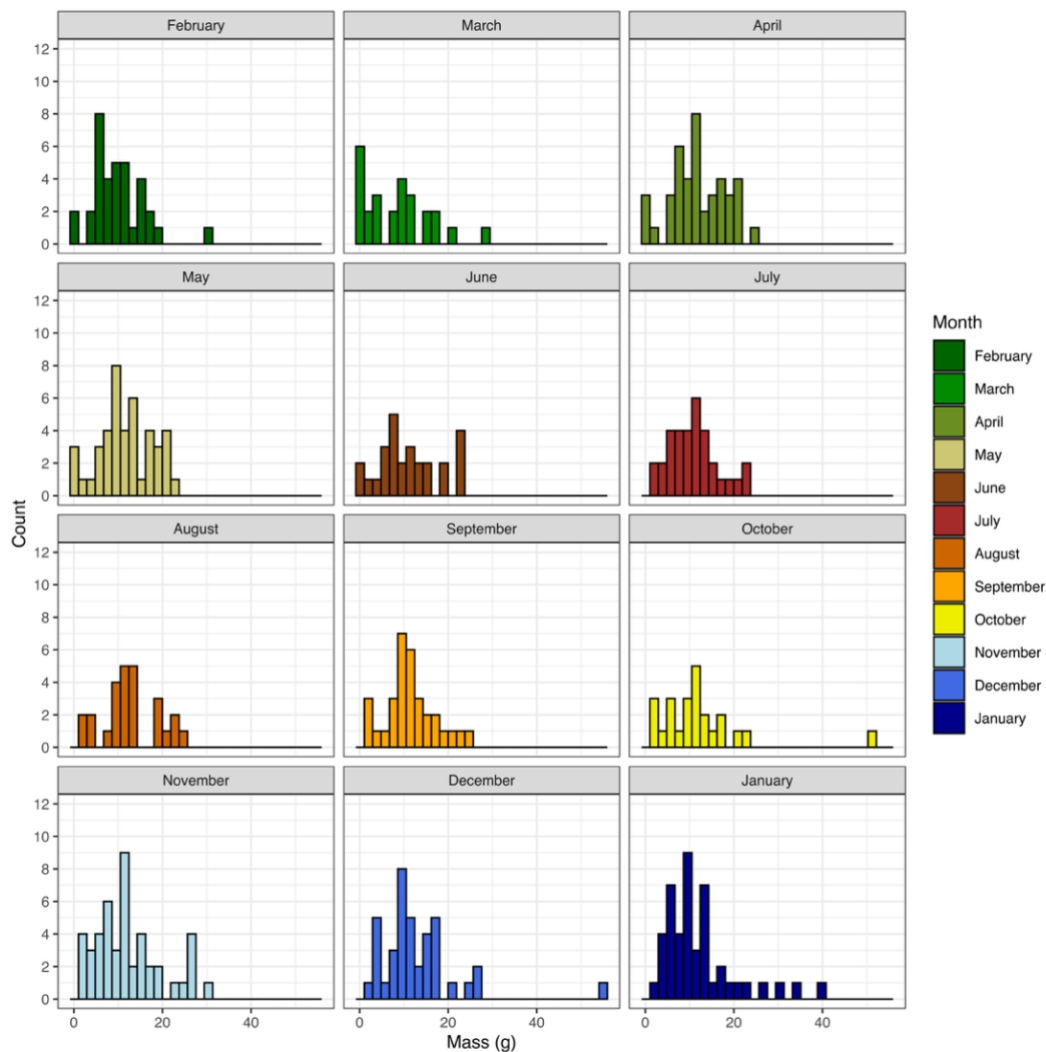


Figure 17: Seasonal mass-frequency distribution of kōaro (*Galaxias brevipinnis*) captured in the Millar Road wetland. Data are from the initial 12 Gee's minnow traps deployed monthly from February 2025 to January 2026. The figure shows the frequency of individual body masses recorded each month, illustrating temporal variation in mass distribution across the sampling period.

3.3.4 Kōaro mass-length relationship

Kōaro mass scaled strongly with total length across the study period ($\log_{10}(\text{wet mass}) \sim \log_{10}(\text{total length})$; $R^2 = 0.91$, $F_{1,416} = 4017$, $p < 0.001$; Figure 18). The estimated allometric exponent was 3.58 (95 % CI: 3.47 - 3.69), exceeding 3 and therefore consistent with positive allometry. This regression describes the local mass-length relationship and was not used to estimate body condition.

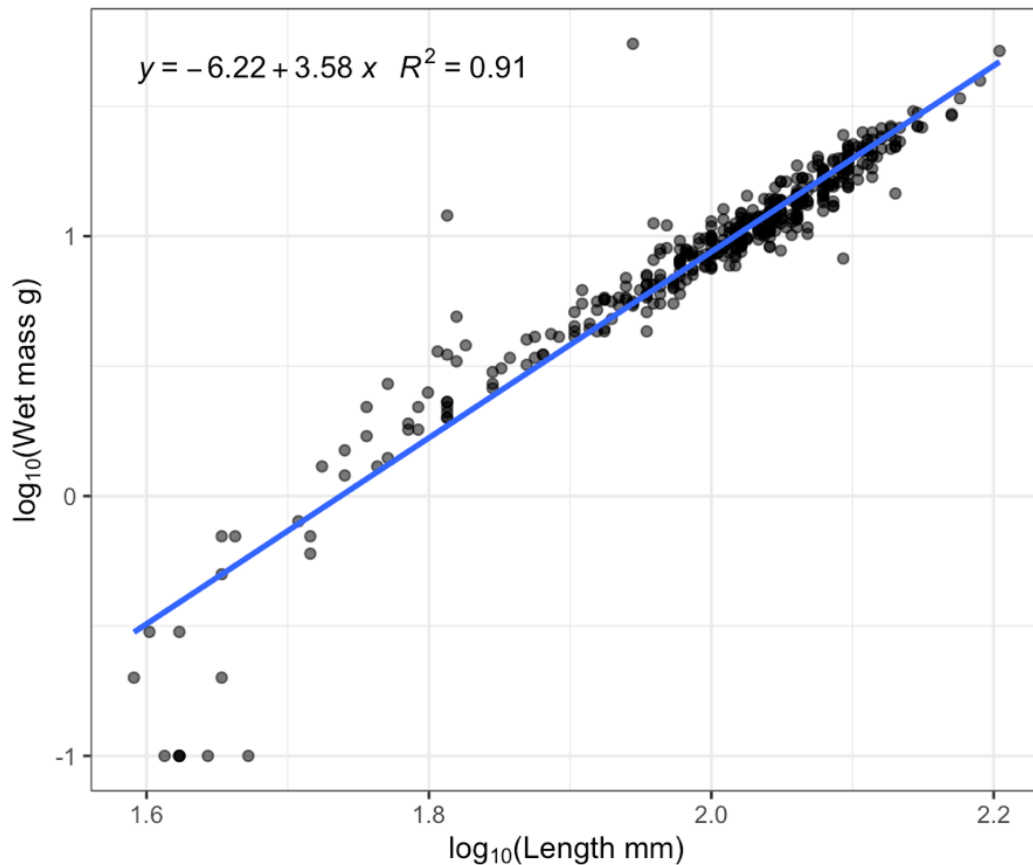


Figure 18: Log–log relationship between total length (mm) and wet mass (g) for kōaro (*Galaxias brevipinnis*) captured at the Millar Road wetland between February 2025 and January 2026 ($n = 419$). Points represent individual fish. The solid blue line shows the fitted linear regression of $\log_{10}(\text{wet mass})$ on $\log_{10}(\text{total length})$. The regression equation and coefficient of determination (R^2) are displayed on the plot ($p < 0.001$).

3.3.5 Kōaro condition

When benchmarked against the national length–weight relationship for kōaro (Jellyman et al., 2013), individuals from the Millar Road wetland exhibited a mean log-residual condition of 0.028 (SD = 0.130; $n = 419$; Figure 19). A one-sample t-test indicated that mean condition differed significantly from zero ($t_{417} = 4.41$, $p < 0.001$), a result supported by a Wilcoxon signed-rank test ($V = 67,388$, $p < 0.001$). Mean relative weight (W_r) was 112 %, with a median of 108 %.

Monthly mean condition values ranged from -0.038 (June) to 0.095 (December). A linear model indicated a significant relationship between condition and month ($\beta = 1.785 \times 10^{-4} \pm 5.736 \times 10^{-5}$ SE, $p = 0.002$).

Condition was also significantly associated with body length ($\beta = 7.785 \times 10^{-4} \pm 2.848 \times 10^{-4}$ SE, $p = 0.007$; Figure 20). In a multiple regression including both month and length, both predictors remained significant ($F_{2,415} = 9.53$, $p < 0.001$, $R^2 = 0.044$).

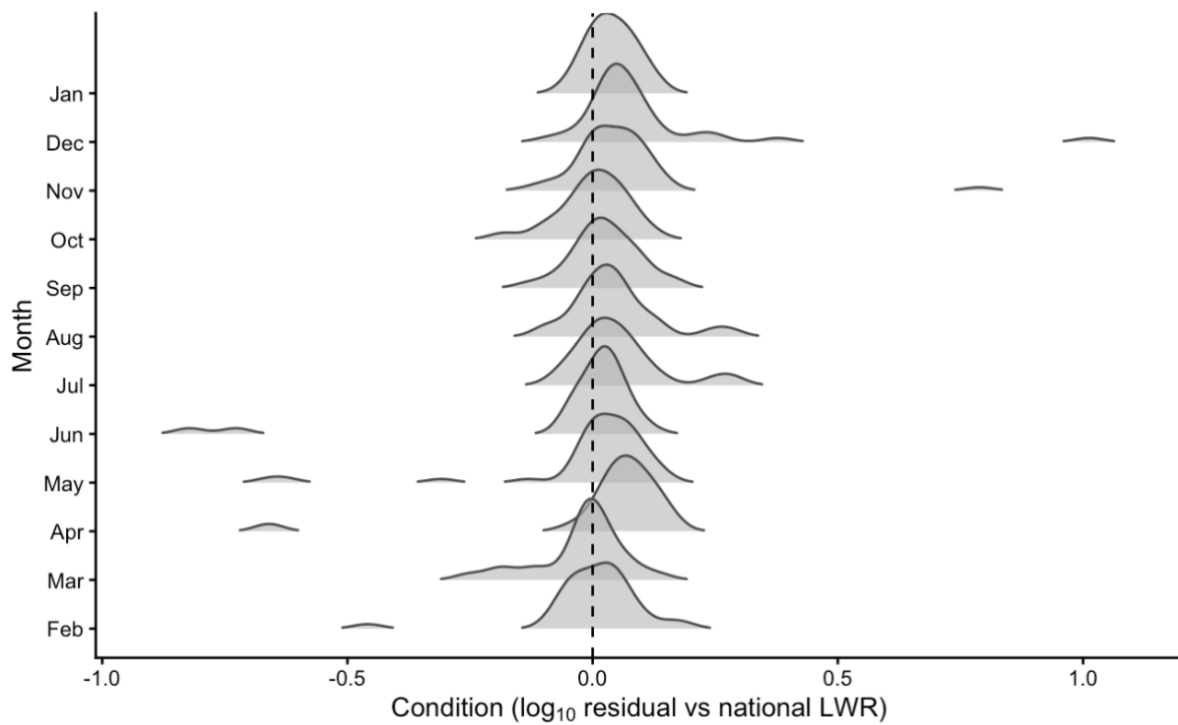


Figure 19: Monthly distribution of kōaro (*Galaxias brevipinnis*) condition relative to the national length–weight relationship (Jellyman et al., 2013). Condition is expressed as the \log_{10} residual between observed weight and expected weight derived from the national equation. Values greater than zero indicate individuals heavier than predicted for their length, while values below zero indicate individuals lighter than predicted. Ridgelines represent kernel density distributions for each month, and the dashed vertical line indicates the national expectation (residual = 0). Monitoring began in February 2025 and continued monthly until January 2026.

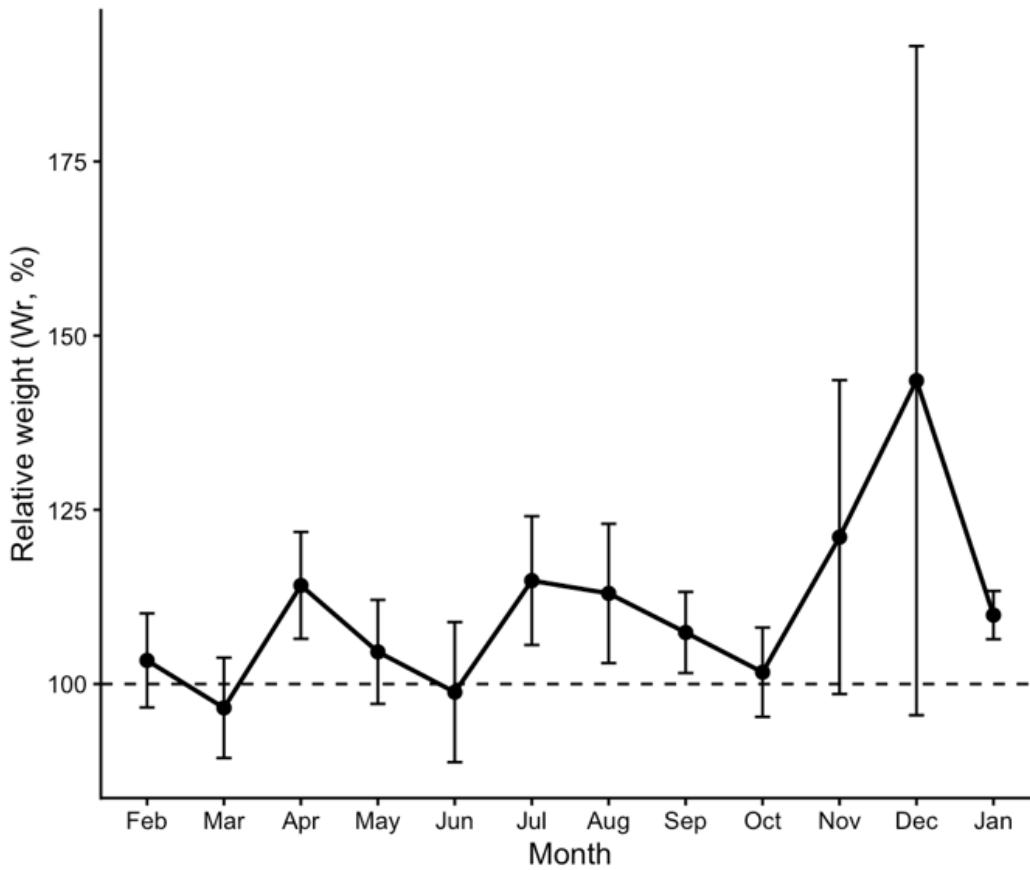


Figure 20: Monthly variation in relative weight (W_r) of kōaro (*Galaxias brevipinnis*) at the Millar Road wetland between February 2025 and January 2026. Relative weight was calculated as $100 \times (\text{observed mass} / \text{expected mass})$ using the national length–weight relationship for kōaro (Jellyman et al., 2013). Points represent individual fish, lines show monthly means, and error bars indicate $\pm 95\%$ confidence intervals. The dashed horizontal line represents $W_r = 100$, corresponding to the national expected mass for a given length.

3.3.6 Kōaro biomass

Mean biomass per unit effort (BPUE; g trap^{-1}), calculated using $n = 12$ traps, varied among sampling months (Figure 21). Monthly mean BPUE ranged from 12.9 g trap^{-1} in October (95 % CI: 2.83 - 23.0) to 37.9 g trap^{-1} in November (95 % CI: 8.63 - 67.2), indicating substantial temporal variation in kōaro biomass within the sampled reach.

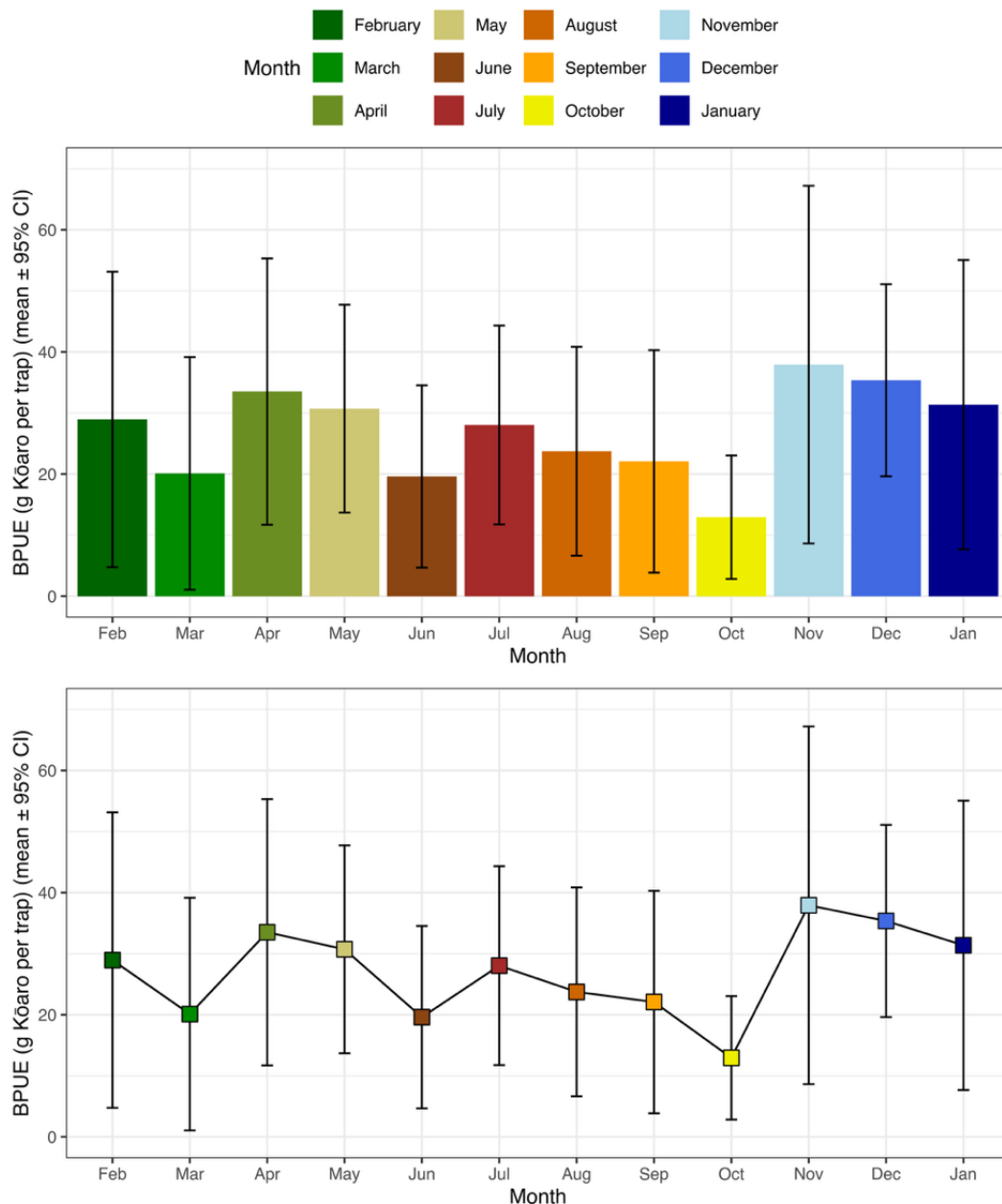


Figure 21: Monthly variation in mean kōaro (*Galaxias brevipinnis*) biomass per unit effort (BPUE; g kōaro per trap) in the Millar Road wetland. Data were derived from the initial 12 Gee's minnow traps sampled monthly from February 2025 to January 2026. Bars and points represent monthly mean BPUE values, and error bars indicate the 95 % confidence interval (CI).

3.3.7 Kōaro recruitment

Kōaro abundance varied seasonally across the study period. Mean CPUE from the initial 12 traps were lowest during late winter and early spring and increased through summer, reaching a peak in late summer to early autumn before declining towards winter (Figure 13). This seasonal pattern was consistent when analyses were repeated using the full trap array (Appendix A All Traps).

Seasonal variation was also evident in kōaro size (Figure 16). Length distributions differed among months, with smaller individuals becoming more prevalent during late summer and early autumn (Figure 14). Larger individuals were present throughout the year.

Juvenile kōaro (< 70 mm) were recorded in multiple sampling months, with counts ranging from 1 individual in January to 8 individuals in March. Juveniles were first detected in March and were subsequently recorded intermittently through the remainder of the study period (Figure 22).

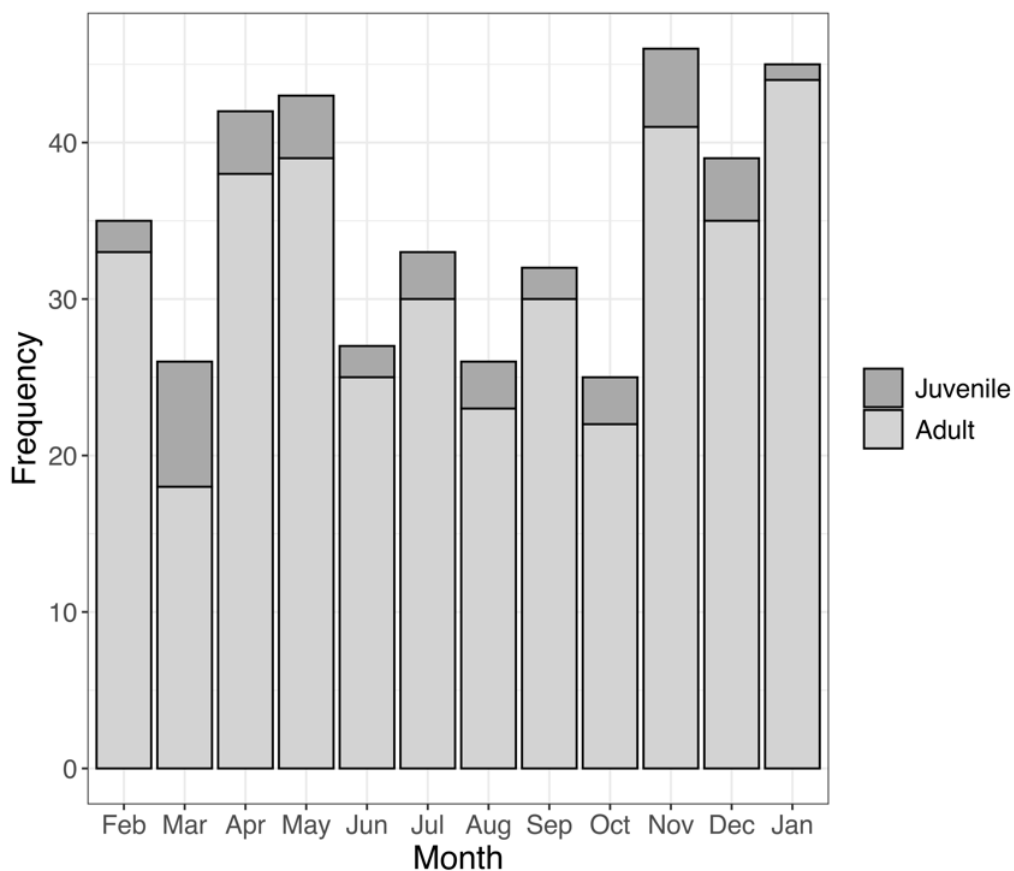


Figure 22: Proportion of adult and juvenile kōaro (*Galaxias brevipinnis*) in the Millar Road wetland. Data were derived from the initial 12 Gee's minnow traps sampled monthly from February 2025 to January 2026. Juveniles were defined as individuals <70 mm total length.

The proportion of juvenile kōaro (< 70 mm total length) varied across months, with the highest predicted probability occurring in March (Figure 23). However, the proportion of juveniles did not differ significantly among months (binomial GLM, $\chi^2_{11} = 14.7$, $p = 0.197$).

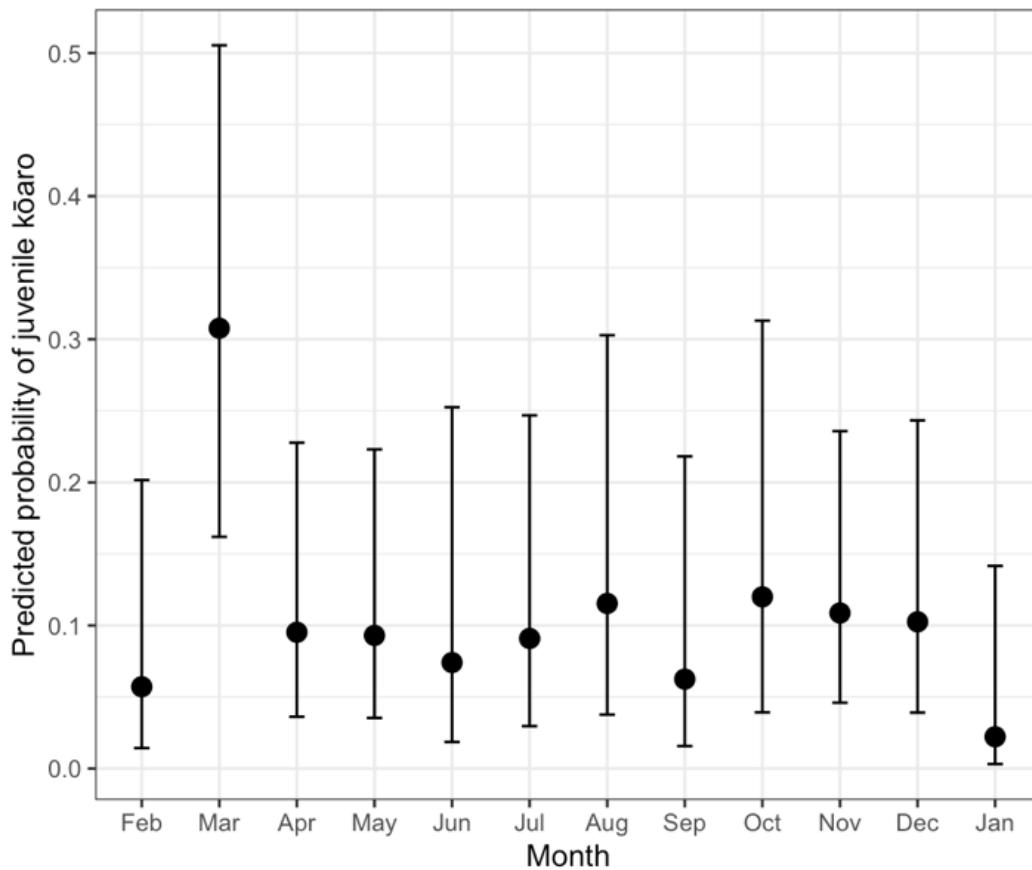


Figure 23: Model-predicted probability of kōaro (*Galaxias brevipinnis*) being juvenile (< 70 mm total length) by month, estimated using a binomial generalised linear model. Data were derived from the initial 12 Gee’s minnow traps sampled monthly from February 2025 to January 2026. Points show predicted probabilities and error bars indicate 95 % confidence interval.

3.3.8 Kōaro-habitat associations

Kōaro presence-absence was analysed using a binomial generalised linear mixed-effects model with trap and month included as random intercepts to account for repeated sampling. The model included habitat structure variables (shade, raupō cover, aquatic vegetation, and grasses) and co-occurring fish taxa (trout, common bullies, and kōura) as fixed effects (Table 3).

Among habitat variables, raupō cover was significantly negatively associated with kōaro presence ($\beta = -0.76 \pm 0.31$ SE, $z = -2.50$, $p = 0.013$), indicating that kōaro were less likely to occur in traps with higher raupō cover (Table 3).

None of the co-occurring fish variables showed a statistically significant association with kōaro presence at $\alpha = 0.05$, although kōura exhibited a positive but non-significant association with kōaro presence ($\beta = 0.71 \pm 0.42$ SE, $z = 1.70$, $p = 0.089$).

Random effect variance estimates for both trap and month were close to zero, indicating limited residual variation in kōaro presence attributable to differences among traps or months after accounting for fixed effects.

Table 3: Results of a generalized linear model examining the effects of habitat variables and co-occurring species on kōaro (Galaxias brevipinnis) presence in the Millar Road wetland. Estimates (β) are logit-scale coefficients, with associated standard errors (SE), z-values, and p-values. Habitat predictors included ordinal cover scores (0–3) for shade, raupō, and aquatic vegetation, and presence/abundance measures of grasses, trout, common bully, and kōura. Negative coefficients indicate a decrease in the probability of kōaro presence with increasing predictor values, whereas positive coefficients indicate an increase.

Predictor	Estimate (β)	SE	z	p
Shade (0–3)	-0.11	0.44	-0.25	0.80
Raupō (0–3)	-0.76	0.31	-2.50	0.013
Aquatic vegetation (0–3)	0.53	0.64	0.83	0.41
Grasses	0.65	0.86	0.76	0.45
Trout	-0.001	0.73	-0.00	0.999
Common bully	-0.001	0.014	-0.07	0.95
Kōura	0.71	0.42	1.70	0.089

3.3.9 Influence of hydrology on kōaro

Mean lake level varied across the sampling period (February - December 2025). Mixed-effects models indicated that trout CPUE increased with increasing lake level ($\beta = 3.35 \times 10^{-4} \pm 1.69 \times 10^{-4}$ SE, $p = 0.049$). In contrast, kōaro CPUE declined as lake level increased ($\beta = -0.00232 \pm 0.00104$ SE, $p = 0.026$). Trout CPUE showed little trap-level variability, whereas kōaro CPUE varied substantially among traps. Lake level data were unavailable for January 2026 and this month was excluded from hydrology-linked analyses.

3.4 Kōaro comparison (2019 and 2025)

To control for seasonal variation, kōaro abundance was compared between the March 2019 and March 2025 sampling events at the initial 12 traps. 36 kōaro were recorded in March 2019 and 26 in March 2025 (Table 4).

Table 4: Summary statistics for kōaro (Galaxias brevipinnis) total length (mm) recorded in Millar Road wetland. Data were derived from the initial 12 Gee's minnow traps sampled during March 2019 and March 2025 and pooled across all monthly sampling occasions in 2025/2026. Values shown include sample size (n), mean length, median length and standard deviation (SD).

Date	n	Mean	Median	SD
March 2019	36	100.6	101.0	17.9
March 2025	26	89.5	101.5	31.8
All months 2025/26	313	105.0	110.0	23.1

Mean kōaro length pooled across all sampling months in 2025/2026 (103.0 ± 22.0 mm, $n = 419$), like March 2019 values, whereas March 2025 alone showed greater variability and a lower mean length (Table 4). Mean kōaro CPUE across the sampling period showed no evidence of an interannual shift when March 2019 was compared with monthly CPUE values from the 2025 sampling period (Figure 24).

When CPUE was compared directly between March 2019 and March 2025 at the trap level, no significant difference was detected (negative binomial GLM: $\beta = -0.054$, $SE = 0.083$, $z = -0.66$, $p = 0.511$; Figure 25).

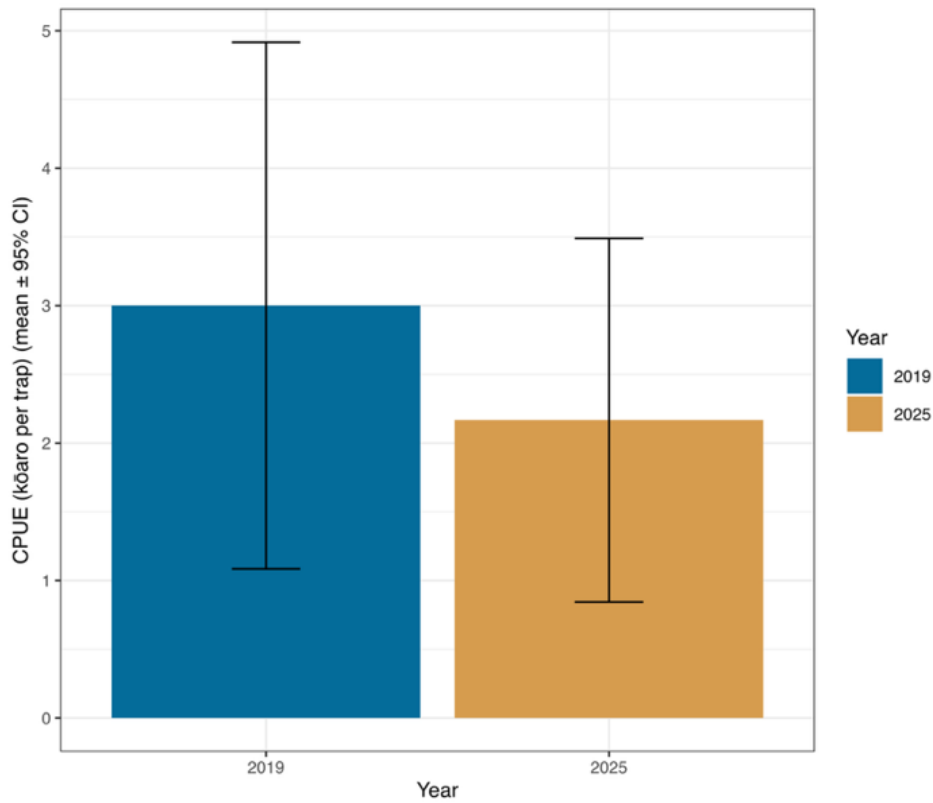


Figure 24: Comparison of kōaro (*Galaxias brevipinnis*) mean catch per unit effort (CPUE; individuals per trap) in the Millar Road wetland. Data were derived from the initial 12 Gee's minnow traps sampled during March 2019 and March 2025. Bars and represent monthly mean CPUE values, and error bars indicate the 95 % confidence interval (CI).

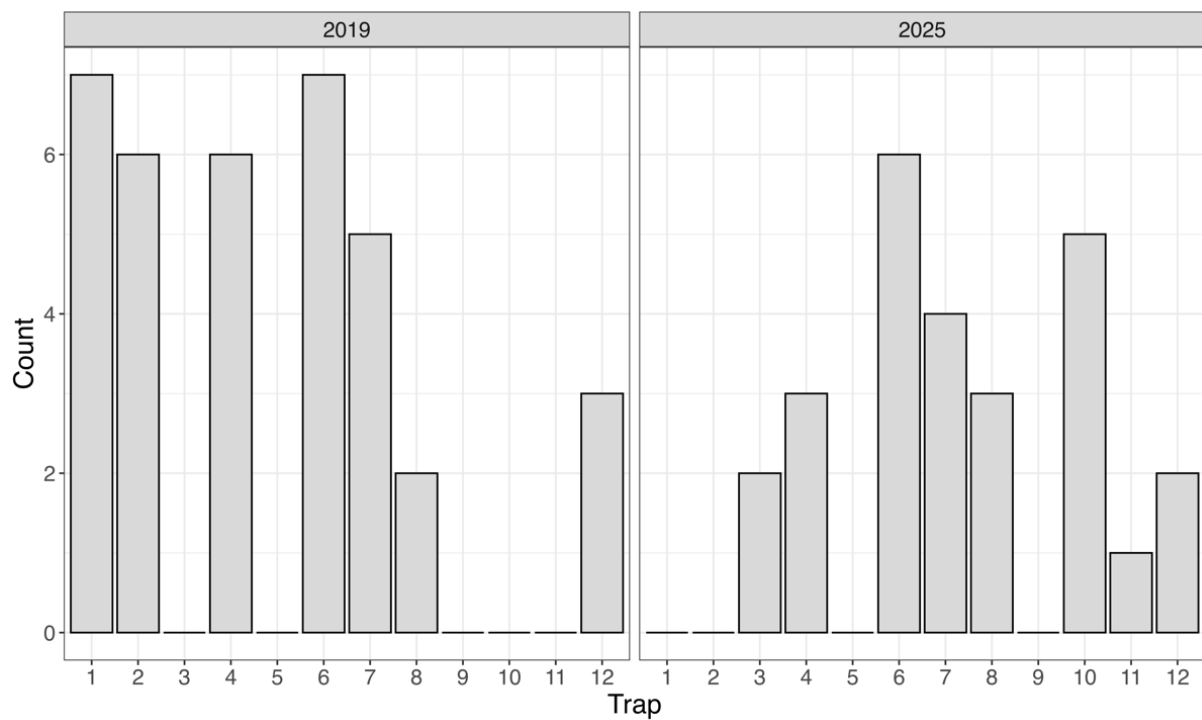


Figure 25: Comparison of kōaro (*Galaxias brevipinnis*) Catch Per Unit Effort (CPUE; individuals per trap) in the Millar Road wetland. Data were derived from 12 Gee's minnow traps sampled during March 2019 and March 2025.

Kōaro size was compared between the March 2019 and March 2025 sampling events. Median total length was similar between years (101.0 mm in 2019; 101.5 mm in 2025), and no significant difference in length distribution was detected (Wilcoxon rank-sum test, $p = 0.39$; Figure 26).

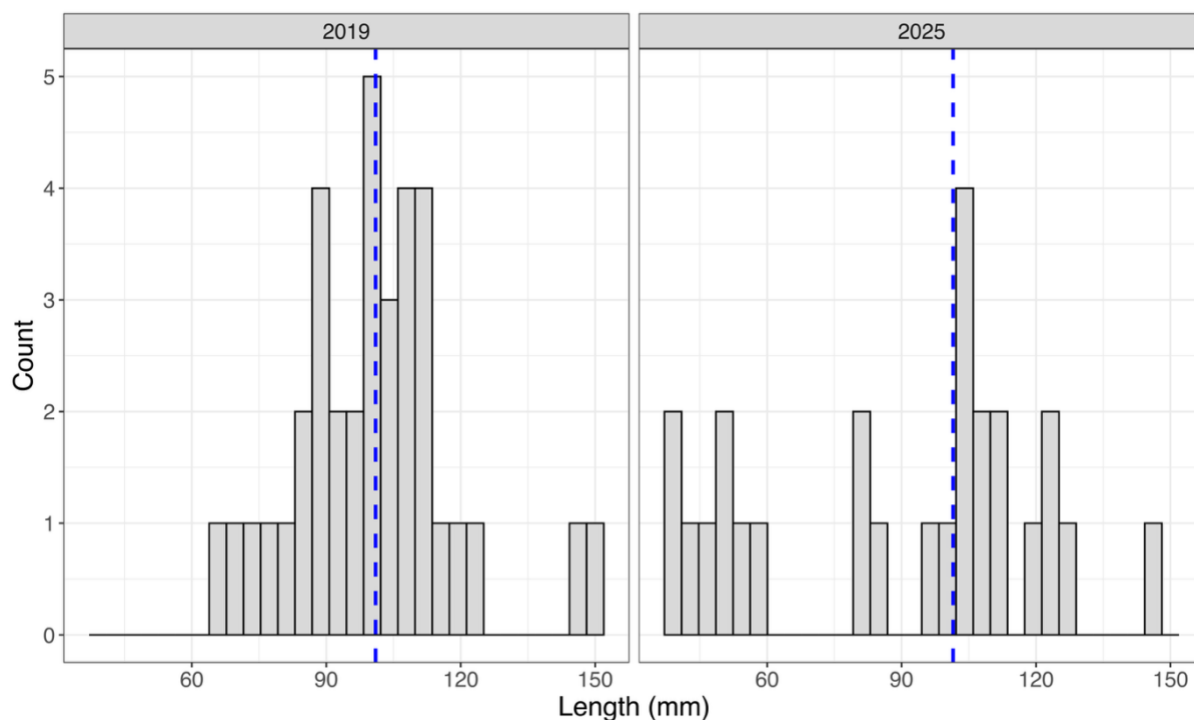


Figure 26: Comparison of kōaro (*Galaxias brevipinnis*) total length (mm) between March 2019 and March 2025 sampling events at the 12 monitored traps in the Millar Road wetland. Histograms show length-frequency distributions for each year respectively (March 2019: $n = 36$; March 2025: $n = 26$). The dashed blue vertical line in each panel indicates the median total length for that corresponding year.

In contrast to length, kōaro mass differed between the March 2019 and March 2025 sampling events. Median mass was slightly higher in March 2025 (8.85 g) than in March 2019 (8.45 g), and this difference was statistically significant (Wilcoxon rank-sum test, $p = 0.015$; Figure 27).

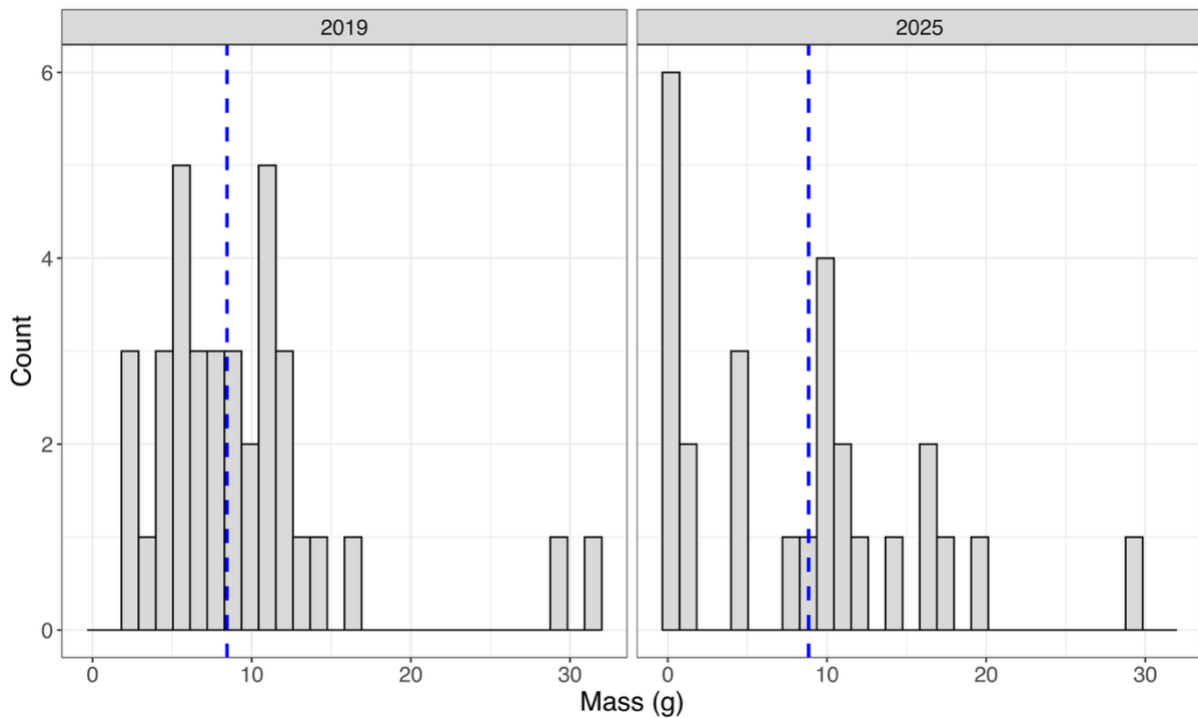


Figure 27: Comparison of kōaro (*Galaxias brevipinnis*) Mass (g) between March 2019 and March 2025 sampling events at the 12 monitored traps in the Millar Road wetland. Histograms show mass-frequency distributions for each year (March 2019: $n = 36$; March 2025: $n = 26$). The dashed vertical line in each panel indicates the median total mass for that year.

Across all samples, the proportion of juveniles was higher in 2025 than in 2019 (Table 5). In 2019, juveniles comprised 2.8 % of captured kōaro (1 of 36 individuals), whereas in 2025 juveniles accounted for 9.8 % of captures (41 of 419 individuals).

Table 5: Comparison of kōaro (*Galaxias brevipinnis*) length-class composition between 2019 and 2025. Individuals were classified as juveniles (<70 mm total length) or adults (≥ 70 mm) to assess the relative contribution of juvenile fish in each sampling year. Values show total counts and the proportion of juveniles within each year's sample.

Year	Month	Adults	Juveniles	Total	% Juveniles
2019	March	35	1	36	2.8 %
2025	March	18	8	26	30.8 %
2025	All months	278	35	313	11.2 %

A direct comparison of March sampling events showed a marked difference in juvenile representation between years (Figure 28). In March 2019, juveniles were almost absent (1 individual), whereas in March 2025 juveniles comprised 8 of 26 captured kōaro. Fisher's exact test indicated that the odds of capturing a juvenile were significantly higher in March 2025 than in March 2019 (odds ratio = 14.9, $p = 0.003$).

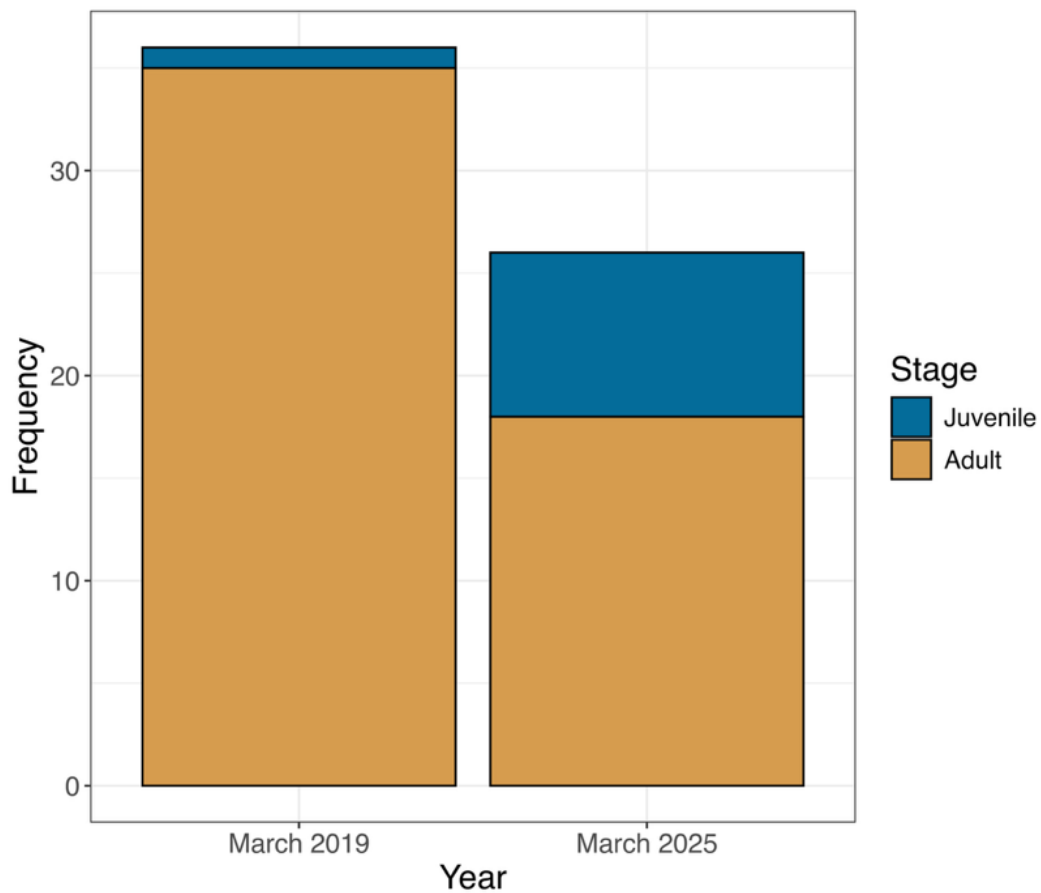


Figure 28: Comparison of adult and juvenile kōaro (*Galaxias brevipinnis*) between March 2019 and March 2025 sampling events at the 12 monitored traps in the Millar Road wetland. Individuals were classified as juveniles (<70 mm total length) or adults (≥ 70 mm) to assess differences in size-class composition between sampling years. Values show total counts and the proportion of juveniles within each year.

3.5 Kōaro mark-recapture

A total of 27 kōaro were PIT-tagged during the September 2025 sampling occasion, with recaptures recorded across subsequent sampling months. Overall, 48.1 % of tagged individuals were detected in at least one post-tagging sampling month (Table 6). Detection proportions were similar across October, November, and January.

Table 6: Monthly recapture of PIT-tagged kōaro (*Galaxias brevipinnis*) following tagging in September 2025 at the Millar Road wetland. Values show the number and proportion of tagged individuals detected in each subsequent sampling month ($n = 27$ tagged individuals). *Fin-clipped individuals counted only due to technical issues with the tag reader.

Month	Recaptured (n)	Proportion (%)
October 2025	8	29.6
November 2025	8	29.6
December 2025*	11	42.3
January 2026	6	22.2
All months	13	48.1

* Only fin-clipped individuals counted due to technical issues with the tag reader.

3.5.1 PIT-tagged kōaro movement and site fidelity

Of the 27 PIT-tagged kōaro, 13 individuals (59 %; 95 % CI: 39 - 78 %) were recaptured at least once between October and January (Table 6; Figure 29). Among these recaptured individuals, 2 were detected only at their original trap location, whereas 11 were detected at more than one trap location, indicating limited but measurable within-wetland movement. Across all recapture events ($n = 22$), 8 (36%) occurred at the individual's original trap and 14 (64%) occurred at a different trap.

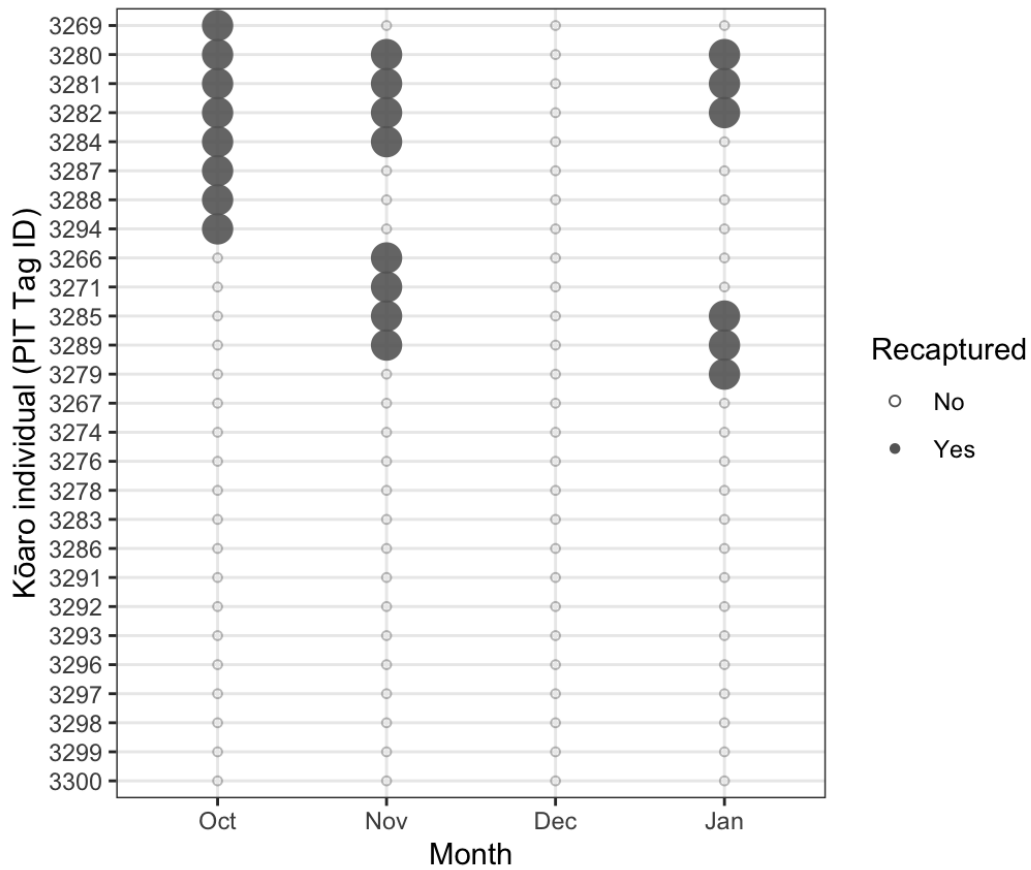


Figure 29: Capture histories of PIT-tagged kōaro (*Galaxias brevipinnis*) in the Millar Road wetland following release. Individuals were PIT-tagged and released in September 2025, and subsequent recaptures were recorded during monthly sampling from October 2025 to January 2026. The y-axis shows individual PIT tag IDs, ordered by the month of first recapture, with individuals not recaptured during the study period shown at the bottom. The x-axis shows sampling month. Large, filled symbols indicate months in which an individual was recaptured, while small open symbols indicate months in which the individual was not recaptured. December shows no recaptures due to technical problems recording individual tag data.

Considering individuals captured more than once, movement between successive recaptures was limited, with a mean stepwise distance of 9.4 m (median 7.1 m; Figure 30). The maximum stepwise displacement recorded was 55.9 m. All movement distances were calculated between successive recapture locations.

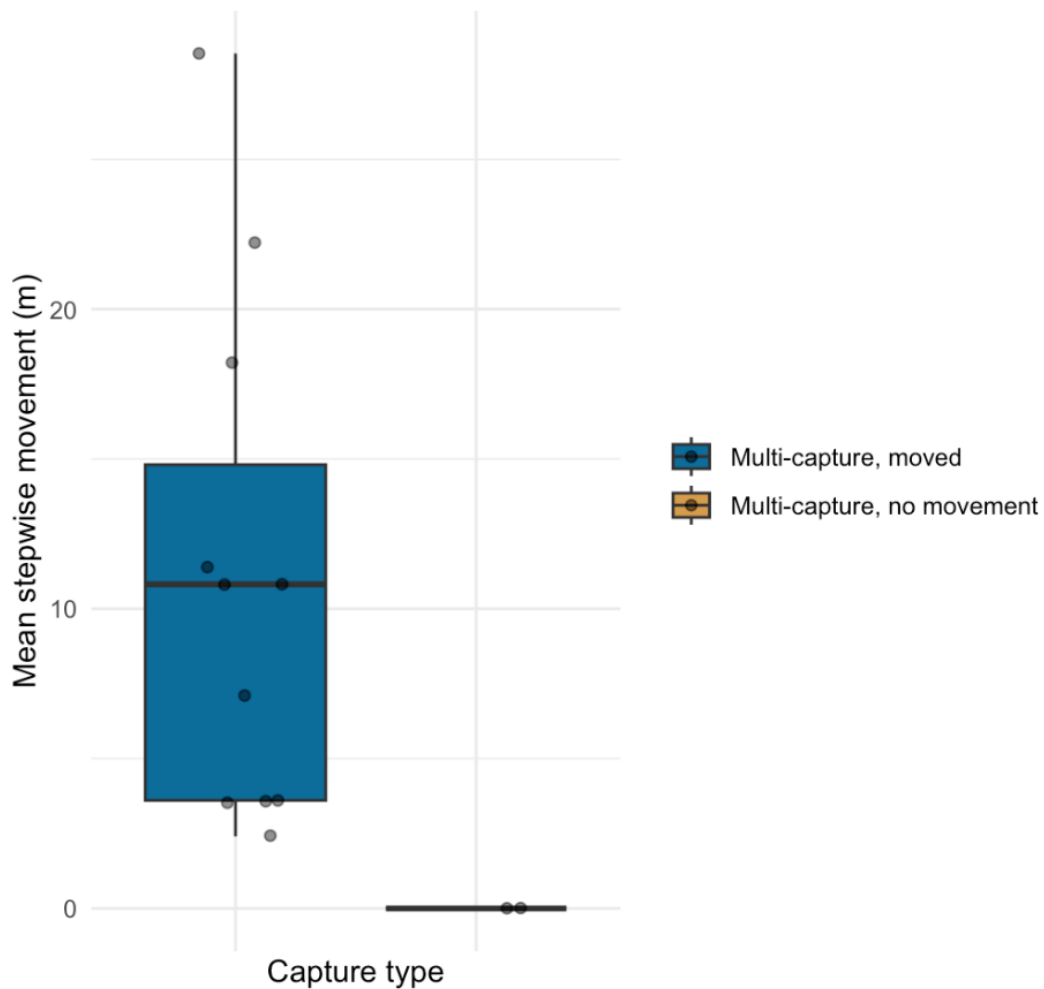


Figure 30: Movement of PIT-tagged kōaro (*Galaxias brevipinnis*) between successive recapture events at Millar Road wetland between September 2025 and January 2026. Boxes show the median and interquartile range, whiskers indicate the range, and points represent individual movements. Only individuals captured more than once were included.

3.5.2 Individual growth post tagging

6 individuals were recaptured in both September and January, allowing paired comparisons of growth. Mean total length increased by 6.33 mm (range -1 to 11 mm; Table 7). A paired *t*-test on log-transformed data indicated a significant increase in length ($t_5 = 3.41$, $p = 0.019$). A Wilcoxon signed-rank test showed a similar directional pattern but did not reach the 0.05 significance threshold ($V = 20$, $p = 0.063$).

Paired analyses indicated consistent growth in kōaro following initial tagging (Table 7; Figure 31). Between September and October (Survey 8 → 9), individuals increased in total length by a mean of 3.3 % (paired *t*-test on log-transformed data: $t_7 = -5.55$, $p <$

0.001), while no significant change in mass was detected. Similar increases in length were observed between September and November (Survey 8 → 10). Over the longer interval between September and January (Survey 8 → 12), mean total length increased by 6.3 mm (95 % CI: 1.56 - 11.10 mm), corresponding to an average proportional increase of 5.8 %, with a significant increase in mass also detected. No paired comparisons were possible for December due to the absence of PIT scanning during that survey.

Table 7: Paired comparisons of individual kōaro (Galaxias brevipinnis) growth between the initial tagging event in September 2025 and subsequent recapture surveys, excluding December. Mean absolute and proportional changes in total length and body mass are shown for each interval. Statistical significance was assessed using paired t-tests on log-transformed data.

Interval (Survey)	Interval (Month)	<i>n</i>	Metric	Mean change	% change	p-value
8 → 9	Sep → Oct	8	Length (mm)	+3.6	+3.3 %	<0.001
			Mass (g)	+0.4	Insignificant	0.44
8 → 10	Sep → Nov	8	Length (mm)	+3.6	+3.3 %	<0.001
			Mass (g)	+0.4	Insignificant	0.44
8 → 12	Sep → Jan	6	Length (mm)	+6.3	+5.8 %	0.019
			Mass (g)	+1.9	+17 %	0.025

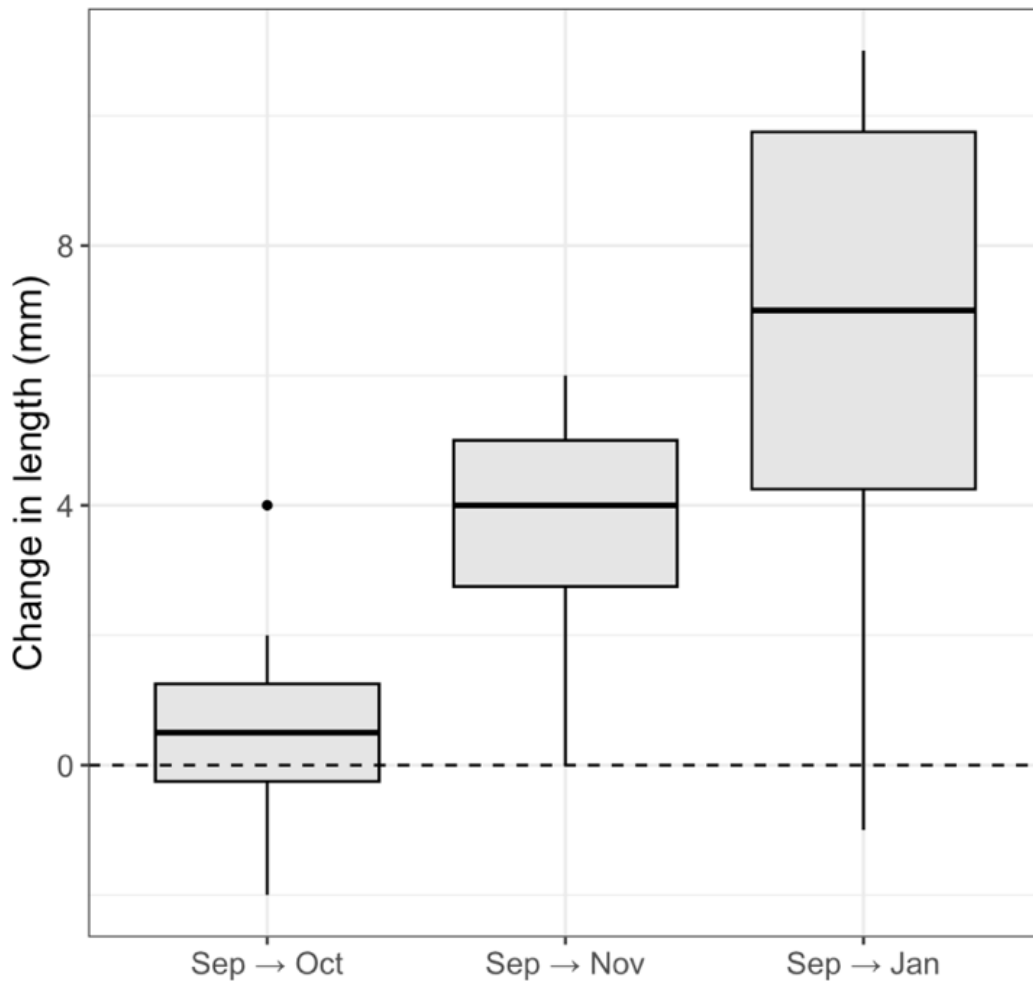


Figure 31: Change in individual kōaro (*Galaxias brevipinnis*) total length (Δ length, mm) relative to initial tagging in September 2025, excluding December. Boxes show the median and interquartile range, whiskers indicate the range, and points represent individual fish. Positive values indicate growth.

3.5.3 Population estimate

Lincoln-Petersen mark–recapture estimates of kōaro abundance varied across months (Table 8). Mean estimated kōaro abundance was 121 ± 44 individuals.

Estimated population size within the trapped reach was lowest in October (75 individuals) and December (96 individuals), intermediate in November (138 individuals), and highest in January (174 individuals). These estimates represent short-term closed-population estimates between marking and recapture events and are interpreted as indices of relative abundance rather than absolute population size.

Table 8. Lincoln–Petersen mark–recapture estimates of kōaro abundance by month at all sites in the Millar Road wetland between September 2025 and January 2026. *M* represents the number of individuals marked during the initial tagging event, *C* the total number of individuals captured during the recapture survey, and *R* the number of marked individuals recaptured. Estimated population size (\hat{N}) represents short-term closed population estimates between marking and recapture events and should be interpreted as indices of relative abundance rather than absolute population size.

Month	(M)	(C)	(R)	Estimated \hat{N}
October	26	25	9	75
November	26	46	9	138
December	26	39	11	96
January	26	45	7	174
Mean \pm SD				121 \pm 44

3.5.4 Monthly spatial variation in kōaro CPUE

Kōaro CPUE exhibited marked spatial and temporal heterogeneity across the 12 initial traps during the February - January sampling period (Figure 32). Across all trap-month combinations, CPUE ranged from 0 to 12 individuals per trap-month (median = 2; mean = 2.17). Zero catches occurred in 27.8 % of trap–month observations, indicating moderate zero inflation in the dataset.

Monthly CPUE values were classified into low, medium, and high categories using global quantiles calculated across all trap-month combinations, enabling direct comparison among months. Within individual months, CPUE classes were unevenly distributed among traps, with some traps falling into the upper quantile in multiple months, while others were repeatedly classified as low or recorded zero catch.

The identity of traps classified as high CPUE was not constant across months, demonstrating temporal shifts in the relative contribution of individual traps to total kōaro catch. However, median CPUE values summarised across the 12-month period revealed persistent differences among traps (Figure 33), suggesting sustained spatial heterogeneity in kōaro distribution within the wetland.

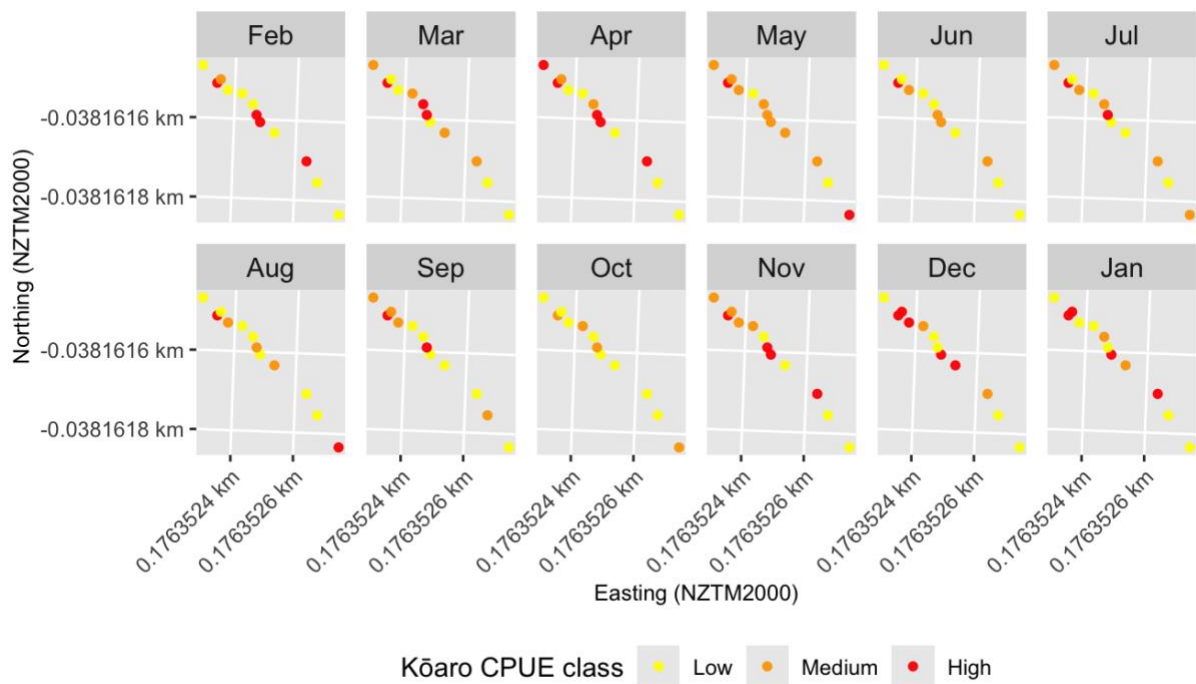


Figure 32: Spatial distribution of kōaro (*Galaxias brevipinnis*) catch per unit effort (CPUE) across the 12 initial traps in the Millar Road Wetland over the February–January sampling period. Panels represent monthly sampling occasions, with trap locations fixed across panels to facilitate temporal comparison. CPUE values were classified into Low (0–1 kōaro), Medium (2–3 kōaro), and High (≥ 4 kōaro) categories using global quantiles calculated across all trap–month observations (0%, 33%, 66%, 100% = 0, 1, 3, 12) to allow direct comparison among months. Axes are shown in NZTM2000 coordinates (EPSG:2193), with tick labels expressed in kilometres to indicate spatial scale. X axis indicates latitudinal position of the sites and Y axis indicate longitudinal position of the sites. Visual inspection suggests a seasonal concentration effect, with February–April and November–January characterised by a greater frequency of high CPUE classifications, indicating temporally clustered use of particular wetland areas.

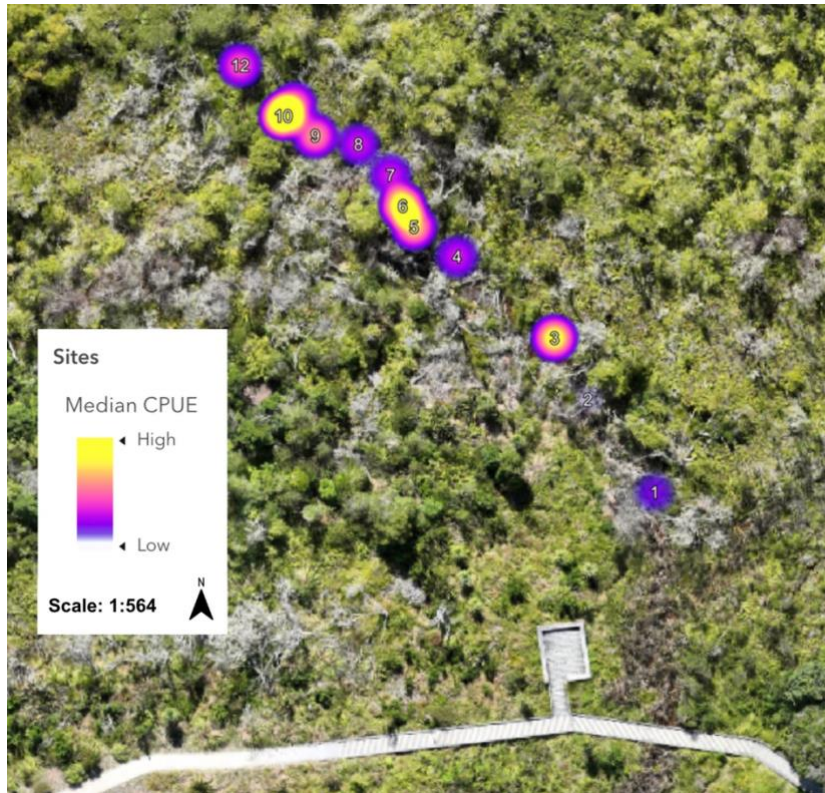


Figure 33: Overall spatial distribution heat map of kōaro (*Galaxias brevipinnis*) CPUE across the 12 initial traps, summarised as the median CPUE per trap over the 12-month sampling period symbolised over high-resolution aerial imagery. Colour intensity represents median CPUE, with warmer colours indicating higher values to cooler colours indicating lower values. Median values were used due to strong zero inflation and right-skewed catch distributions, providing a robust estimate of typical trap performance across months. Map projection is NZTM2000 (EPSG:2193). Traps exhibiting consistently higher median CPUE indicate areas of sustained kōaro use within the wetland and may represent spatially stable core-use areas under prevailing hydrological conditions.

3.6 Common bullies in MRW

3.6.1 Size structure

A total of 1403 common bullies (*Gobiomorphus cotidianus*) were captured during the study, representing the majority of fish recorded across the sampling period by abundance. Length and mass distributions were strongly right-skewed, indicating a predominance of small-bodied individuals (Figure 34; Figure 35).

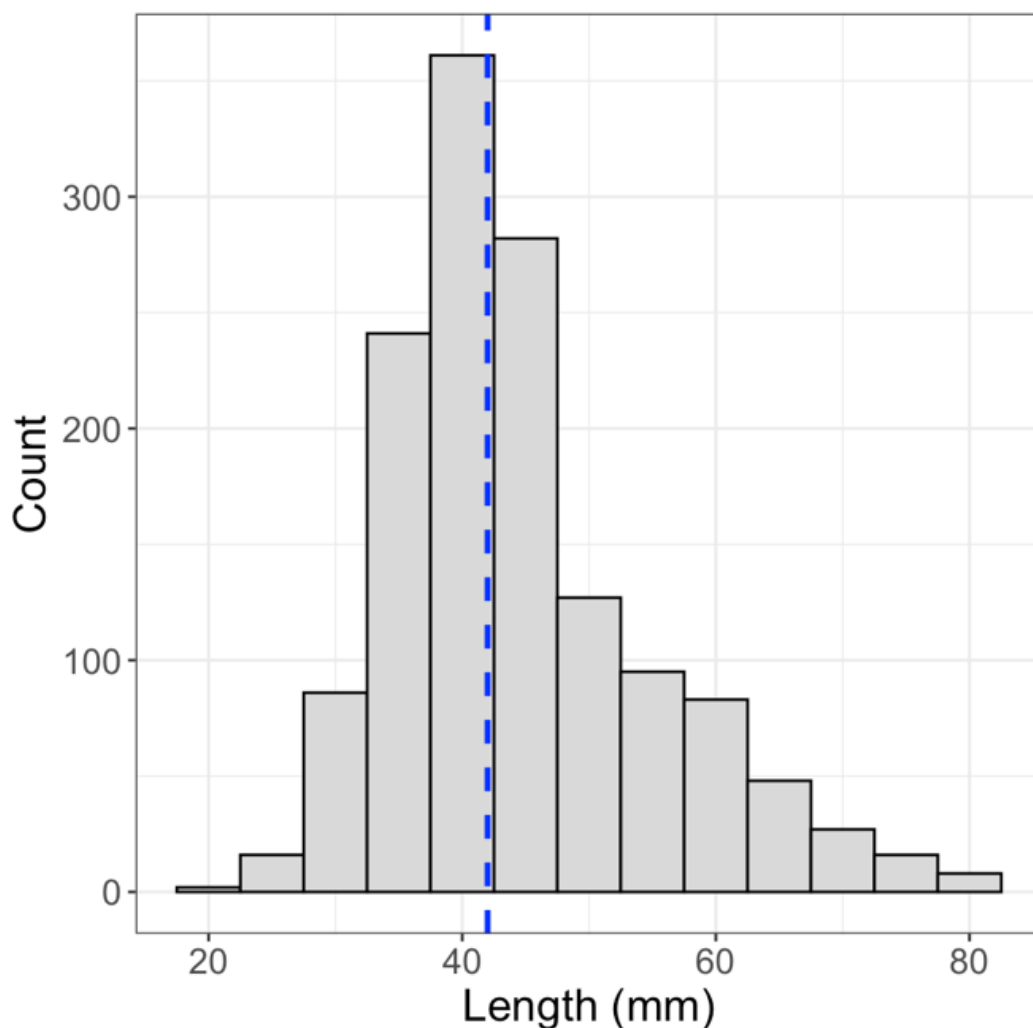


Figure 34: Length-frequency distribution of common bullies (*Gobiomorphus cotidianus*) at Millar Road wetland. Data comes from all 20 Gee's minnow traps which were set monthly from February 2025 to January 2026. The histogram summarises the size structure of individuals recorded across the sampling period ($n = 1,392$), with the dashed vertical line indicating the median total length. The distribution is right-skewed, reflecting a predominance of smaller-bodied individuals.

Total length ranged from 20 to 80 mm (mean = 44.6 mm; median = 42 mm), with most individuals clustered at smaller size classes. Body mass ranged from 0.05 to 8.0 g (mean = 1.09 g; median = 0.7 g), with the upper tail of the distribution driven by a small number of larger individuals.

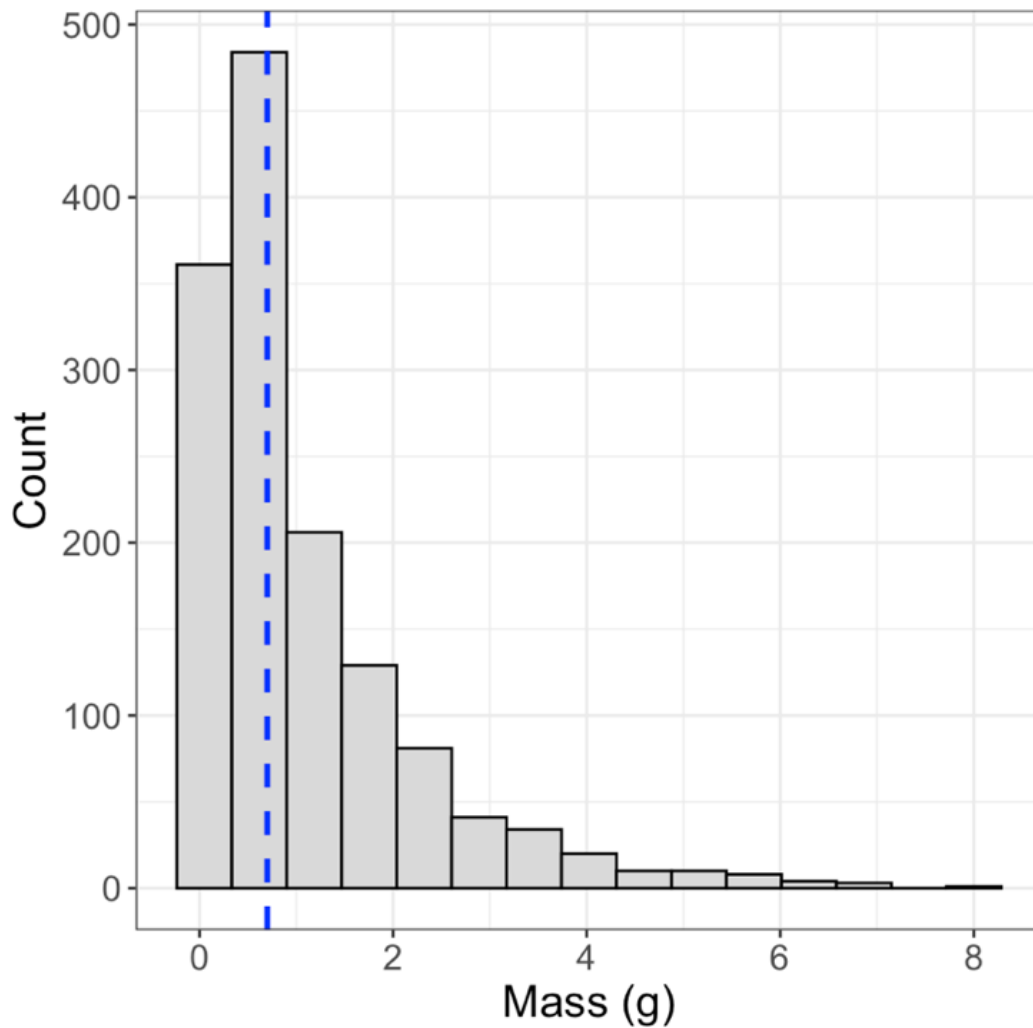


Figure 35: Mass frequency distributions of common bullies (*Gobiomorphus cotidianus*) at Millar Road wetland. Data comes from all 20 Gee's minnow traps which were set monthly from February 2025 to January 2026. The histogram summarises body mass variation among individuals recorded during the study ($n = 1,392$), with the dashed vertical line indicating the median body mass. The strongly right-skewed distribution reflects a high proportion of low-mass individuals and a small number of larger fish.

3.6.2 Seasonal abundance patterns

Monthly captures of common bullies showed pronounced seasonal variation across the sampling period (Figure 36). Captures were lowest during late summer and winter months, increased markedly from September, and peaked in late spring and early

summer. The highest number of captures was recorded in November, with elevated counts persisting through December and January before declining again in autumn.

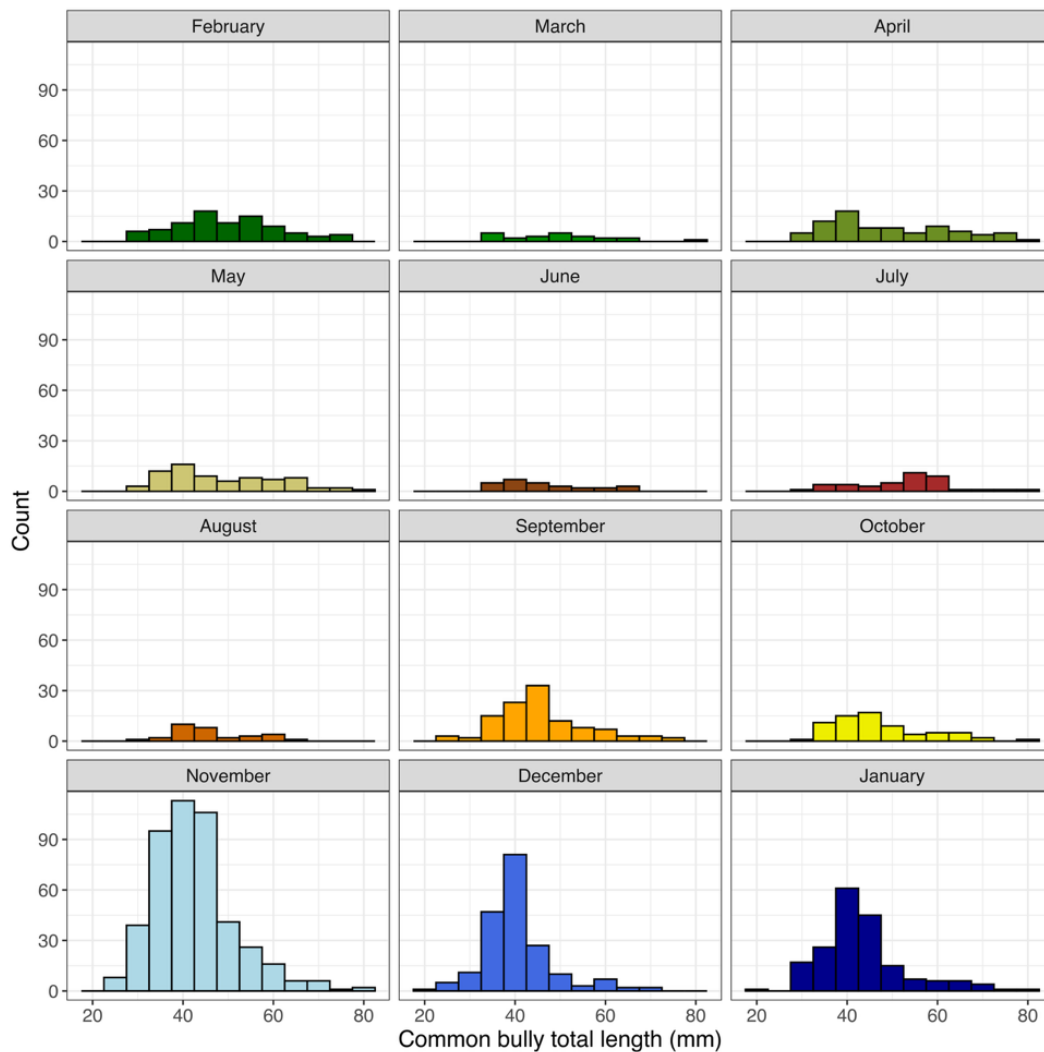


Figure 36: Monthly variation in size of common bullies (*Gobiomorphus cotidianus*) at Millar Road wetland. Data comes from all 20 Gee’s minnow traps which were set monthly from February 2025 to January 2026. Bars represent the total number of individuals recorded across all traps in each month, illustrating seasonal variation in relative abundance.

3.6.3 Co-occurrence with kōaro

Across 210 trap deployments, kōaro and common bullies co-occurred in 117 deployments (55.7 %; Figure 37). Kōaro were captured in the absence of common bullies in 34 deployments (16.2 %), while common bullies were captured without kōaro in 56 deployments (26.7 %). Neither species was recorded in 3 deployments (1.4 %).

Common bullies were present in 77.5 % of deployments in which kōaro were captured, while kōaro were present in 67.6 % of deployments in which common bullies were captured, indicating substantial spatial overlap in trap use by both species.

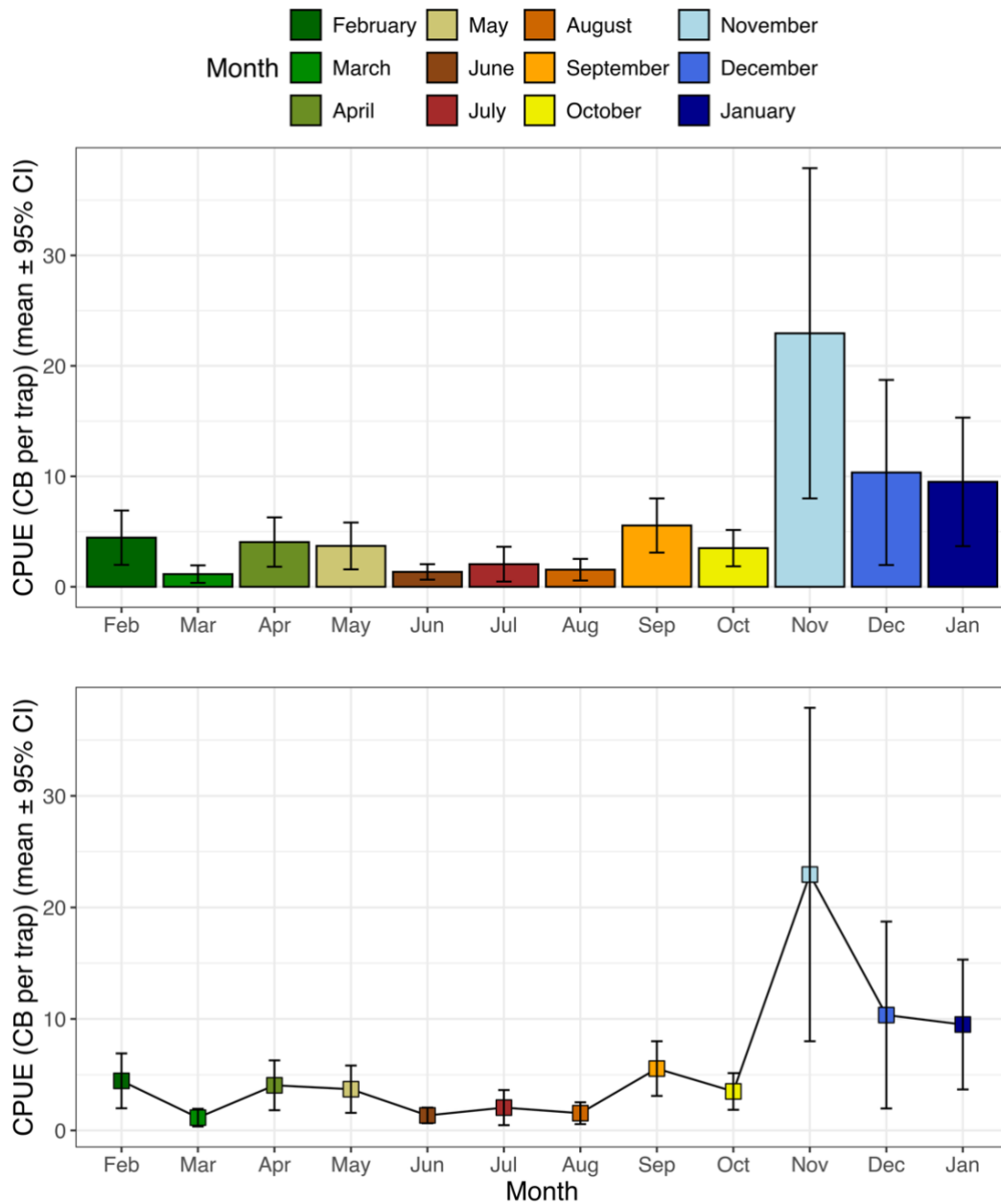


Figure 37: Monthly mean common bully (*Gobiomorphus cotidianus*) catch per unit effort (CPUE; individuals per trap per 24-hour sampling occasion) from February 2025 to January 2026. Bars and points show mean CPUE across traps, with error bars indicating 95 % confidence intervals.

Despite frequent co-occurrence, trap-level abundances of kōaro and common bullies were not significantly associated (Spearman's $\rho = -0.024$, $p = 0.728$, Figure 38).

Similarly, no relationship was detected between trap-month CPUE values for kōaro and common bullies (Spearman's $\rho = -0.024$, $p = 0.728$).

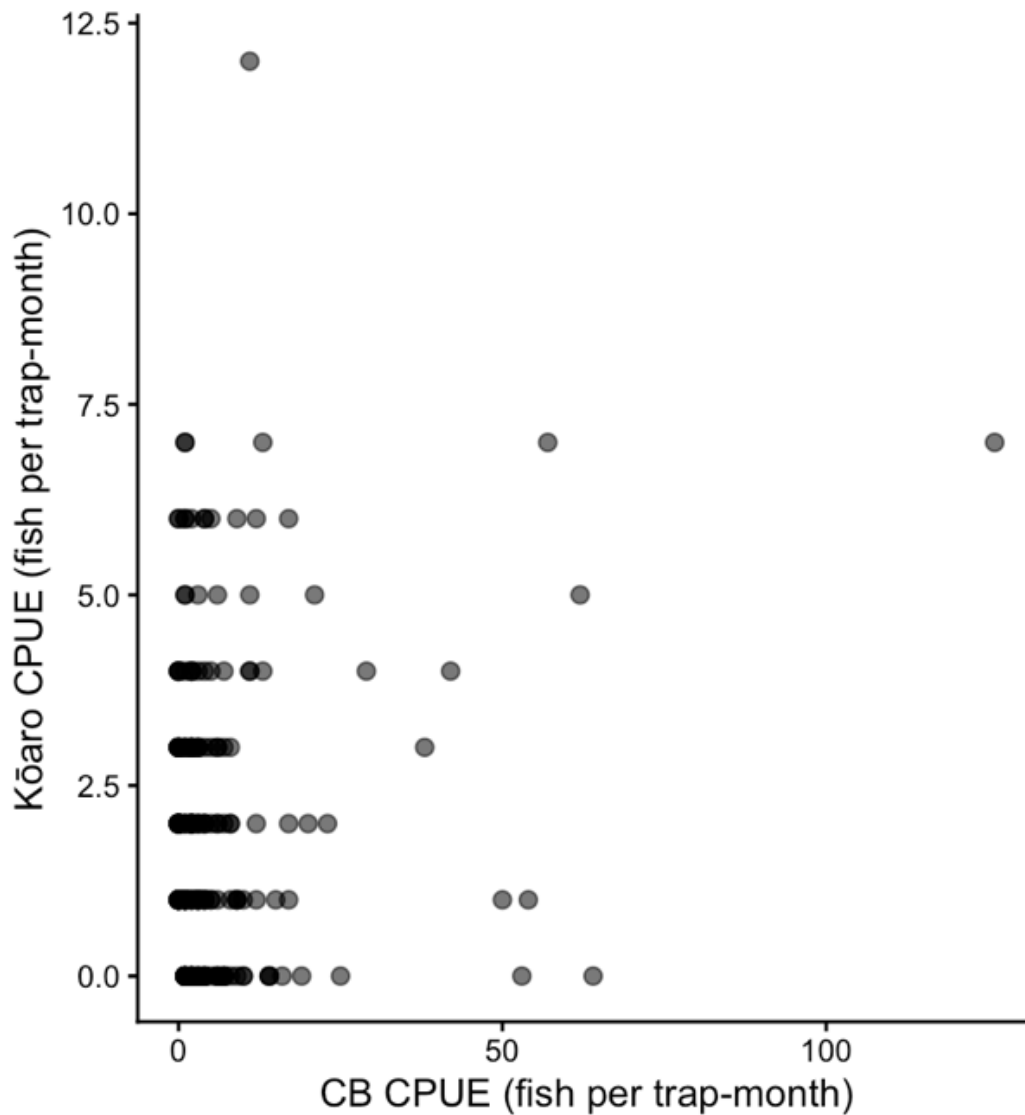


Figure 38: Relationship between kōaro (*Galaxias brevipinnis*) and common bully (*Gobiomorphus cotidianus*) catch per unit effort (CPUE) at the trap-month scale at Millar Road wetland. Each point represents one trap deployment in one month. CPUE values are expressed as per month. Data comes from all 20 Gee's minnow traps which were set monthly from February 2025 to January 2026.

3.6.4 Relative dominance and seasonal contrasts

Monthly totals showed marked variation in the relative numerical dominance of common bullies and kōaro across the sampling period (Figure 39). For example, in

November, 459 common bullies and 46 kōaro were recorded, whereas in March total captures were similar between species (23 common bullies and 26 kōaro).

Across most months, common bullies contributed a larger proportion of the combined catch than kōaro. Monthly bully:kōaro ratios ranged from 0.89 to 9.98, with the highest ratios occurring during late spring and summer (Figure 40).

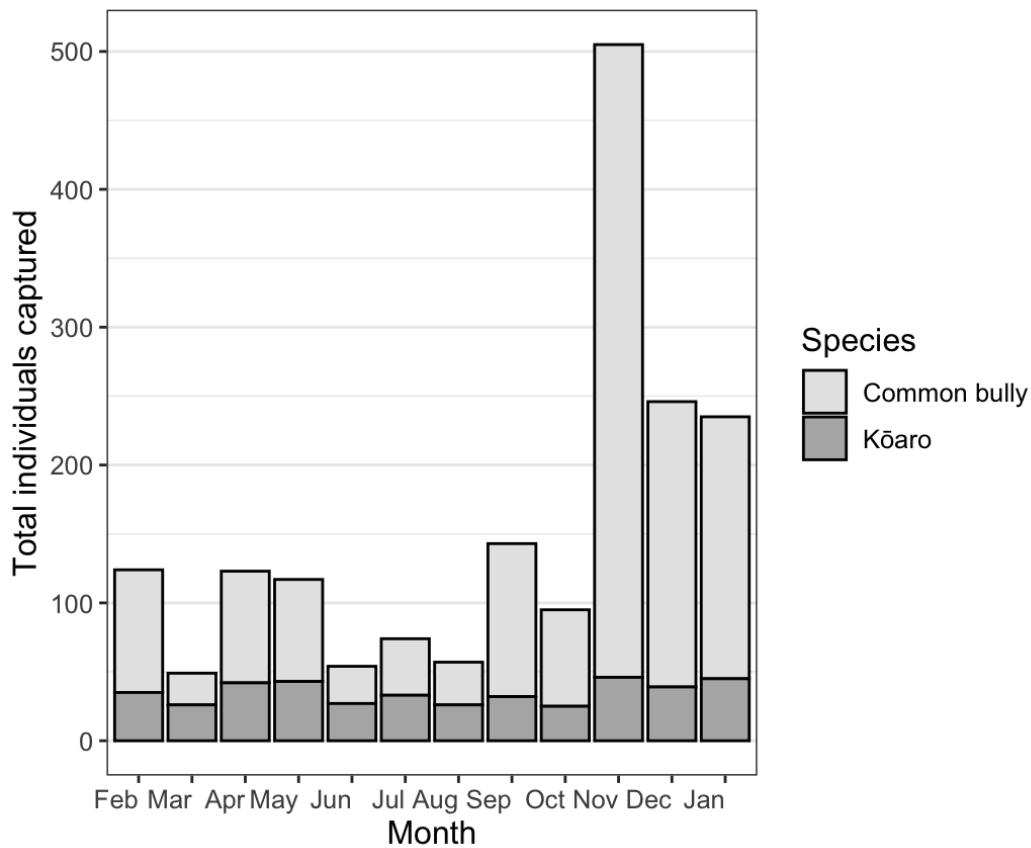


Figure 39: Monthly total counts of kōaro (*Galaxias brevipinnis*) and common bully (*Gobiomorphus cotidianus*) at Millar Road wetland. Data comes from all 20 Gee’s minnow traps which were set monthly from February 2025 to January 2026. Bars are stacked to illustrate seasonal variation in absolute abundance and relative numerical dominance between species.

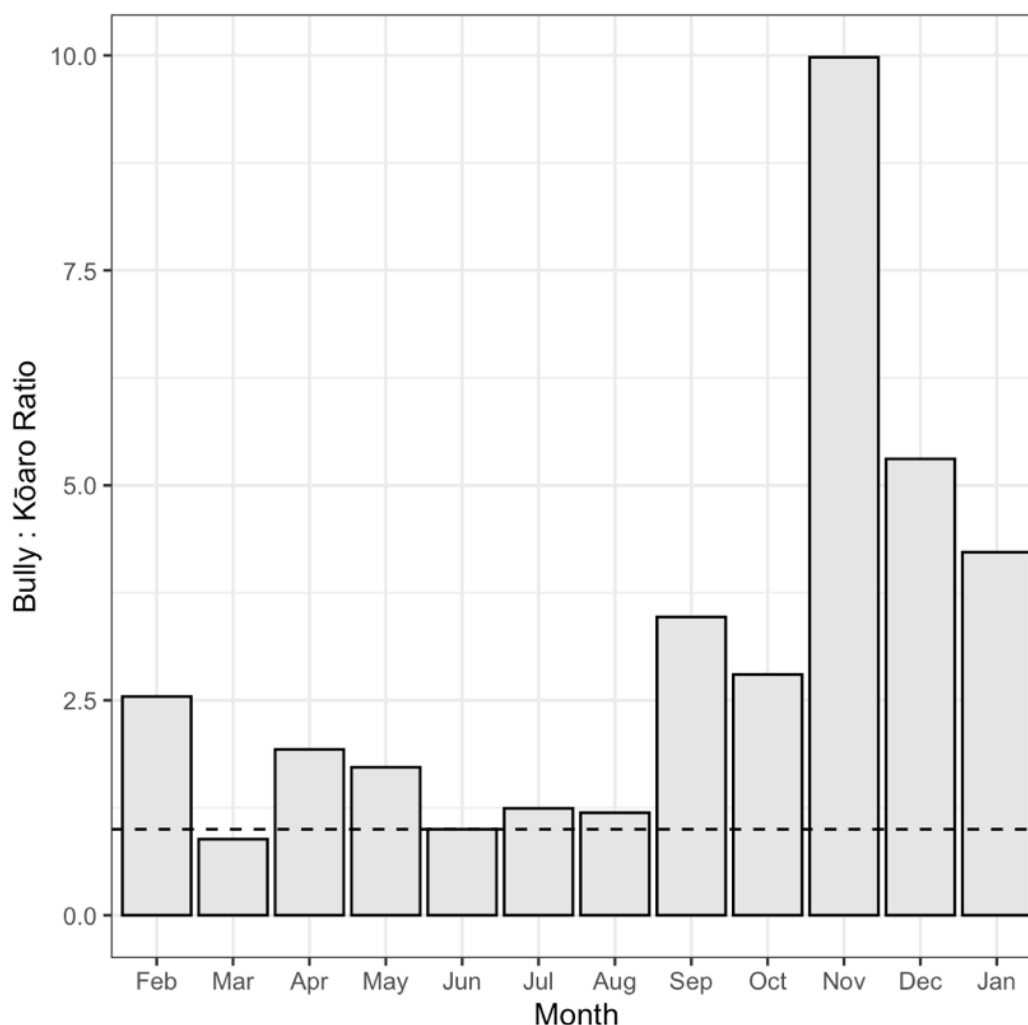


Figure 40: Monthly ratio of common bully (*Gobiomorphus cotidianus*) to kōaro (*Galaxias brevipinnis*) at Millar Road wetland. Data comes from all 20 Gee's minnow traps which were set monthly from February 2025 to January 2026. Values represent the total number of common bullies divided by the total number of kōaro recorded across all traps within each month. The dashed horizontal line indicates a ratio of 1, representing equal numerical abundance of the two species.

3.6.5 Common bully recruitment

Evidence of common bully recruitment was apparent from the seasonal occurrence of small individuals (≤ 32 mm total length) that comprised 7.5 % of total common bullies caught (Wilhelm et al., 2007). Juveniles were captured in eight of the twelve sampling months, indicating extended recruitment across the year rather than a single discrete pulse.

Juvenile proportions were highest during late spring and summer, peaking in November (10.2 % of captures, Figure 41), December (8.7 %), and January (9.5 %).

In contrast, juveniles were absent from captures in March and June and occurred at low frequencies during winter months. These patterns suggest that recruitment in MRW is seasonal, with strongest recruitment occurring during warmer months.

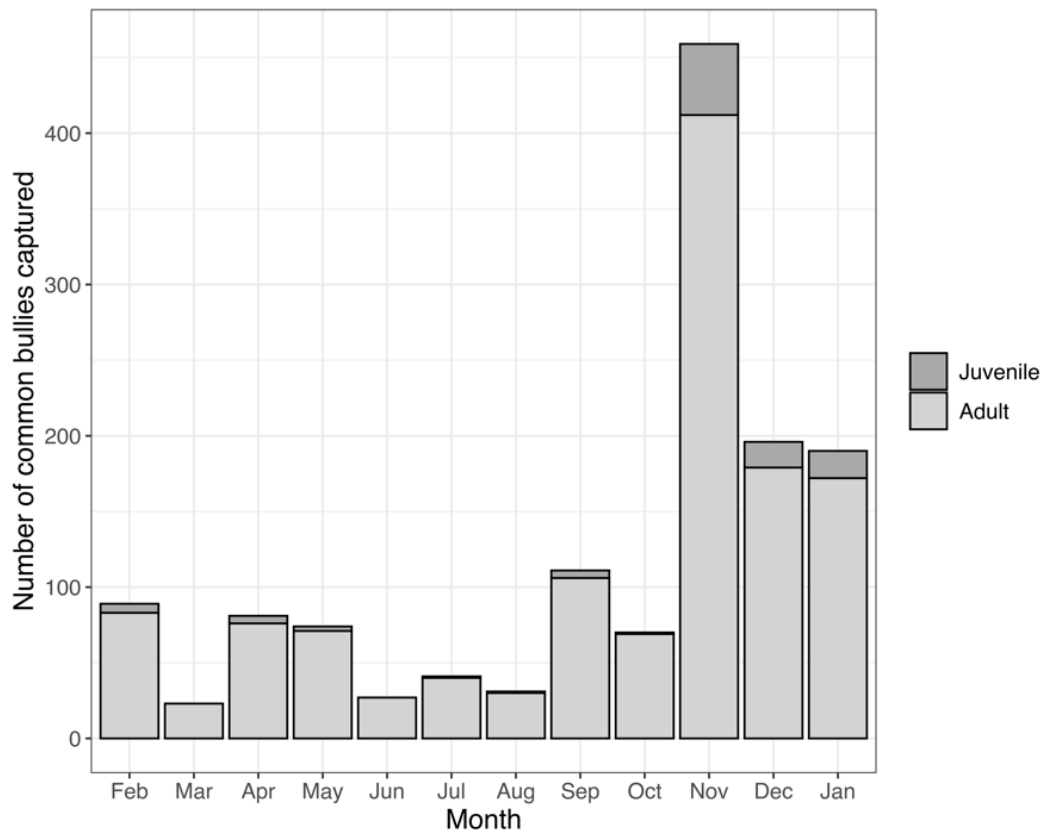


Figure 41: Monthly proportion of juvenile to adult common bullies (*Gobiomorphus cotidianus*) captured at the Millar Road wetland from February 2025 to January 2026. Juveniles were defined as individuals ≤ 32 mm total length. Bars represent the proportion of juveniles to adults within total monthly captures, illustrating seasonal variation in recruitment.

3.7 Kōura in MRW

3.7.1 Seasonal abundance

A total of 162 kōura (*Paranephrops planifrons*) were captured across the study period, spanning 12 monthly sampling occasions and 19 trap locations. Kōura were recorded in all months from February to January, although monthly abundance varied markedly (Figure 42).

Captures were lowest during late summer and winter (February - July), with between 2 and 4 individuals recorded per month. Abundance increased during spring and early summer, peaking in September (27 individuals), November (25 individuals),

December (23 individuals), and January (25 individuals), before declining again in late summer.

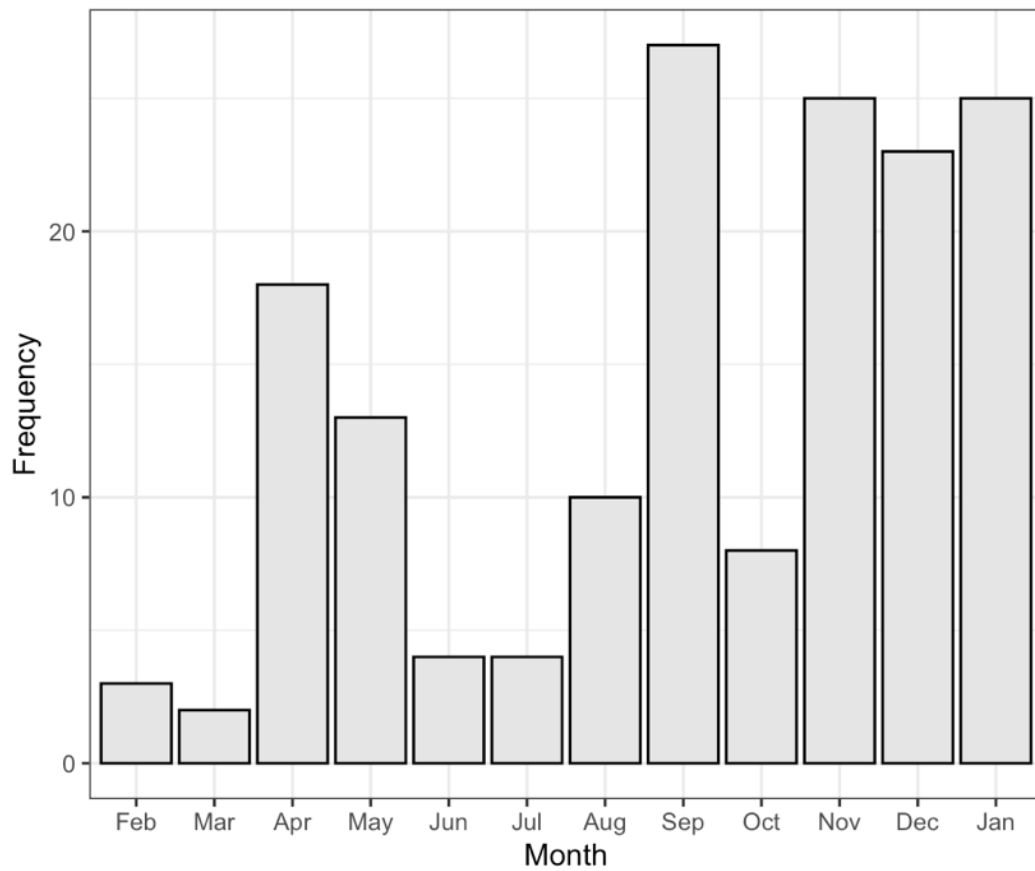


Figure 42: Monthly counts of kōura (*Paranephrops planifrons*) at Millar Road wetland. Data comes from all 20 Gee's minnow traps which were set monthly from February 2025 to January 2026. Bars represent the total number of individuals recorded on each monthly sampling occasion, illustrating seasonal variation in kōura abundance.

3.7.2 Size structure

Orbit–carapace length (OCL) was measured for all captured kōura. Overall OCL ranged from 7 to 28 mm (mean = 16.5 mm; SD = 4.54 mm; median = 16 mm), indicating the presence of multiple size classes within the population (Figure 43).

Monthly OCL distributions showed temporal variation, with smaller individuals more prevalent during autumn and winter months and larger individuals more frequently observed during spring and summer. Mean monthly OCL was highest in November (19.6 mm) and lowest in May (10.9 mm).

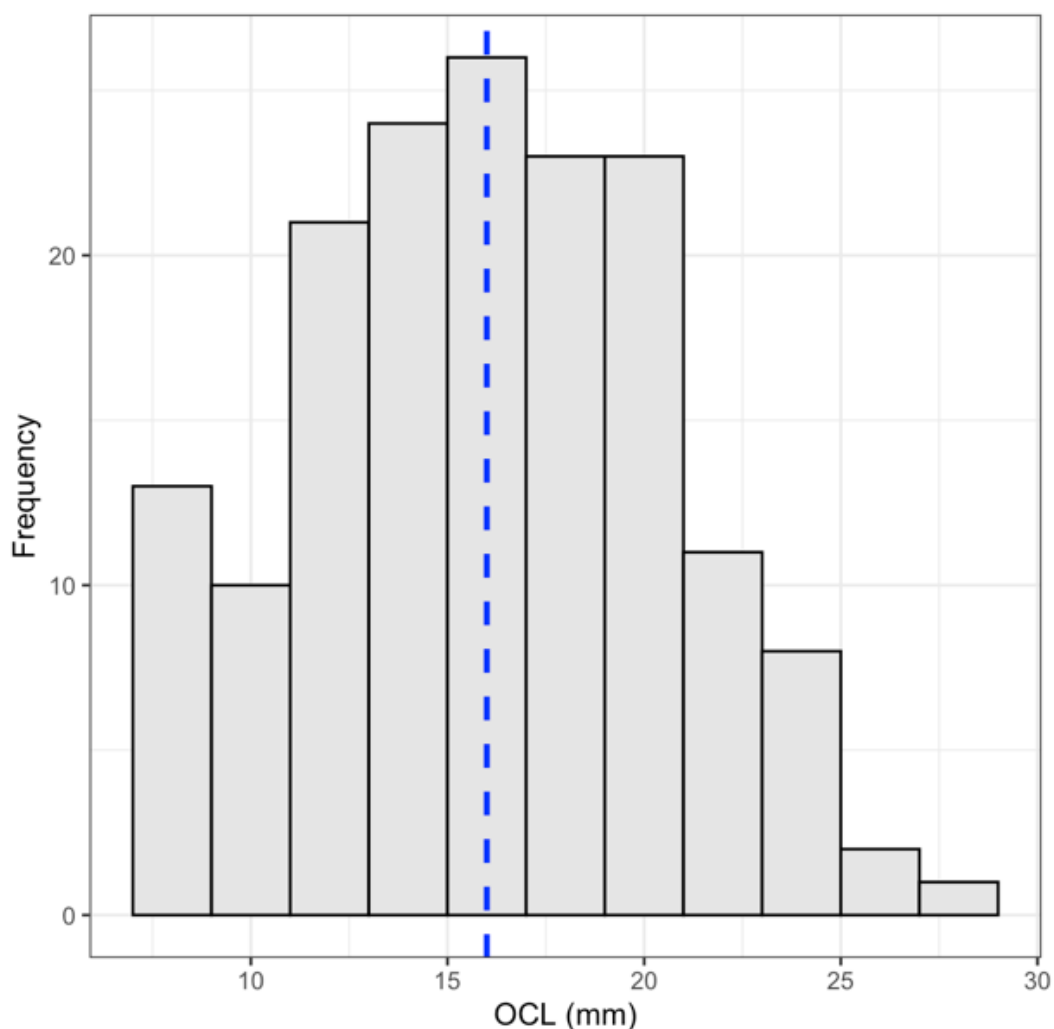


Figure 43: Distribution of orbit carapace length (OCL, mm) of kōura (*Paranephrops planifrons*) at Millar Road wetland. Data were obtained from all 20 Gee's minnow traps set monthly between February 2025 and January 2026 ($n = 162$). The histogram displays the frequency of individuals within successive OCL size classes, illustrating the size structure of the population across the sampled reach. The dashed blue vertical line indicates the mean OCL of the sampled population, providing a measure of central tendency relative to the observed size distribution.

Wet mass, estimated from OCL, ranged from 0.26 to 18.2 g (mean = 4.44 g; SD = 3.43 g; median = 3.26 g; Figure 44). Monthly mean mass broadly reflected patterns observed in OCL, with heavier individuals occurring more frequently during spring and summer months, particularly in November (mean = 6.88 g) and January (mean = 5.23 g).

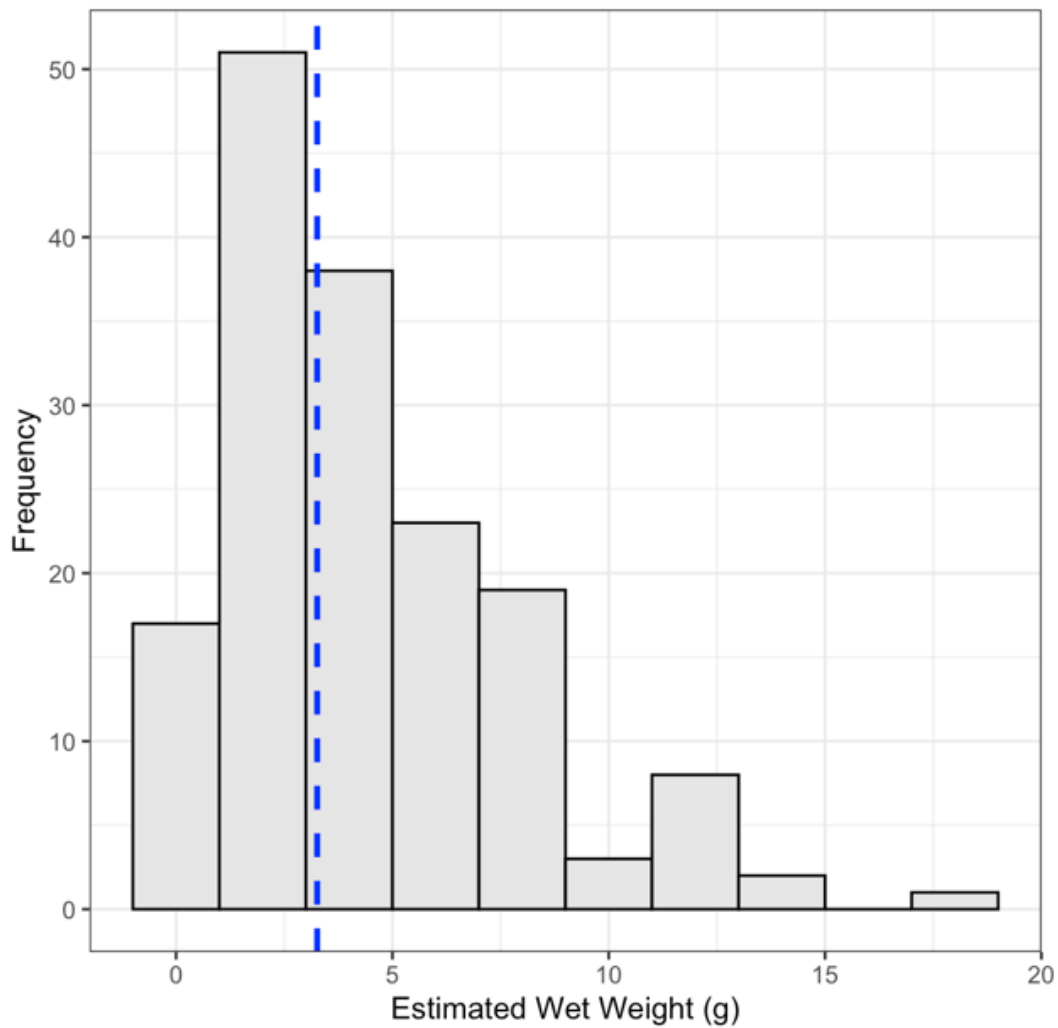


Figure 44: Distribution of wet mass for kōura (*Paranephrops planifrons*) at Millar Road wetland. Data comes from all 20 Gee’s minnow traps which were set monthly from February 2025 to January 2026. Mass values were estimated from orbit–carapace length (OCL) and illustrate seasonal variation in individual body size.

3.7.3 Recruitment patterns

Kōura recruitment was detected in 7 of the 12 months sampled, with juveniles (OCL ≤ 10 mm) present during late summer and autumn and intermittently throughout the year

(Figure 45). Recruitment was most pronounced between February and May, when juveniles comprised up to 31 % of monthly captures (May: 4 of 13 individuals).

In contrast, some months showed no detected juveniles despite moderate adult abundance, including April, October, and November. Overall, juveniles accounted for approximately 18 % of all kōura captures, and captures were dominated by smaller size classes.

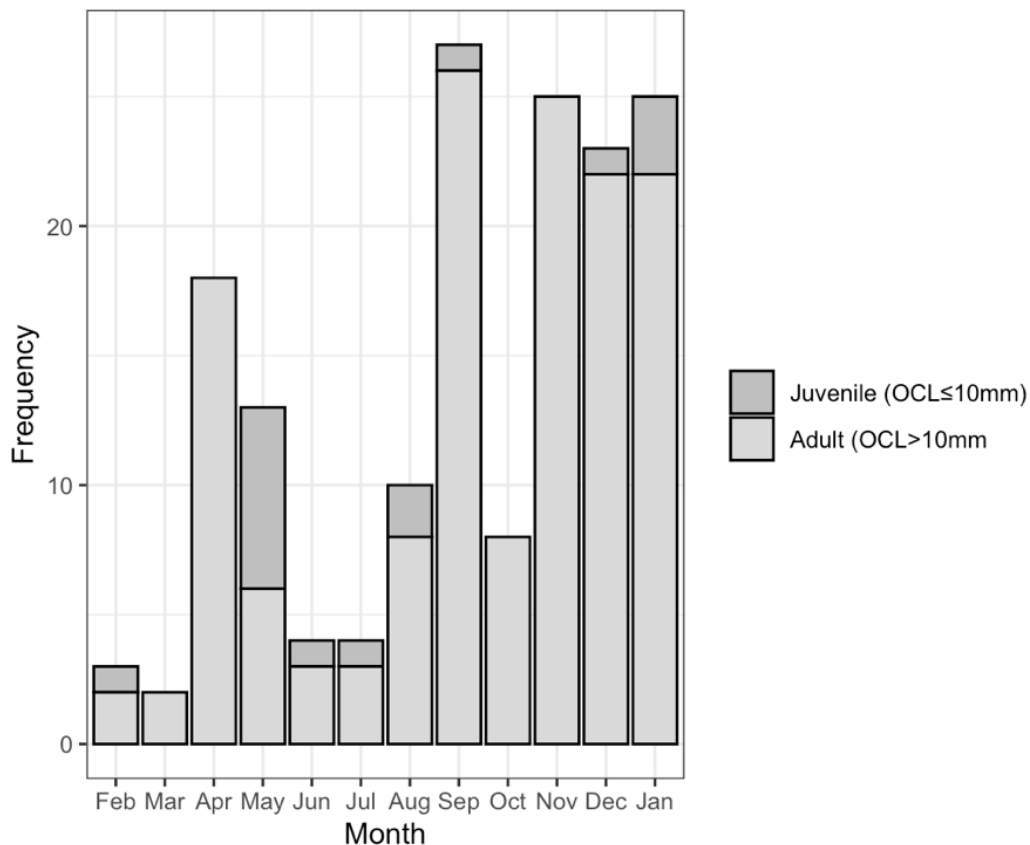


Figure 45: Monthly size-class composition of kōura (*Paranephrops planifrons*) at Millar Road wetland. Data comes from all 20 Gee’s minnow traps which were set monthly from February 2025 to January 2026. Stacked bars show the relative contributions of juvenile (OCL ≤ 10 mm) and adult (OCL > 10 mm) individuals to total monthly captures.

3.8 Rainbow trout in MRW

3.8.1 Occurrence and frequency

Rainbow trout (*Oncorhynchus mykiss*) were detected on three sampling occasions during the 12-month study period (Figure 46). Across these months, trout were

captured in a total of 11 trap-months, indicating infrequent occurrence within the wetland relative to native fish species.

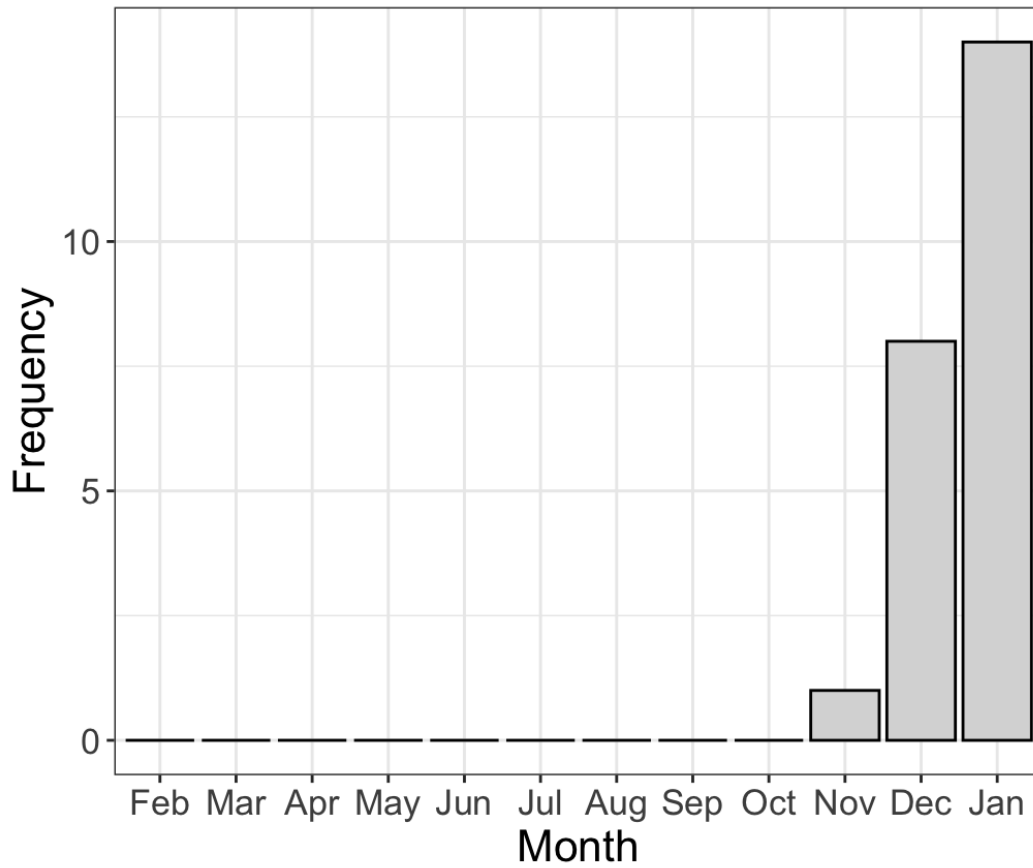


Figure 46: Frequency of rainbow trout (*Oncorhynchus mykiss*) detections at Millar Road wetland. Data comes from all 20 Gee's minnow traps which were set monthly from February 2025 to January 2026. Bars indicate sampling months in which trout were recorded.

A total of 23 trout were captured during the sampling period. Figure 47 shows total length ranged from 49 to 76 mm, with a mean (\pm SD) of 60.5 ± 7.5 mm and a median of 60 mm. The relatively low standard deviation indicates a narrow size distribution, with most individuals clustered around the 55 - 65 mm size class.

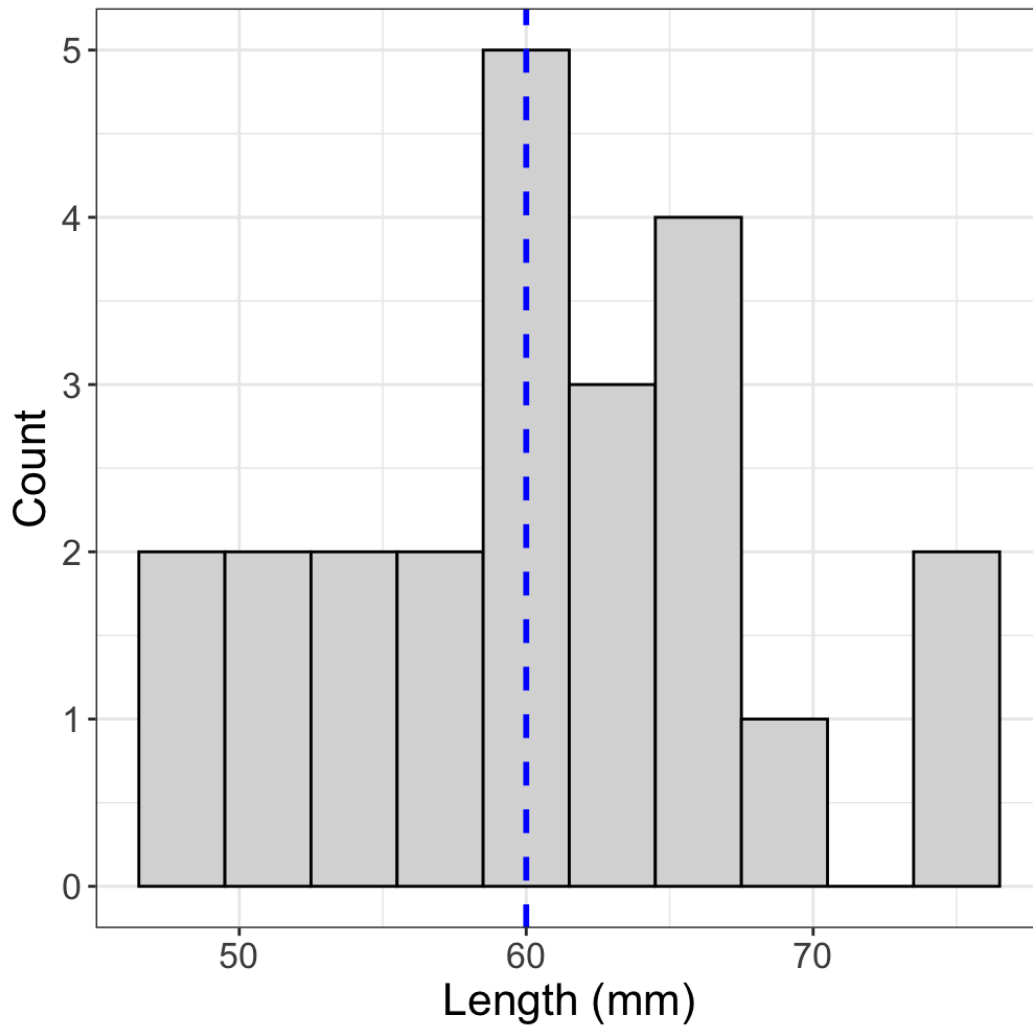


Figure 47: Length-frequency distribution of rainbow trout (*Oncorhynchus mykiss*) at Millar Road wetland. Data comes from all 20 Gee's minnow traps which were set monthly from February 2025 to January 2026. The histogram summarises the size structure of individuals recorded across the sampling period ($n = 28$), with the dashed vertical line indicating the median total length. The distribution shows a narrow size range.

Wet mass of trout ranged from 1.2 to 4.4 g, with a mean (\pm SD) of 2.4 ± 0.81 g and a median of 2.3 g ($n = 23$; Figure 48). The distribution of mass values was moderately right skewed, reflecting a dominance of lighter individuals. As with length, the range of mass values were narrow.

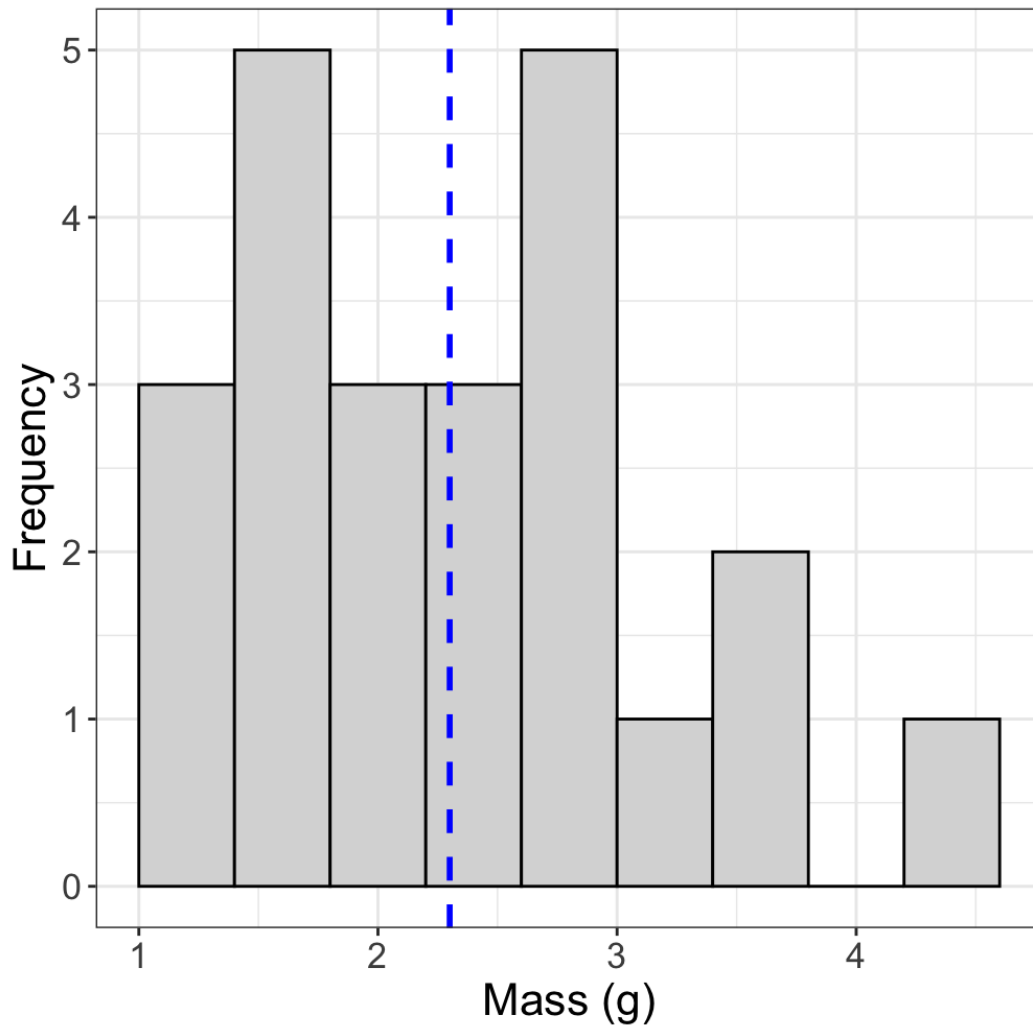


Figure 48: Mass-frequency distribution of rainbow trout (*Oncorhynchus mykiss*) at Millar Road wetland. Data were collected from Gee's minnow traps set monthly from February 2025 to January 2026. The histogram summarises the mass structure of individuals recorded across the sampling period ($n = 28$), with the dashed vertical line indicating the median mass. The distribution is slightly right skewed, reflecting a dominance of lighter individuals.

3.8.2 Spatial distribution

Trout detections were spatially clustered, with captures concentrated at upstream trap locations within the wetland (Figure 49). Few detections occurred at downstream traps, indicating a strong spatial gradient in trout occurrence along the wetland.

Spatial patterns in trout captures were further examined in relation to trap position along the wetland. Trout captures declined with decreasing trap position, with higher capture frequencies recorded at upstream traps and progressively fewer detections at downstream locations.

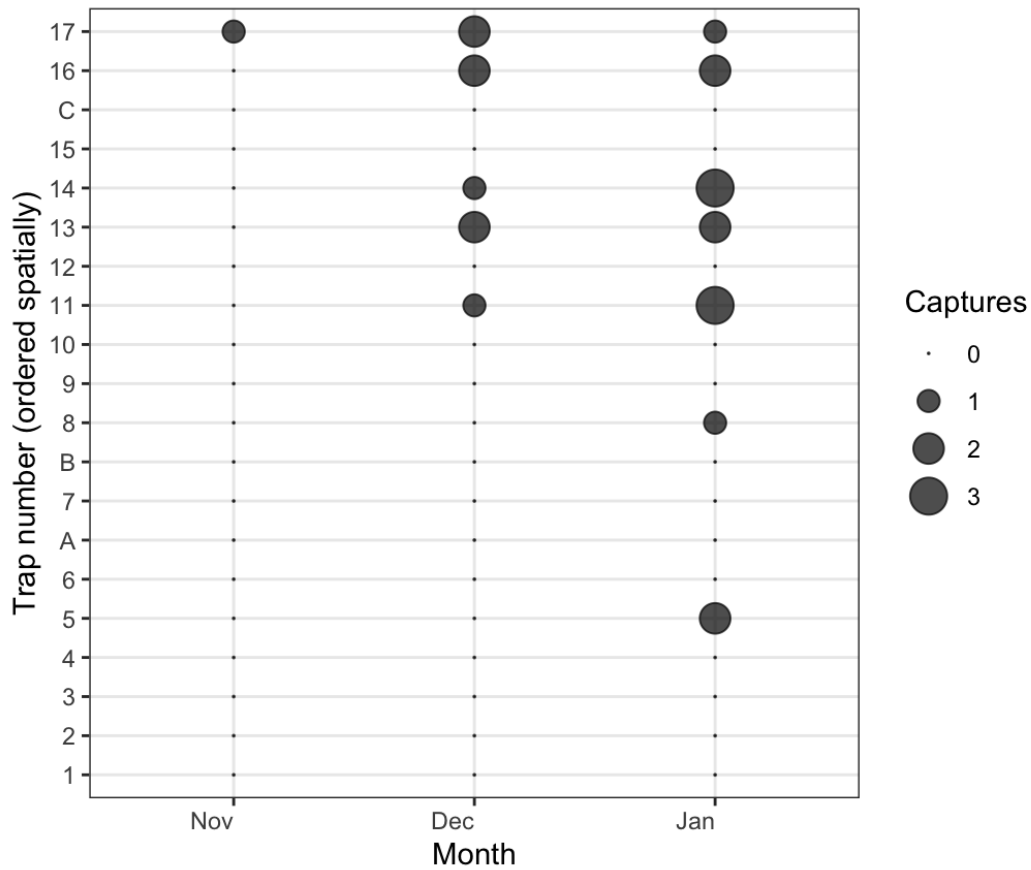


Figure 49: Spatial distribution and relative intensity of rainbow trout (*Oncorhynchus mykiss*) across the Millar Road wetland during 3 months in which trout were detected in the 20 Gee’s Minnow Traps between February 2025 and January 2026. Point size represents the number of trout captured per trap per month, with larger symbols indicating higher capture counts. Trap numbers are ordered spatially along the wetland from downstream to upstream.

3.8.3 Relationship with kōaro

Kōaro CPUE was compared between trap-months with and without trout detections. Kōaro were present in all trap-months irrespective of trout presence, and no significant difference in kōaro CPUE was detected between trout-present and trout-absent trap-months (Wilcoxon rank-sum test, $p = 0.19$).

3.8.4 Environmental drivers

Mixed-effects modelling indicated that trout CPUE increased with increasing lake level ($\beta = 3.35 \times 10^{-4} \pm 1.69 \times 10^{-4}$ SE, $p = 0.049$). When lake level was centred, predicted trout CPUE at mean lake level was low but non-zero, and between-trap variability was minimal, suggesting a system-wide hydrological influence on trout occurrence within the wetland. However, trout were detected in relatively few trap-month combinations

(n = 13), and the effect size was small ($p = 0.049$), indicating that this relationship should be interpreted cautiously.

3.9 Stable isotope analysis

I characterised the MRW food web using stable isotope analysis (SIA). The overall food web (Figure 50) showed a diversity of basal resources and invertebrate consumers. There appeared to be two dominant energy channels based on autochthonous production and allochthonous inputs. Important autochthonous basal resources with more depleted $\delta^{13}\text{C}$ values included biofilms, filamentous algae (Chlorophyta), and the pondweed *Potamogeton cheesemanii*. In contrast, allochthonous basal resources with a more enriched $\delta^{13}\text{C}$ value included coarse particulate organic matter from trees (*Salix* sp.), ground ferns (*Blechnum novae-zealandiae*) and raupō (*Typha orientalis*). Fine benthic organic matter was also sampled with more enriched $\delta^{13}\text{C}$ values. Two terrestrial plants (a grass *Dactylis glomerata* and an herb *Lotus pedunculatus*) were included in the SIA for reference but these were relatively uncommon plants and likely unimportant to the MRW food web.

The basal resources helped to sustain a variety of invertebrate consumers (Figure 50). The invertebrates with more depleted $\delta^{13}\text{C}$ values suggesting greater reliance on autochthonous carbon sources included the hydroptilid caddisfly *Oxyethira*, true fly larvae from the families Chironomidae, Simuliidae, and Limoniidae (*Limonia* sp.), freshwater molluscs (the snails *Potamopyrgus antipodarum*, *Austropeplea tomentosa*, and the pea clam *Sphaerium novaezealandiae*), and scirtid beetle larvae. Predatory invertebrates seemingly more reliant on these prey included tanypod true fly larvae (Chironomidae) and the caddisfly *Psilochorema* sp. Another predatory invertebrate with a relatively depleted $\delta^{13}\text{C}$ value was the dragonfly nymph *Hemicordulia australiae*. The depleted $\delta^{15}\text{N}$ value for this predator suggested that its likely prey (e.g., microcrustaceans feeding on biofilms) were not characterised by SIA.

Invertebrates with more enriched $\delta^{13}\text{C}$ values suggesting greater reliance on allochthonous carbon sources included larval caddisflies (*Triplectides* sp.) and the dixid midge *Paradixa fuscinervis*. Adult caddisflies also had more enriched $\delta^{13}\text{C}$ values due to dominance of obligate shredders including the leptocerid *Triplectides dolichos* and the oeconesid *Oeconesus maori*. Adult moths too had more enriched $\delta^{13}\text{C}$ values but depleted $\delta^{15}\text{N}$ values helping to discriminate them from the caddisflies. The

predatory pond skater *Microvelia macregori* also had more enriched $\delta^{13}\text{C}$ values but relatively depleted $\delta^{15}\text{N}$ values, suggesting that it preys mainly on terrestrial insects like moths trapped on the water surface. The omnivorous kōura (*Paranephrops planifrons*) possessed more enriched $\delta^{13}\text{C}$ and $\delta^{15}\text{N}$ values, suggesting that it consumes animal matter in addition to terrestrial detritus. Other predatory invertebrates with relatively enriched $\delta^{13}\text{C}$ values included the polycentropodid caddisfly *Polypsectropus* sp. and the lycosid spider *Anoteropsis* sp.

The two fish species assessed at the time of sampling were kōaro (*Galaxias brevipinnis*) and the common bully (*Gobiomorphus cotidianus*). To further assess the differences in their trophic niches using SIA (Figure 50), I first plotted standard ellipses (Figure 51) and calculated the standard ellipse area (SEA) using Bayesian inference (Figure 52). There was no significant difference in the area occupied in the isospace for the two fish species ($P = 0.182$), suggesting the same extent of individual variation. However, the degree of trophic overlap was asymmetric, indicating that the two species were partitioning trophic niche space (Figure 51). Using Bayesian inference, I estimated the degree of trophic overlap as being $15.7\% \pm 5.3\%$ (1 standard deviation).

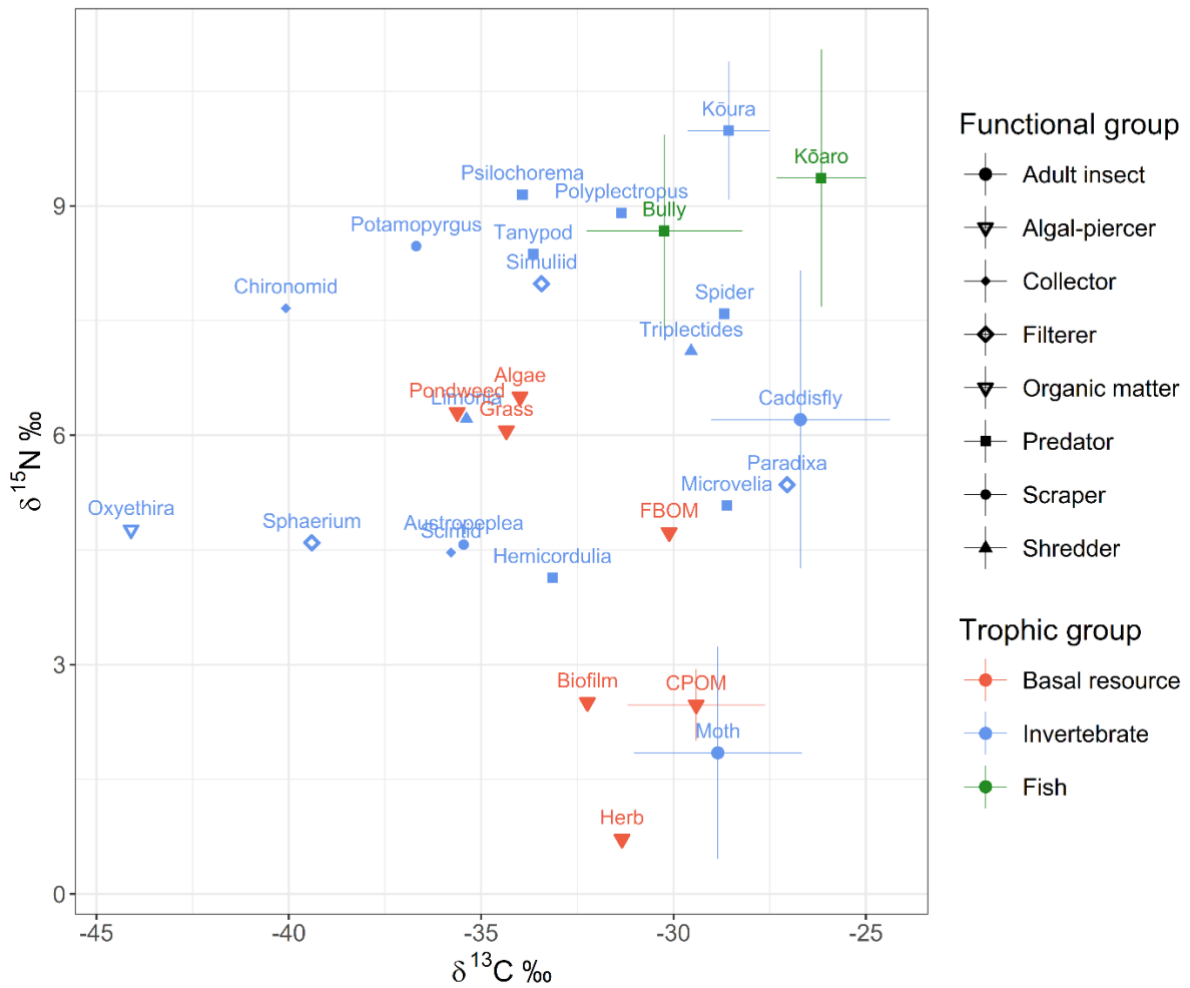


Figure 50: Stable isotope biplot of $\delta^{13}\text{C}$ and $\delta^{15}\text{N}$ (‰) describing the Millar Road Wetland food web on the margins of Lake Ōkāreka. Error bars (± 1 standard deviation) are shown to indicate variation in stable isotope ratios for selected food web components. Symbols indicate functional groups (including invertebrate functional feeding groups), colours indicate broad trophic groups (basal resources, invertebrates, fish). Kōaro, *Galaxias brevipinnis*; Bully, *Gobiomorphus cotidianus*; Kōura, *Paranephrops planifrons*; Caddisfly, including *Leptoceridae* and *Oeconesidae*; Moth, including *Oecophoridae* and *Noctuidae*; FBOM, fine benthic organic matter; CPOM, coarse particulate organic matter.

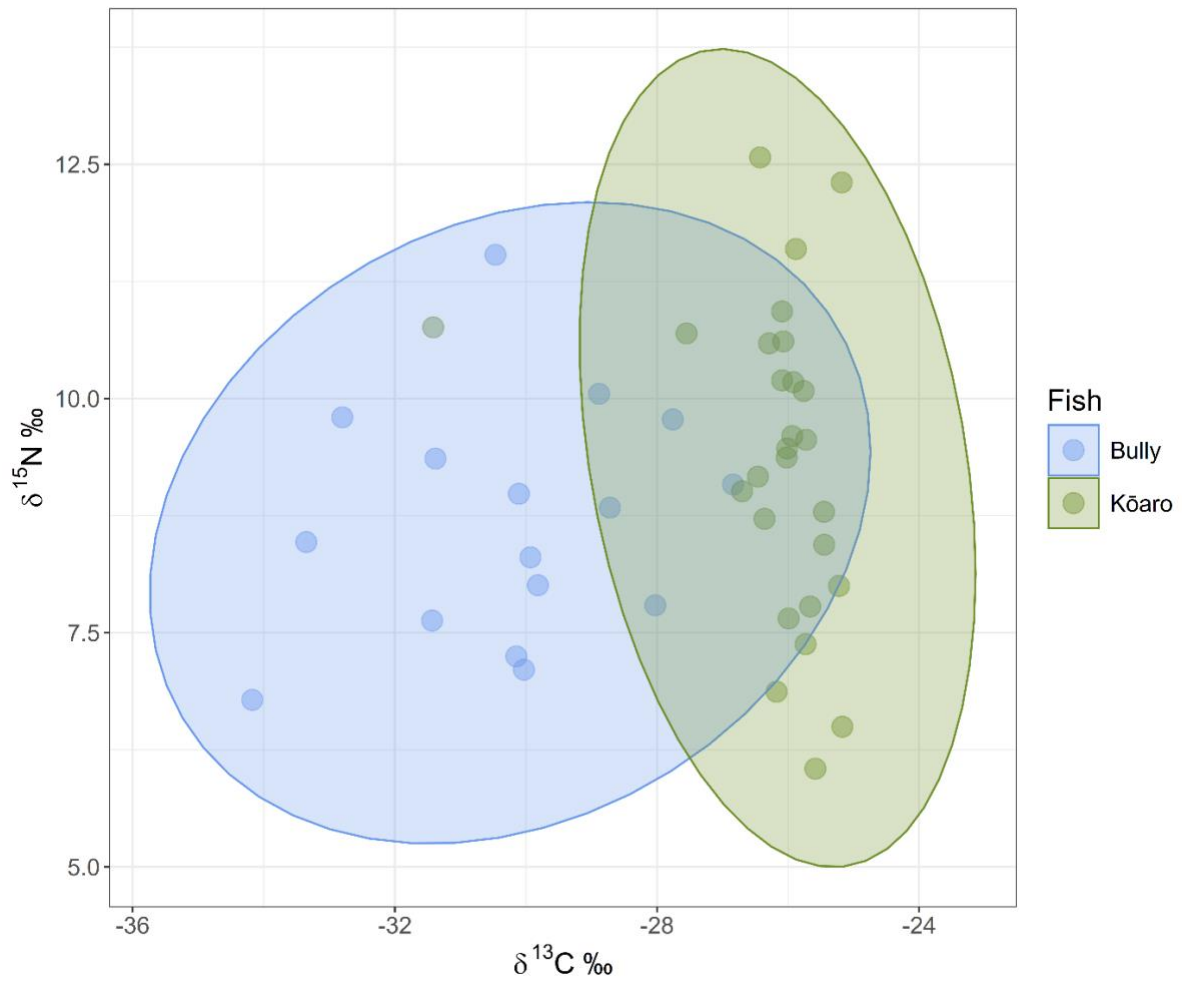


Figure 51: Stable isotope biplot of $\delta^{13}\text{C}$ and $\delta^{15}\text{N}$ (‰) describing the individual variation in fish (Kōaro, *Galaxias brevipinnis*; Bully, *Gobiomorphus cotidianus*) in the Millar Road Wetland food web. Each point represents an individual fish. Standard ellipses indicate the 95 % confidence interval.

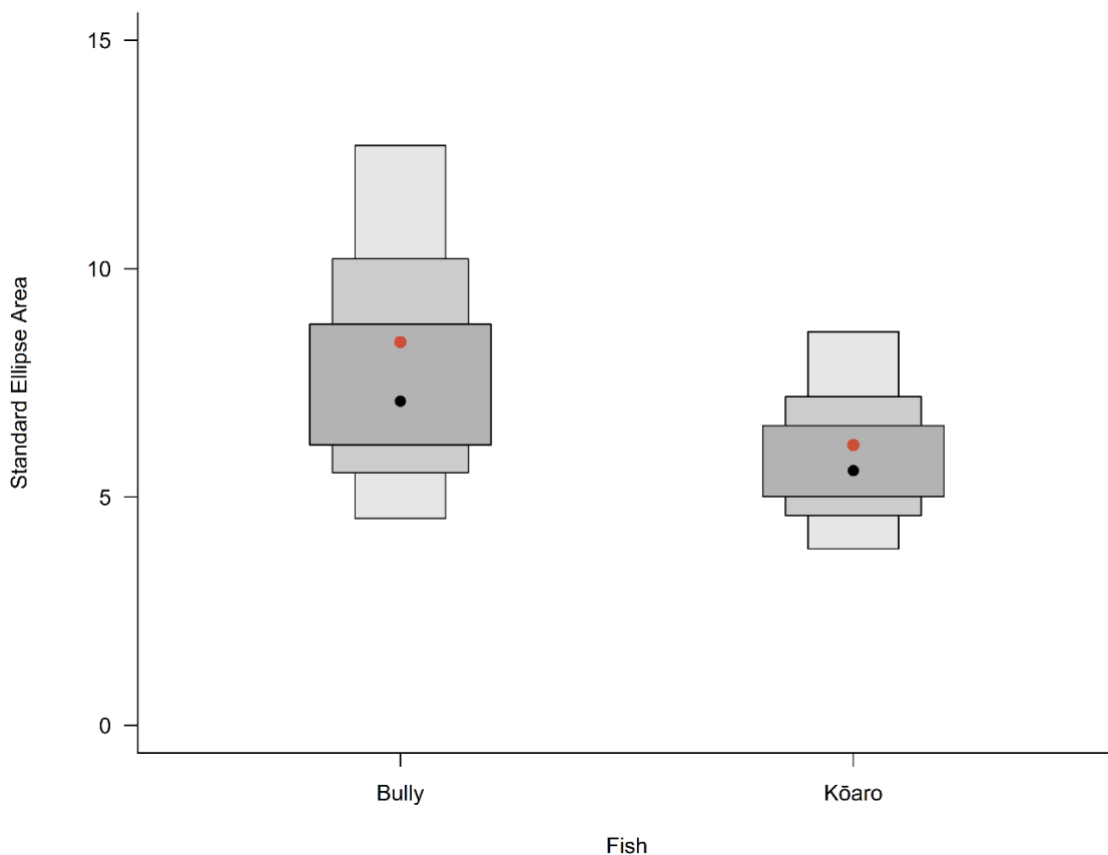


Figure 52: Boxplot describing the variation in the Bayesian Standard Ellipse Area (%²) for individual kōaro (*Galaxias brevipinnis*; and common bully, *Gobiomorphus cotidianus*) in the Millar Road Wetland food web. Boxes indicate the 50 %, 95 % and 99 % credible intervals. The black dot indicates the mode for the estimated values of Bayesian Standard Ellipse Area (%²). The red dot indicates the maximum-likelihood (ML) estimated Standard Ellipse Area (%²) corrected for sample size (SEA-c).

To further test the hypothesis that kōaro were partitioning food resources to coexist with common bully in MRW, I selected four putative invertebrate prey sources (Figure 53). Due to their relative abundance and biomass, these prey could dominate the energetic pathways leading to fish in the MRW food web. I used Bayesian inference in mixing models to help determine the proportion of each prey contributing to the diets of kōaro and common bully (Figure 54). Kōaro appeared to be highly reliant on adult caddisfly, with this group accounting for nearly 70 % of their diet (Figure 54). In contrast, common bully were highly reliant on midge larvae, with this group accounting for 75 % of their diet (Figure 55). To better understand the underlying sources of energy contributing to the diet of kōaro and common bully in MRW, I also modelled sources of autochthonous and allochthonous carbon using basal resources (Figure 53). The results of these mixing models showed that kōaro were more reliant on

allochthonous energy sources, accounting for nearly 100 % of their diet (Figure 55) Common bullies were by contrast far more reliant on autochthonous energy sources, with over 90 % of the diet coming from these carbon sources (Figure 54). The credible intervals derived from the Bayesian analyses supported these summaries (Appendix D Stable Isotope Analysis, Table 9 & Table 10).

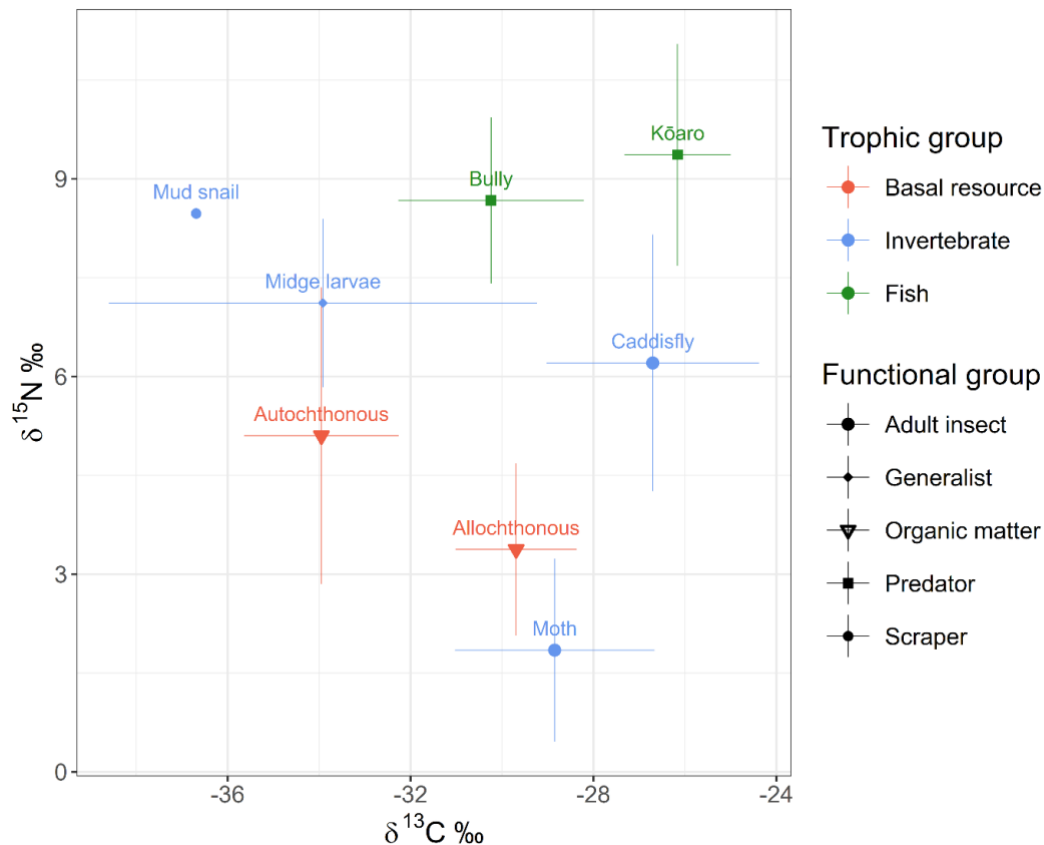


Figure 53: Stable isotope biplot of $\delta^{13}\text{C}$ and $\delta^{15}\text{N}$ (‰) describing putative prey and carbon sources used by fish (Kōaro, *Galaxias brevipinnis*; Bully, *Gobiomorphus cotidianus*) in the Millar Road Wetland food web. These sources were used in Bayesian mixing models. Error bars (± 1 standard deviation) are shown to indicate variation in stable isotope ratios for selected food web components. Symbols indicate functional groups (including invertebrate functional feeding groups), colours indicate broad trophic groups (basal resource, invertebrates, fish). Mud snail, *Potamopyrgus antipodarum*; Midge larvae, *Chironomidae*, *Simuliidae*, *Dixidae*, and *Limoniidae*; Caddisfly, including adult *Leptoceridae* and *Oeconesidae*; Moth, including *Oecophoridae* and *Noctuidae*; Autochthonous, organic matter including biofilms, filamentous algae (*Chlorophyta*), and *Potamogeton cheesemani*; Allochthonous, organic matter including fine benthic organic matter (FBOM) and coarse particulate organic matter (CPOM).

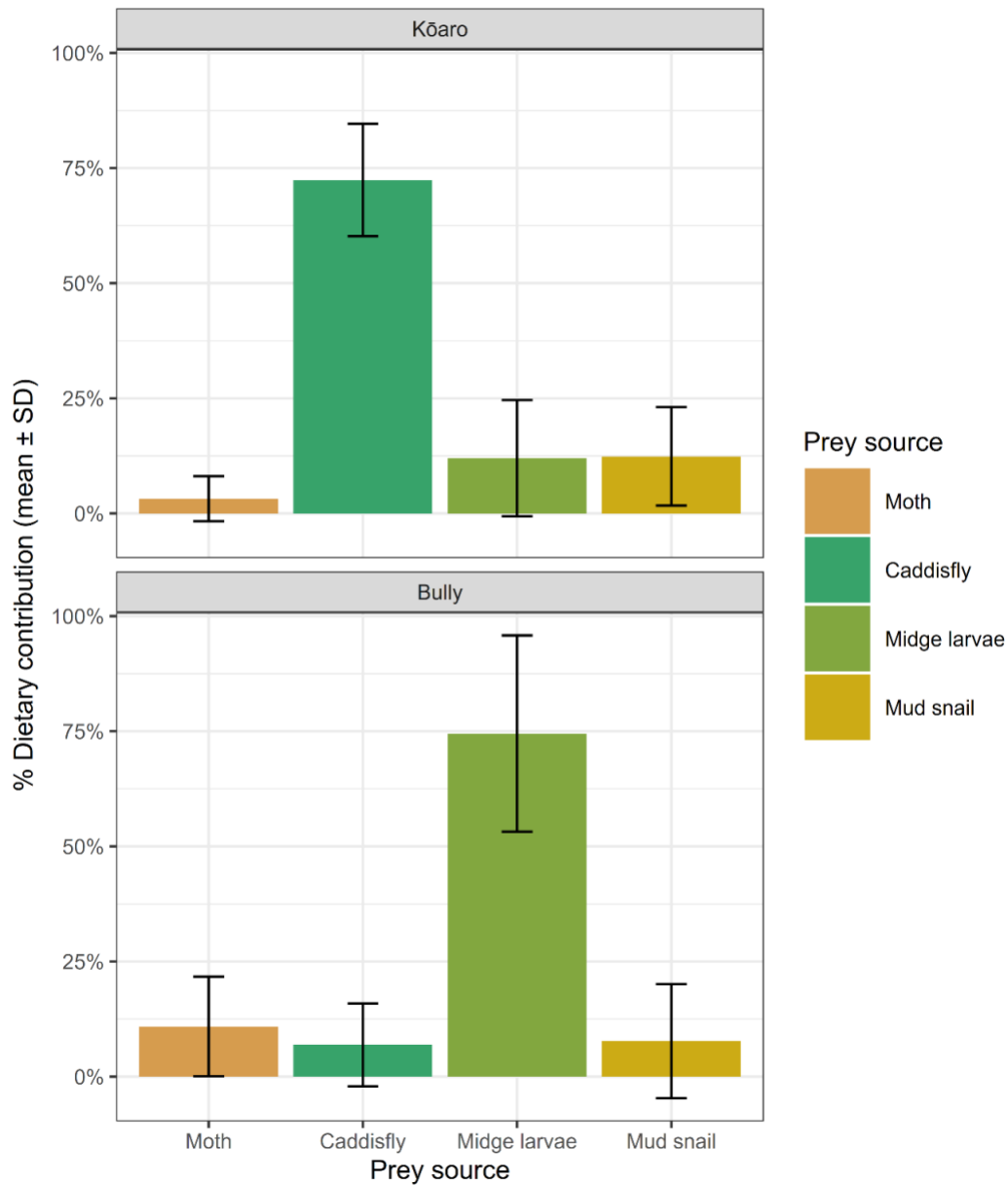


Figure 54: Dietary contribution (mean \pm 1 standard deviation) of different prey sources to kōaro (*Galaxias brevipinnis*) and common bully (*Gobiomorphus cotidianus*) in the Millar Road Wetland food web estimated by a Bayesian mixing model. See Appendix 6.4 for credible intervals from the mixing model.

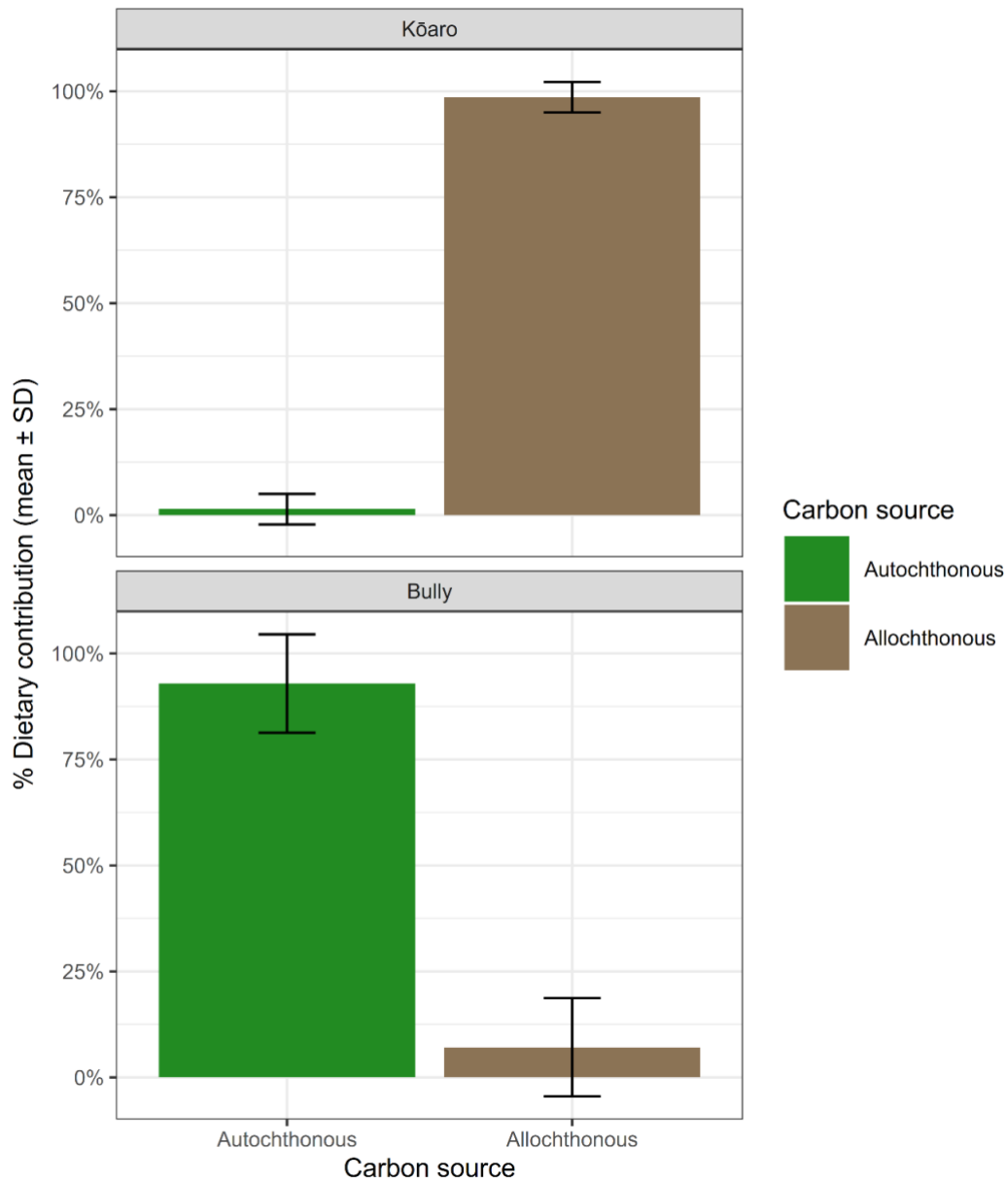


Figure 55: Dietary contribution (mean \pm 1 standard deviation) of different carbon sources to kōaro (*Galaxias brevipinnis*) and common bully (*Gobiomorphus cotidianus*) in the Millar Road Wetland food web estimated by a Bayesian mixing model. See Appendix 6.4 for credible intervals from the mixing model.

Discussion

In my study, I sought to describe the demographics and trophic ecology of the kōaro (*Galaxias brevipinnis*) population in the Millar Road Wetland (MRW). The MRW is a natural wetland located on the north-west shoreline of Lake Ōkāreka in the Rotorua, Te Arawa Lakes region. The kōaro population in the MRW is notable because the wetland does not conform to the typical habitat associated with this galaxiid species. However, with Lake Ōkāreka supporting a remnant population of kōaro (Kusabs, 2019; Rowe, Smith & Grayling, 2008), found by Young (2002) to be relatively abundant compared to Lake Tarawera, the MRW metapopulation may be an important source of breeding adults for the lake. I found that the MRW supports a relatively large number of adult kōaro throughout the year. The recruitment of juveniles to the wetland was more equivocal, but during my sampling I found evidence for a March peak. Kōaro in the wetland appear to coexist with common bullies (toi toi, *Gobiomorphus cotidianus*), and stable isotope analysis indicated niche partitioning, with each species favouring different prey and energetic pathways. The appearance of juvenile rainbow trout (*Oncorhynchus mykiss*) in traps during the summer of 2025/2026 was of concern, because this non-native species is known to compete with and prey upon native fish, including kōaro. In my discussion, I revisit my four key hypotheses and further consider interesting features of the kōaro population in the MRW, including the broader community and ecosystem context of this unique habitat.

4.1 H1: Demographic function of the wetland

My first hypothesis (H1) proposed that isolated wetlands with restricted hydrological connectivity would function as demographic sinks, supporting transient individuals rather than resident populations. Under this expectation, kōaro abundance within MRW would reflect temporary occupancy, with recruitment occurring elsewhere in the lake system. Alternatively, if MRW functions as a refuge habitat, it should support a persistent adult population exhibiting seasonal recruitment and multi-year stability.

The demographic evidence from this study supports the refuge interpretation rather than the demographic sink expectation. Kōaro were detected in over 70 % of trap-months and occurred across all seasons, indicating consistent spatial occupancy

rather than episodic use. Seasonal variation in CPUE was evident, with higher catch rates in late summer and lower values in spring; however, these fluctuations most plausibly reflect seasonal changes in activity, detectability, and habitat redistribution rather than population instability. CPUE patterns were consistent across both the initial 12-trap array and the expanded 20-trap dataset, indicating that temporal trends were not artefacts of sampling design.

Size structure further supports the presence of a resident, internally structured population. Individuals ranged from 39 to 160 mm total length, and multiple size classes were present throughout the sampling period. Smaller individuals were most prevalent in late summer and early autumn, with a March peak consistent with the extended December-April spawning period reported for lacustrine kōaro (Young, 2002; Kusabs, 1989). Recruitment timing in MRW appeared later than peaks reported for Lake Taupō tributaries, where juvenile migration was strongest between August and November (Kusabs, 1989; Young, 2002). In contrast to those well-connected stream systems, MRW is a relatively shallow, low-velocity wetland where hydrological connectivity to the lake is intermittent and spatially constrained. Delayed or protracted recruitment signals may therefore reflect wetland-specific dynamics, including slower larval ingress, altered growth rates under lentic conditions, or seasonal expansion of inundated habitat. Notably, the 2024/2025 summer was relatively dry, and lake levels remained low through much of the recruitment period. If larval ingress depends on surface-water connectivity between Lake Ōkāreka and MRW, reduced lake levels may have delayed or limited successful entry into the wetland until water levels rose sufficiently to reconnect marginal habitats. In this context, the March peak in smaller individuals may reflect hydrologically mediated recruitment timing rather than intrinsic shifts in spawning phenology.

Additionally, adult cannibalism of juveniles, documented by Kusabs (1989), may further reduce detectable juvenile abundance within confined habitats, dampening early recruitment peaks and contributing to the apparent shift in seasonal timing. Although juveniles (<70 mm) comprised a modest proportion of the total population, their repeated detection indicates ongoing recruitment. The absence of statistically significant month-to-month differences in juvenile proportion likely reflects limited sample sizes and potential under-sampling of small individuals, rather than absence of recruitment dynamics.

Mark–recapture results provide further evidence of persistence within MRW. Approximately 48 % of PIT-tagged individuals were recaptured at least once following tagging, with a mean per-occasion recapture probability of ~35 %. Most recaptures occurred at the same trap location, movement distances between successive detections were limited, and individuals exhibited continued growth across spring and early summer. Together, these patterns indicate partial site fidelity and short to medium term residency within the wetland rather than transient occupancy.

Recapture probabilities of this magnitude are comparable to or higher than those reported for passive trapping studies of small-bodied freshwater fishes (e.g., ~21 % in a similar mark–recapture study by Ruetz et al. (2015)) and align with findings from Mitsuo et al. (2013), who documented relatively stationary behaviour with a tendency for localised upstream movement in a freshwater fish species. These patterns are consistent with moderate short-term retention within the sampled reach. Although higher detection probabilities have been reported for kōaro in Lake Taupō tributaries (McEwan & Joy, 2011), those studies employed continuous antenna arrays rather than discrete trapping events. Antenna-based systems typically detect movement more reliably than passive trapping gear (Greenberg & Giller, 2000). However, mark–recapture studies often report substantial numbers of non-recaptured individuals, which may reflect mobility rather than mortality (Gowan et al., 1994, cited in Greenberg & Giller, 2000). While some movement beyond the trapping array cannot be excluded, repeated same-location recaptures and limited observed movement distances in MRW suggest that many individuals remained within the wetland during the study period.

Interannual comparison further strengthens this interpretation. Adult abundance and size structure in March 2025 closely matched those recorded in March 2019 despite a six-year interval. Although juvenile representation differed between years, this variability aligns with interannual fluctuations in recruitment strength documented for kōaro elsewhere (Hicks et al., 2020; Toorchi & Closs, 2023). The stability of adult cohorts across years suggests sustained survival within MRW rather than reliance on continual immigration from Lake Ōkāreka.

Body condition and growth patterns further support the refuge interpretation. Kōaro in MRW exhibited positive allometric growth and maintained stable body condition across seasons, with no pronounced post-spawning decline. Seasonal and size-related

predictors explained only a small proportion of variance in condition, suggesting that individual level variability rather than environmental constraint dominated.

Relative weight exceeded national expectations based on length–mass relationships, with individuals consistently heavier for their length than predicted. When benchmarked against the nationally derived length–weight relationship for kōaro (Jellyman et al., 2013), individuals from MRW were 6-12 % heavier for their length, with a mean relative weight (Wr) of 112 %. These values indicate that individuals were not obviously energetically constrained within the wetland and are inconsistent with expectations for populations occupying marginal or sink habitats.

A marked increase in kōaro condition in December followed a spike in juvenile common bully abundance in November. Although direct gut-content data were not collected, this temporal alignment suggests that recruitment pulses of small bullies may provide a short-term energetic subsidy for larger kōaro. This interpretation aligns with evidence from Lake Rotoaira, where large kōaro (>90 mm) consumed common bullies (Rowe et al., 2002), and supports broader observations of opportunistic piscivory in galaxiids. In this context, native predator-prey coupling may reduce competitive tension within the assemblage, such that high bully densities represent a potential energetic resource rather than a competitive burden.

I used a national length–mass relationship for kōaro in conjunction with a modified relative weight approach to estimate individual condition in MRW. Using a nationally derived benchmark avoided circularity associated with locally calculated residuals and enabled comparison against a broad reference population. I considered this approach to be more appropriate than Fulton’s condition factor, which assumes isometric growth and can perform poorly for elongate species such as galaxiids. Nevertheless, establishing “condition” from length-mass relationships presents inherent challenges. Deviations from a national benchmark assume morphological consistency among populations; however, kōaro inhabiting lentic wetlands may exhibit habitat-associated phenotypic plasticity, potentially adopting a more robust body form than stream-dwelling conspecifics. In such cases, elevated relative weight may reflect morphological adaptation as well as energetic status. Furthermore, relative weight integrates structural tissue, reproductive investment, and lipid reserves, limiting its capacity to distinguish among components of physiological condition. Additional metrics, including the Hepatosomatic Index (HSI), Gonadosomatic Index (GSI), and

muscle lipid content, would provide greater resolution of energetic status. Despite these limitations, concordant evidence from growth patterns, seasonal stability in condition, and prey availability supports the interpretation that kōaro in MRW are not severely energetically constrained.

Taken together, these findings indicate that MRW supports a persistent, locally structured kōaro population characterised by multi-cohort presence, seasonal recruitment, adult survival, and continued growth. The demographic patterns observed are inconsistent with transient occupancy and instead align with expectations for a resident population inhabiting a functional refuge habitat. Accordingly, H1 was not supported; contrary to the expectation that MRW would function as a demographic sink, multiple lines of evidence demonstrate that it supports a stable, resident kōaro population.

4.2 H2: Environmental filtering and trout limitation

My second hypothesis (H2) proposed that trout predation would constrain kōaro persistence unless environmental conditions within MRW acted as an abiotic filter limiting trout establishment. If trout predation governed assemblage structure within the wetland, trout presence would be expected to suppress kōaro occupancy or abundance. Alternatively, if shallow depths, structural complexity, restricted connectivity, and periodic low dissolved oxygen acted as environmental filters, trout abundance should remain low while kōaro persist within their broader tolerance range.

The results support the environmental filtering interpretation. Rainbow trout were detected infrequently, occurring in only three sampling months and in a small number of trap deployments across the 12-month study period. When present, trout were represented exclusively by small juveniles (maximum length 76 mm) and did not appear to form a resident population. This contrasts sharply with the persistent, widespread detection of kōaro and indicates that trout do not establish sustained occupancy within MRW under typical conditions. It is also plausible that short-term increases in native prey abundance influence trout incursions. Common bully abundance increased markedly in November, followed by a modest increase in trout detections in subsequent months. Although the trout captured were small juveniles, elevated densities of small-bodied native fishes may temporarily enhance foraging opportunities and attract trout into upstream wetland margins during periods of

increased connectivity. Such dynamics likely reflect opportunistic predator tracking of prey pulses rather than sustained establishment, consistent with the absence of any detectable decline in kōaro abundance during trout-present periods.

Trout occurrence was also spatially restricted. Captures were concentrated in upstream sections of the wetland and declined significantly downstream, with trap position explaining approximately 31 % of variation in trout captures. This pattern suggests that only a limited portion of MRW provides conditions temporarily suitable for trout access, likely reflecting proximity to hydrological connection points and slightly deeper or more hydraulically connected habitats. Downstream zones characterised by shallow water, dense macrophyte cover, and low velocities are known to reduce salmonid foraging efficiency and habitat suitability (Jellyman & McIntosh, 2008; Stuart-Smith et al., 2007), indicating that much of MRW is physically structured in ways that disadvantage trout.

Hydrology emerged as a key mediator of this dynamic. Trout CPUE increased with rising lake level, indicating that elevated water levels enhance connectivity between MRW and Lake Ōkāreka (or nearby streams). Under lower lake levels, connectivity is reduced and trout access should decline. Alternatively, there may be spillover during high-flow events in Boyes Stream, a nearby trout breeding stream connected to the lake. Irrespective of the exact pathway, trout incursions appear episodic, conditional, and hydrologically mediated rather than constant. Even during elevated lake levels, incursions remained spatially constrained and transient, with only juveniles captured.

Physicochemical variability likely reinforces this filtering effect. Episodic dissolved oxygen minima, particularly in shallow vegetated sections of the wetland, approached levels known to induce physiological stress in salmonids. Rainbow trout exhibit reduced feeding efficiency, impaired growth, and increased stress under sustained DO concentrations below approximately 5-6 mg L⁻¹, with sensitivity at concentrations as low as 3 mg L⁻¹ (Dean & Richardson, 1999). Although low-oxygen events within MRW were episodic rather than chronic, such conditions may limit trout performance or prevent prolonged residency. In contrast, native galaxiids exhibit greater tolerance of hypoxia, with scaleless species able to supplement branchial respiration via cutaneous oxygen uptake (Dean & Richardson, 1999). The wetland therefore appears periodically harsh for salmonids, yet within the tolerance range of kōaro, reinforcing the role of environmental filtering in limiting trout establishment.

Dissolved oxygen and temperature data further support this interpretation. Although mean conditions were similar between logger sites (mean daily temperature ~ 10.9 °C; mean DO ~ 6.2 - 6.4 mg L⁻¹), episodic extremes differed, with minima declining to ~ 2 mg L⁻¹ at one site. These short hypoxic events likely contribute to the absence of resident trout, even where connectivity allows occasional access. In contrast, kōaro persisted across seasons and sites despite these conditions, consistent with their greater tolerance of low dissolved oxygen and ability to exploit fine-scale habitat heterogeneity.

Although dissolved oxygen was measured at only two locations, broader spatial patterns in fish distribution were consistent with an asymmetric filtering effect. Trout captures were concentrated upstream and declined downstream, whereas kōaro remained widespread, including during periods of lowest dissolved oxygen. Temperature was negatively correlated with DO, such that periods of higher thermal stress coincided with increased hypoxia risk. Together, these patterns indicate that episodic low-oxygen conditions likely constrain trout residency or growth, while kōaro persist under these conditions.

Crucially, kōaro abundance did not decline during trout-present months. Kōaro were detected in all trap-months, and CPUE showed no significant reduction when trout occurred, indicating that trout incursions did not translate into measurable demographic suppression. All trout captured were juveniles, limiting their capacity for piscivory and reducing their potential ecological impact. In systems where salmonids strongly influence galaxiid populations, impacts are typically driven by larger individuals; such size classes were absent here, suggesting that environmental conditions also constrain trout growth to ecologically ineffective sizes.

Instead, predation and competitive pressure within MRW appear weak and episodic rather than chronic. While juvenile trout may overlap in diet with kōaro (Kusabs & Swales, 1991), such interactions are likely brief and spatially constrained. Increased connectivity following high-flow events may elevate encounter rates, but environmental harshness appears to prevent sustained top-down or exploitative suppression.

Together, these findings indicate that MRW functions as a hydrologically mediated refuge for kōaro. Connectivity permits occasional trout access, but incursions remain

limited, transient, and insufficient to suppress kōaro populations. Environmental filtering, including shallow depth and episodic low dissolved oxygen, constrains trout establishment and long-term growth. Under current conditions, the balance between connectivity and environmental harshness restricts sustained trout presence while allowing kōaro persistence.

H2 is therefore supported: trout do not structure the kōaro population within MRW because abiotic and hydrological constraints limit sustained predator pressure.

Under projected climate scenarios involving increased hydrological variability and more frequent extreme events, the context-dependent nature of MRW's refuge function becomes particularly relevant. Groundwater-fed systems may buffer short-term drought and temperature extremes through groundwater inputs and structural complexity (Stuart, 2021), yet altered lake level regimes could increase predator access. Conversely, increasing temperatures may reduce dissolved oxygen availability, intensifying environmental harshness. The persistence of kōaro under current variability suggests tolerance to short-term physicochemical stress, but future shifts in connectivity and oxygen dynamics may alter the balance between refuge function and predator exposure.

4.3 H3: Trophic structure and resource use

My third hypothesis (H3) proposed that fish inhabiting the MRW would rely predominantly on aquatic invertebrates that use primary production in the wetland. Under this expectation, kōaro diets would reflect strong dependence on autochthonous prey sources. Alternatively, if aquatic prey availability were limited and/or kōaro exhibited trophic plasticity, individuals would rely substantially on terrestrial invertebrate inputs as a resource subsidy to sustain their observed biomass.

Stable isotope analysis refuted my prediction that kōaro rely on autochthonous production. Basal resources were clearly separated in $\delta^{13}\text{C}$ space, revealing two dominant energy pathways: an autochthonous channel derived from in-stream primary production and an allochthonous channel derived from terrestrial organic matter. Kōaro isotopic signatures aligned overwhelmingly with the allochthonous pathway. Mixing models estimated that approximately 98 % of kōaro carbon was derived from terrestrial sources, with adult caddisflies contributing nearly 70 % of dietary composition. This pattern indicates strong reliance on terrestrial or emergent prey

rather than benthic aquatic production. The prominence of adult caddisflies in the diet of kōaro may represent a favoured seasonal prey source dominant at the time of sampling. Alternatively, the light trapping was more successful than benthic sampling in capturing caddisflies, and larval forms still may have represented an important food source for kōaro in the MRW. Two of the caddisflies caught in the MRW (*Triplectides dolichos* and *Oeconesus maori*) are obligate shredders that rely on terrestrial inputs of leaf litter, thus helping to explain the strong influence of allochthonous carbon in the trophic position of kōaro.

The wetland also supported autochthonous production. Chironomids, simuliids, freshwater molluscs, and hydroptilid micro-caddis (small algal-piercers that often exploit filamentous algae) were associated with depleted $\delta^{13}\text{C}$ signatures consistent with benthic primary production and Chlorophyta (filamentous green algae). In general, the autochthonous resources supported smaller invertebrate prey, like orthoclad midges and hydroptilid micro-caddisflies, which may be less energetically rewarding for the larger kōaro compared to the smaller common bully. Instead, the trophic position of kōaro may have reflected opportunistic exploitation of larger-bodied adult aquatic insects, likely captured near the surface or within vegetated margins. These two contrasting energy pathways reinforce trophic niche partitioning and likely contribute to the ability of both species to coexist at high densities within the same system.

My results showed the importance of allochthonous carbon for kōaro, yet their diet was dominated by aquatic insects, particularly detritivorous caddisflies. This suggests that kōaro are not relying directly on terrestrial invertebrates, but rather on aquatic prey whose production is itself supported by terrestrial inputs. Moths were included in the mixing models but contributed little to the diet of either fish species, likely reflecting sampling bias associated with light trapping rather than true dietary importance. Previous studies have demonstrated considerable trophic plasticity in kōaro (Kusabs & Swales, 1991). In stream systems where kōaro co-occur with rainbow trout, dietary overlap has been reported, with kōaro occupying a more subordinate, benthic-feeding role. In contrast, kōaro in MRW appear to dominate surface and water-column feeding niches, while bullies are more strongly associated with benthic prey. Differences in microhabitat use may therefore explain prey partitioning within the wetland. Rather than being constrained by limited in-stream production, kōaro in MRW appear to

exploit a detrital pathway in which terrestrial leaf inputs subsidise aquatic insect production, which in turn supports higher trophic levels. Such trophic flexibility likely enhances persistence in a shallow, hydrologically variable system. Terrestrial subsidies, even when mediated through aquatic insects, may provide relatively stable energy inputs compared to in-stream primary production, particularly under environmental variability (Rooney et al., 2006; Vidal et al., 2020).

In this context, trophic plasticity represents an important component of habitat flexibility. The ability to exploit different prey sources allow kōaro to persist in a habitat that would traditionally be considered suboptimal based on classical stream associations. By integrating allochthonous energy pathways, kōaro reduce dependence on potentially variable aquatic prey production within the wetland (Rooney et al. 2006).

H3 is therefore partially supported in its alternative form: kōaro within MRW rely substantially on terrestrial resource subsidies and the detrital food web rather than exclusively on autochthonous production, demonstrating a trophic flexibility that likely contributes to their persistence in this unconventional wetland habitat.

The dominance of allochthonous energy pathways for kōaro suggests that the integrity of the refuge is closely tied to intact riparian vegetation and strong terrestrial–aquatic connectivity. Such reliance may buffer kōaro against decreased stability in autochthonous production associated with increased disturbance and altered flow regimes under climate change (Vidal et al., 2020; Coughlan, 2022).

4.4 H4: Coexistence with common bully

My fourth hypothesis (H4) proposed that in a simplified or resource-limited wetland system, kōaro and common bullies would exhibit substantial dietary overlap, increasing the potential for interspecific competition. Alternatively, coexistence within MRW may be facilitated by trophic niche differentiation, with kōaro relying more heavily on terrestrial or water-column prey sources and common bullies primarily exploiting aquatic benthic prey.

The results support the alternative hypothesis of niche differentiation. Although common bullies dominated the assemblage numerically, no significant negative

relationship was detected between bully and kōaro CPUE at the trap scale. Kōaro abundance was not suppressed in months or locations where bullies were abundant, and numerical dominance by bullies did not translate into energetic dominance. Despite lower abundance, kōaro contributed substantially greater biomass overall (4,850 g vs. 1,510 g), exceeding bully biomass by more than threefold. Their markedly greater mean individual mass (11.6 g compared to 1.1 g) indicates that kōaro represent the dominant native fish biomass within the wetland. This asymmetry reinforces the interpretation that coexistence occurs without competitive exclusion.

Stable isotope analyses provide a mechanistic explanation for this pattern. Although kōaro and common bullies exhibited similar trophic niche breadth, isotopic niche overlap was limited (~16 %), indicating partial but non-redundant resource use. Mixing models revealed strong prey-specific partitioning: kōaro diets were dominated by adult caddisflies (~69 %), while bullies relied primarily on midge larvae (~75 %). This prey-specific partitioning suggests functional differentiation in foraging behaviour and habitat use. Adult caddisflies are likely captured near the water surface or within marginal vegetation, whereas midge larvae are benthic and closely associated with fine sediments. Such differentiation in prey use is consistent with known ecological differences between galaxiids and benthic gobiids and likely reduces direct competition for food resources despite co-occurrence (McDowall, 2000; Coughlan, 2022).

Stable isotope mixing models focus on underlying carbon sources further supported niche partitioning. Kōaro were overwhelmingly supported by allochthonous carbon, while bullies derived most of their energy from autochthonous production. This near-complete divergence in basal energy pathways indicates that coexistence is structured at the level of primary energy sources rather than simple prey partitioning within a shared benthic pool. Such energy-channel differentiation substantially reduces the likelihood of exploitative competition, even within a spatially constrained wetland.

Temporal patterns further suggest dynamic interactions within the assemblage. A spike in bully abundance during late spring was followed by elevated kōaro condition in early summer, raising the possibility that high densities of small bullies may temporarily augment available prey for larger kōaro individuals. Piscivory in large kōaro has been documented in several studies (Kusabs & Swales, 1991; Rowe et al., 2002). Although my stable isotope sampling preceded this observation and bullies

were not explicitly included as a prey source in the mixing models, future analyses could incorporate juvenile bullies to evaluate their contribution to kōaro diets more directly. Even without direct dietary confirmation, opportunistic feeding during recruitment pulses could plausibly contribute to short-term energetic gains. Such predator-prey coupling would reduce the likelihood of competitive suppression by shifting interactions from exploitative competition toward density-dependent predation within the native assemblage. Elevated juvenile fish densities may also help explain episodic trout incursions, as increases in prey availability can attract opportunistic predators and influence population regulation through food limitation (Chapman, 1966).

My findings align with established ecological differences between galaxiids and gobiids documented in New Zealand freshwater systems (McDowall, 2000). Experimental studies have demonstrated that spatial and trophic segregation can facilitate coexistence between galaxiids and bullies. For example, Cadwallader (1975) showed that interactive segregation between *Galaxias vulgaris* and upland bullies reduced direct interference, with bullies exhibiting greater behavioural flexibility and generalist feeding behaviour. This flexibility was argued to promote coexistence by allowing bullies to exploit a broader range of benthic resources while galaxiids occupied complementary microhabitats. Although the species examined in that study differ from kōaro and common bullies, the underlying mechanism of habitat and resource partitioning appears consistent. The trophic partitioning observed in MRW therefore fits within a broader ecological framework in which coexistence between *Galaxias* and *Gobiomorphus* is structured by behavioural and trophic differentiation rather than competitive exclusion.

H4 is therefore supported in its alternative form: coexistence within MRW is facilitated by trophic niche differentiation and energy-channel partitioning rather than high dietary overlap and intense competition. This differentiation contributes to assemblage stability and reinforces refuge function by allowing high densities of native species to persist without competitive exclusion.

Summary

5.1 Synopsis

In this study, I investigated how a small, ground-fed wetland on the margin of Lake Ōkāreka functions as habitat and potential refuge for kōaro. By integrating population monitoring, mark–recapture, environmental modelling, and stable isotope analysis, I aimed to determine whether Millar Road Wetland (MRW) supports a persistent kōaro population and to identify the mechanisms that enable that persistence.

The results show that MRW supports a locally resident and structured kōaro population. Kōaro were widespread throughout the wetland, occurred across multiple size classes, and exhibited seasonal recruitment, positive allometric growth, and stable body condition. Mark–recapture data demonstrated site fidelity and continued growth, while interannual comparisons revealed stable adult size structure between 2019 and 2025 despite variability in juvenile recruitment. Together, these findings support H1 and indicate that MRW functions as a resident habitat rather than a transient corridor or demographic sink.

Environmental analyses support H2 and show that hydrology mediates refuge strength. Trout occurrence increased with rising lake level, indicating that hydrological connectivity governs predator access. Under typical conditions, trout remained rare, spatially restricted to upstream margins, and represented only small juvenile individuals. The wetland appears too small, shallow, and periodically harsh—particularly during episodic dissolved oxygen minima—to support large predatory salmonids. This asymmetry is consistent with trout sensitivity to hypoxia and the greater tolerance of scaleless native galaxiids, which can supplement oxygen uptake across highly vascularised skin (Dean & Richardson, 1999). Refuge function therefore emerges not from complete exclusion of trout, but from weak and hydrologically constrained predator pressure.

Connectivity lies at the centre of this dynamic. Hydrological connection to Lake Ōkāreka is essential for recruitment, dispersal, and metapopulation exchange, yet increased connectivity also elevates trout access. MRW therefore operates within a

balance: sufficient connection to maintain demographic exchange but limited enough to restrict sustained predator establishment. This tension between demographic necessity and predator exposure highlights the context-dependent nature of refuge function within the wetland.

Stable isotope analysis revealed that coexistence within MRW is further stabilised by trophic differentiation. Kōaro relied predominantly on allochthonous carbon, largely via emergent aquatic insects supported by terrestrial detrital inputs, whereas common bullies were supported mainly by autochthonous production and benthic invertebrates. This separation in primary energy pathways reduces exploitative competition and supports coexistence at high densities. Kōura contributed to internal energy cycling without undermining kōaro persistence. The wetland therefore supports a native-dominated, trophically coherent food web rather than a simplified assemblage shaped by salmonid suppression.

Collectively, these findings demonstrate that refuge function at MRW arises from interacting hydrological buffering, structural complexity, environmental filtering, and trophic partitioning operating across spatial and temporal scales.

5.2 Implications and limitations

This study shows that small, ground-fed wetlands can function as ecosystem-scale refugia for native freshwater fishes embedded within invaded lake systems. MRW sustains a persistent kōaro population while limiting sustained trout establishment through hydrological mediation and environmental harshness. Refuge strength, however, is dynamic rather than fixed. Elevated lake levels increase connectivity and partially erode refuge conditions, while groundwater buffering stabilises hydrology and dampens short-term rainfall effects.

Connectivity emerges as both essential and risky. Without connection to the lake and surrounding waterways, MRW could become demographically isolated. Yet excessive connectivity increases predator access. Understanding and managing this balance will be critical under climate change, where altered precipitation regimes and lake-level variability may shift the threshold between protection and exposure.

A key limitation is that dissolved oxygen concentrations and temperature were monitored at only two fixed locations and could not be assigned to individual traps at the time scale of fish sampling. This limits formal inference about whether kōaro select specific microhabitats in response to oxygen minima and prevents testing oxygen as a trap-scale predictor of CPUE in mixed-effects models. As a result, my interpretation of dissolved oxygen as a physiological filter is mechanistic but indirect, based on episodic logger minima, trout size structure, and broad spatial patterns rather than direct fish-oxygen matching.

Trait-based vulnerability assessments indicate that kōaro are among the most climate-sensitive native freshwater fishes due to narrow thermal tolerance and limited dispersal capacity (Canning et al., 2025). The persistence of a robust population within MRW therefore highlights the potential importance of small wetlands as climatic strongholds within fragmented lake systems.

The assumption that MRW is too small and harsh to support persistent trout requires further testing. While current data show only episodic juvenile presence, long-term shifts in hydrology or thermal regimes could alter habitat suitability. Similarly, although episodic dissolved oxygen minima likely constrain trout more than kōaro, direct experimental comparisons of hypoxia tolerance were beyond the scope of this study. Although relative weight provided useful comparative insight into somatic condition, incorporating direct physiological indices such as HSI, GSI, or lipid content would strengthen inference about energetic status and refine assessment of refuge quality.

The broader metapopulation role of MRW also remains unresolved. While adult stability and recruitment patterns indicate local persistence, it is unclear whether the wetland functions primarily as a source, sink, or seasonal refuge within the Lake Ōkāreka system. Clarifying this role is critical for understanding the true conservation value of MRW at the landscape scale.

Despite these limitations, the convergence of demographic, environmental, and trophic evidence provides strong support for interpreting MRW as a hydrologically mediated refuge, shaped by asymmetric environmental filtering.

5.3 Future research directions

Several key questions arise from this work.

First, how common are MRW-like systems across the Arawa Lakes? Identifying additional ground-fed wetlands or similar and assessing their fish assemblages would clarify whether MRW represents an isolated stronghold or part of a broader refuge network.

Second, what role does MRW play within the Lake Ōkāreka metapopulation? Genetic analyses, otolith chemistry, or expanded PIT-tag tracking could determine whether individuals recruit from the lake into the wetland, emigrate from the wetland into the lake, or move bidirectionally. Establishing whether MRW functions as a source, sink, or stepping-stone habitat is essential for regional management.

Third, are kōaro in MRW locally adapted to variable dissolved oxygen conditions? Comparative physiological experiments across populations could test whether wetland residents exhibit enhanced hypoxia tolerance relative to lake or stream populations. Future work should quantify physicochemical habitat selection directly by pairing fish sampling with trap-adjacent DO and temperature measurements (or deploying additional loggers across the trap gradient). This would allow mixed-effects models that test whether kōaro CPUE increases in areas with higher minimum DO, whether trout occurrence tracks oxygen refugia, and whether hydrological expansion during high lake levels changes the spatial distribution of oxygen stress. A logical next step would be moving toward species distribution modelling that integrates hydrology, habitat structure, and physicochemical predictors to predict when and where refuge conditions are strongest.

Fourth, how will climate-driven changes in hydrology influence connectivity thresholds and trout access? Integrating hydrological modelling with predator detection data would allow prediction of future refuge stability under altered lake-level regimes.

Finally, restoration ecology offers important opportunities. If degraded wetlands were restored to improve structural complexity, riparian integrity, and groundwater buffering, could they support similar refuge dynamics? Understanding the minimum habitat size

and physicochemical conditions required to exclude large predators while sustaining native fishes would directly inform management.

The results of this study indicate that refuge function at MRW does not arise from a single mechanism, but from the interaction of climate variability, hydrological connectivity, environmental filtering, habitat structure, and trophic organisation. Rather than conceptualising MRW as simply “trout-free”, the evidence suggests a more nuanced system in which connectivity is both essential and risky: it sustains demographic exchange with Lake Ōkāreka yet periodically permits predator access. Environmental harshness linked to episodic hypoxia, combined with shallow depths and complex habitat structure, limit trout residency and prevent growth to ecologically impactful sizes, while trophic partitioning and strong allochthonous support stabilise native coexistence.

I developed a conceptual model to help describe these interactions and processes. Figure 56 synthesises these drivers and illustrates how the MRW functions as a hydrologically-mediated refuge emerging from landscape-scale processes rather than static habitat attributes.

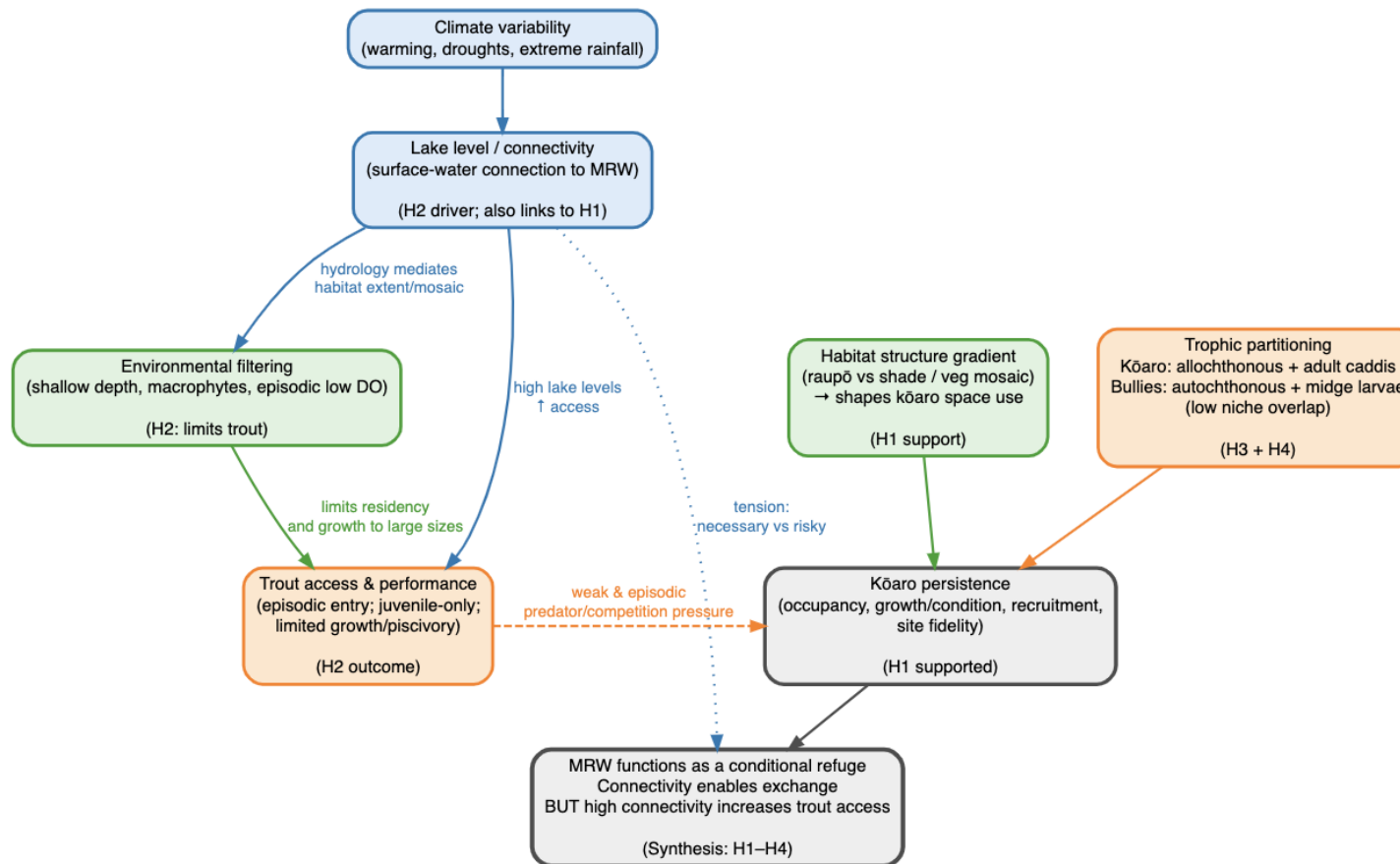


Figure 56: Conceptual model of the Millar Road Wetland (MRW) as a hydrologically mediated refuge for kōaro. Coloured groupings represent interacting drivers identified in this study: climate and hydrology (blue tones) regulate surface-water connectivity; environmental filtering processes (green tones), including shallow depth, macrophyte structure, and episodic low dissolved oxygen, asymmetrically constrain trout residency and growth; biotic interactions (orange tones) reflect trophic partitioning and habitat-mediated space use; and predator dynamics (red tones) illustrate episodic trout access and limited piscivory. Together, these interacting processes support persistent kōaro occupancy while restricting sustained predator pressure. Refuge function emerges not from absolute predator exclusion, but from a context-dependent balance between necessary hydrological connectivity for demographic exchange and environmental constraints that limit trout establishment.

5.4 Conclusion

The Millar Road Wetland is an important refuge for kōaro because it sustains a persistent, structured population while limiting sustained predator pressure through hydrological variability and environmental filtering. The quality of the refuge is environmentally contingent, arising from a balance of connectivity and constraints rather than isolation alone.

This study demonstrates that small, spring-fed wetlands can function as dynamic refugia within invaded lake systems. Determining how strongly the MRW contributes to the wider Lake Ōkāreka metapopulation, as a source, seasonal refuge, or demographic buffer, will be critical for safeguarding kōaro under ongoing climatic and hydrological change in this lake and the wider Arawa Lakes region.

References

- Albert, J. S., Destouni, G., Duke-Sylvester, S. M., Magurran, A. E., Oberdorff, T., Reid, A. J., ... Winemiller, K. O. (2021). Scientists' warning to humanity on the freshwater biodiversity crisis. *Ambio*, 50(1), 85–94.
- Allibone, R. M.; Caskey, D. 2000: Timing and habitat of koaro (*Galaxias brevipinnis*) spawning in streams draining Mt Taranaki, New Zealand. *New Zealand Journal of Marine and Freshwater Research* 34: 593-595.
- Allibone, R. M., & Wallis, G. P. (1993). Genetic variation and diadromy in some native New Zealand galaxiids (Teleostei: Galaxiidae). *Biological Journal of the Linnean Society*, 50(1), 19–33.
- Allan, H., Unmack, P., Duncan, R. P., and Lintermans, M. (2018). Potential impacts of PIT tagging on a critically endangered small-bodied fish: A trial on the surrogate Mountain Galaxias. *Transactions of the American Fisheries Society* 147:1078-1084. doi: <https://doi.org/10.1002/tafs.10102>
- Bell, C. P. (2001). The ecology of koaro (*Galaxias brevipinnis*) in Manson Creek, North Canterbury. Unpublished MSc thesis, University of Canterbury. Christchurch, New Zealand.
- Brown JH, Kodric-Brown A (1977) Turnover rates in insular biogeography: effect of immigration on extinction. *Ecology* 58: 445-449. doi: 10.2307/1935620.
- Canning, A. D., Zammit, C., & Death, R. G. (2025). The implications of climate change for New Zealand's freshwater fish. *Canadian Journal of Fisheries and Aquatic Sciences*, 82, 1–15. <https://doi.org/10.1139/cjfas-2024-0127>
- Caut, S., Angulo, E. and Courchamp, F. (2009), Variation in discrimination factors ($\Delta^{15}\text{N}$ and $\Delta^{13}\text{C}$): the effect of diet isotopic values and applications for diet reconstruction. *Journal of Applied Ecology*, 46: 443-453. <https://doi.org/10.1111/j.1365-2664.2009.01620.x>
- Cazzolla Gatti, R. (2016). Freshwater biodiversity: a review of local and global threats. *International Journal of Environmental Studies*, 73(6), 887-904.

- Closs, G. P., A. S. Hicks, and P. G. Jellyman. 2013. Life histories of closely related amphidromous and non-migratory fish species: A tradeoff between egg size and fecundity. *Freshwater Biology* 58, 6: 1162–1177.
- Coughlan, J. (2022). Trophic ecology and food-web structure of lowland wetland streams. Unpublished Master's thesis. University of Otago, Dunedin, New Zealand.
- Darestani, M. M. (2023). Assessing the effects of landlocking in three New Zealand diadromous fish species using next generation sequencing. Doctoral thesis, University of Otago, Dunedin, New Zealand.
- David, B. O., Jarvis, M., Özkundakci, D., Smith, J., Duggan, I. C., Koh, S. S., ... King, T. M. (2022). First observations and early life-history aspects of lake rearing galaxiid larvae in the lower Waikato River Basin, New Zealand. *New Zealand Journal of Marine and Freshwater Research*, 57(4), 495–517. <https://doi.org/10.1080/00288330.2022.2068620>
- Dean, T.L. and Richardson, J. (1999), Responses of seven species of native freshwater fish and a shrimp to low levels of dissolved oxygen. *New Zealand Journal of Marine and Freshwater Research*, 33: 99-106. <https://doi.org/10.1080/00288330.1999.9516860>
- Delgado, M. L., & Ruzzante, D. E. (2020). Investigating diadromy in fishes and its loss in an-omics era. *iScience*, 23(12).
- Dudgeon, D., Arthington, A. H., Gessner, M. O., Kawabata, Z. I., Knowler, D. J., Lévêque, C., ... & Sullivan, C. A. (2006). Freshwater biodiversity: importance, threats, status and conservation challenges. *Biological Reviews*, 81(2), 163-182.
- Dunn, N. R., Closs, G. P., Crow, S. K., David, B. O., Goodman, J. M., Griffiths, M., Hicks, A. ... & Makan, T. (2023). *Conservation status of New Zealand freshwater fishes, 2023*. Department of Conservation, Wellington, New Zealand
- Eikaas, H. S. (2004). The effect of habitat fragmentation on New Zealand native fish: A GIS approach. Doctoral thesis. University of Canterbury, Christchurch, New Zealand.
- Franklin, C. E., Foster, N. L., & Whelan, M. M. (2018). Impact of climate change on cold-water fish habitats. *Environmental Biology of Fishes*, 101(10), 1515–1527.

- Foden, W. B., Butchart, S. H., Stuart, S. N., Vié, J. C., Akçakaya, H. R., Angulo, A., ... & Mace, G. M. (2013). Identifying the world's most climate change vulnerable species: a systematic trait-based assessment of all birds, amphibians and corals. *PloS One*, 8(6), e65427.
- Gende, S. M., Edwards, R. T., Willson, M. F., & Wipfli, M. S. (2002). Pacific salmon in aquatic and terrestrial ecosystems: Pacific salmon subsidize freshwater and terrestrial ecosystems through several pathways, which generates unique management and conservation issues but also provides valuable research opportunities. *BioScience*, 52(10), 917-928.
- Goldberg, J., Trewick, S.A., & Paterson, A.M. (2008) Evolution of New Zealand's terrestrial fauna: a review of molecular evidence. *Philosophical Transactions of the Royal Society*. B3633319–3334
- Greenberg, L.A. and Giller, P.S. (2000), The potential of flat-bed passive integrated transponder antennae for studying habitat use by stream fishes. *Ecology of Freshwater Fish*, 9: 74-80. <https://doi.org/10.1034/j.1600-0633.2000.90108.x>
- Hanski I (1999) Metapopulation Ecology. *New York: Oxford University Press*. 328pp.
- Harrison, I., Abell, R., Darwall, W., Thieme, M. L., Tickner, D., & Timboe, I. (2018). The freshwater biodiversity crisis. *Science*, 362(6421), 1369-1369.
- Hayes, J. W. (1996). Observations of surface feeding behaviour in pools by koaro, *Galaxias brevipinnis*. *Journal of the Royal Society of New Zealand*, 26(1), 139–141. <https://doi.org/10.1080/03014223.1996.9517508>
- Hicks, A. S., Jarvis, M. G., Easton, R. R., Waters, J. M., David, B. O., Norman, M. D., & Closs, G. P. (2021). Life history plasticity affects the population structure and distribution of the widespread migratory fish *Galaxias brevipinnis*. *Marine and Freshwater Research*, 72, 542–550.
- Hoare, R.J.B., Rhode, B.E., Emmerson, A.W. 2011 (and updates): Larger moths of New Zealand: Image gallery and online guide. <https://www.landcareresearch.co.nz/discover-our-research/biodiversity/plants-invertebrates-fungi-and-bacteria/invertebrate-systematics/moths-and-butterflies/larger-moths-of-new-zealand>

- Jackson, A.L., Inger, R., Parnell, A.C. and Bearhop, S. (2011). Comparing isotopic niche widths among and within communities: SIBER – Stable Isotope Bayesian Ellipses in R. *Journal of Animal Ecology*, 80: 595-602. <https://doi.org/10.1111/j.1365-2656.2011.01806.x>
- Jackson A, Parnell A (2023). SIBER: Stable Isotope Bayesian Ellipses in R. R package version 2.1.9, <<https://CRAN.R-project.org/package=SIBER>>
- Jellyman, P., Booker, D., Crow, S., Bonnett, M., & Jellyman, D. (2013). Does one size fit all? An evaluation of length–weight relationships for New Zealand’s freshwater fish species. *New Zealand Journal of Marine and Freshwater Research*, 47(4), 450–468. <https://doi.org/10.1080/00288330.2013.781510>
- Jellyman, P. G., & McIntosh, A. R. (2008). The influence of habitat availability and adult density on non-diadromous galaxiid fry settlement in New Zealand. *Journal of Fish Biology*, 72(1), 143–156. doi: <https://doi.org/10.1111/j.1095-8649.2007.01694.x>
- Jolly, M. E., Warburton, H. J., Bowie, S., Challies, E., Jellyman, P. G., & McIntosh, A. R. (2024). Isolation management to protect threatened native galaxiid fish species: Lessons from Aotearoa New Zealand. *Aquatic Conservation*, 34(7), Article e4220.
- Jowett, I. G., & Richardson, J. (1996). Distribution and abundance of freshwater fish in New Zealand rivers. *New Zealand Journal of Marine and Freshwater Research*, 30(2), 239–255.
- Joy, M. K., Death, R. G. (2013) Freshwater biodiversity. In Dymond, J.R. ed. *Ecosystem services in New Zealand – conditions and trends*. Manaaki Whenua Press, Lincoln, New Zealand.
- Kaufuss, U., Lee, D. E., Robinson, J. H., Wallis, G. P., & Schwarzhans, W. W. (2020). A Review of *Galaxias* (Galaxiidae) Fossils from the Southern Hemisphere. *Diversity*, 12(5), 208. <https://doi.org/10.3390/d12050208>
- King, K. J., Young, K. D., Waters, J. M., & Wallis, G. P. (2003). Preliminary genetic analysis of koaro (*Galaxias brevipinnis*) in New Zealand lakes: Evidence for allopatric differentiation among lakes but little population subdivision within lakes. *Journal of the Royal Society of New Zealand*, 33(3), 591–600.

- Koehn, J. D., Hobday, A. J., Pratchett, M. S., & Gillanders, B. M. (2011). Climate change and Australian marine and freshwater environments, fishes and fisheries: synthesis and options for adaptation [Paper in special issue: Climate change and Australian aquatic environments, fish and fisheries. Koehn, J. D.; Hobday, A. J.; Pratchett, M. S. and Gillanders, B. M. (eds)]. *Marine and Freshwater Research*, 62(9), 1148–1164. <https://doi.org/10.1071/MF11139>
- Kusabs, I. A. (1989). The biology and general ecology of the Koaro (*Galaxias brevipinnis*) in some tributary streams of Lake Taupo. Unpublished MSc thesis, University of Waikato, Hamilton, New Zealand.
- Kusabs, I. A. (2015). Kōura (*Paranephrops planifrons*) populations in the Te Arawa lakes: An ecological assessment using the traditional Māori tau kōura harvesting method and recommendations for sustainable management (Thesis, Doctor of Philosophy (PhD)). University of Waikato, Hamilton, New Zealand. Retrieved from <https://hdl.handle.net/10289/9346>
- Kusabs, I.A. (2020). Lake Rotorua kōura and kākahi monitoring programme. Report number 4, prepared for Bay of Plenty Regional Council. Ian Kusabs and Associates Ltd, Rotorua, New Zealand.
- Kusabs, I., Bates, C., & Goodwin, M. (2019) Kōaro Survey – Millar Road Wetland, Lake Ōkāreka. Report prepared for Bay of Plenty Regional Council. Ian Kusabs & Associates Ltd.
- Kusabs, I. A., Hicks, B. J., Quinn, J. M., Perry, W. L., & Whaanga, H. (2018). Evaluation of a traditional Māori harvesting method for sampling kōura (freshwater crayfish, *Paranephrops planifrons*) and toi toi (bully, *Gobiomorphus* spp.) populations in two New Zealand streams. *New Zealand Journal of Marine and Freshwater Research*, 52(4), 603–625. <https://doi.org/10.1080/00288330.2018.1481437>
- Kusabs, I. A., & Swales, S. (1991). Diet and food resource partitioning in koaro, *Galaxias brevipinnis* (Günther), and juvenile rainbow trout, *Oncorhynchus mykiss* (Richardson), in two Taupo streams, New Zealand. *New Zealand Journal of Marine and Freshwater Research*, 25(3), 317–325. <https://doi.org/10.1080/00288330.1991.9516485>

- Leathwick, J. R., Rowe, D., Richardson, J., Elith, J., & Hastie, T. (2005). Using multivariate adaptive regression splines to predict the distributions of New Zealand's freshwater diadromous fish. *Freshwater Biology*, 50(12), 2034-2052.
- Ling, N. (2010) Socio-economic drivers of freshwater fish declines in a changing climate: a New Zealand perspective. *Journal of Fish Biology* 77:1983–1992.
- McDowall, R. M. (1990) *New Zealand Freshwater Fishes: A Natural History and Guide*. Auckland, New Zealand: Heinemann Reed and MAF Publishing Group.
- McDowall, R. M. (1998). Driven by diadromy: Its role in the historical and ecological biogeography of the New Zealand freshwater fish fauna. *Italian Journal of Zoology*, 65(sup1), 73–85.
- McDowall, R.M. (2006). Crying wolf, crying foul, or crying shame: alien salmonids and a biodiversity crisis in the southern cool-temperate galaxioid fishes? *Reviews in Fish Biology and Fisheries*, 16(3–4), 233–422.
- McDowall, R.M. and Chadderton, W.L. (1999), *Galaxias gollumoides* (Teleostei: Galaxiidae), a new fish species from Stewart Island, with notes on other non-migratory freshwater fishes present on the island. *Journal of the Royal Society of New Zealand*, 29: 77-88
- McDowall, R. M., Robertson, D. A., & Saito, R. (1975). Occurrence of galaxiid larvae and juveniles in the sea. *New Zealand Journal of Marine and Freshwater Research*, 9(1), 1–9.
- McDowall, R. M., & Suren, A. M. (1995). Emigrating larvae of koaro, *Galaxias brevipinnis* Günther (Teleostei: Galaxiidae), from the Otira River, New Zealand.
- McEwan, A. J., and Joy, M. K. (2011). Monitoring a New Zealand freshwater fish community using passive integrated transponder (PIT) technology; lessons learned and recommendations for future use. *New Zealand Journal of Marine and Freshwater Research* 45:121-133.
- McEwan, A.J., Joy, M.K. (2014a). Diel habitat use of two sympatric galaxiid fishes (*Galaxias brevipinnis* and *G. postvectis*) at two spatial scales in a small upland stream in Manawatu, New Zealand. *Environmental Biology of Fishes* 97, 897–907.

- McEwan, A.J., Joy, M.K. (2014b) Habitat use of redfin bullies (*Gobiomorphus huttoni*) in a small upland stream in Manawatu, New Zealand. *Environ Biol Fish* **97**, 121–132.
- Main, M. R. (1988). Factors influencing the distribution of kokopu and koaro (Pisces: Galaxiidae). Unpublished MSc thesis, University of Canterbury.
- Main, M. R., & Winterbourn, M. J. (1987). Diet and feeding of koaro (*Galaxias brevipinnis*) in forested, South Westland streams. *Mauri Ora* 14, 77-86
- Mitsuo, Y., Ohira, M., Tsunoda, H., & Yuma, M. (2013). Movement patterns of small benthic fish in lowland headwater streams. *Freshwater Biology*, 58(11), 2345–2354. <https://doi.org/10.1111/fwb.12214>
- Morrongiello John R., Beatty Stephen J., Bennett James C., Crook David A., Ikedife David N. E. N., Kennard Mark J., Kerezszy Adam, Lintermans Mark, McNeil Dale G., Pusey Bradley J., Rayner Thomas (2011) Climate change and its implications for Australia's freshwater fish. *Marine and Freshwater Research* **62**, 1082-1098.
- National Environmental Monitoring Standards. (2022, June). *Macroinvertebrates: Collection and processing of macroinvertebrate samples from rivers and streams* (Version 1.0.0).
- Nielsen, J.M., Clare, E.L., Hayden, B., Brett, M.T., Kratina, P. (2018). Diet tracing in ecology: Method comparison and selection. *Methods in Ecology and Evolution*.; 9: 278–291. <https://doi.org/10.1111/2041-210X.12869>. NIWA (2023) Impacts of sediment on kōaro [Fact sheet]. National Institute of Water and Atmospheric Research, Hamilton, New Zealand. https://niwa.co.nz/sites/default/files/Sediment%20factsheet_ko%CC%84aro_0.pdf
- O'Conner, W. G., & Koehn, J. D. (1998). Spawning of the broad-finned Galaxias, *Galaxias brevipinnis* Günther (Pisces: Galaxiidae) in coastal streams of southeastern Australia. *Ecology of Freshwater Fish*, 7(2), 95-100.
- Pianka, E. R. (1974). Niche overlap and diffuse competition. *Proceedings of the National Academy of Sciences USA* 71: 2141–2145.
- Petersen, C. G. J. (1896). The yearly immigration of young plaice into the Limfjord from the German Sea. *Report of the Danish Biological Station*, 6, 1–48.

- Phillips, W.J., 1940. Food supply and deterioration of trout in the Thermal lakes District, North Island. *Transactions and Proceedings of the New Zealand Institute* 55: 381-391.
- R Core Team (2022). R: a language and environment for statistical computing. R Foundation for Statistical Computing. Vienna, Austria.
- Ramírez-Álvarez, R., Contreras, S., Vivancos, A., Reid, M., López-Rodríguez, R., & Górski, K. (2022). Unpacking the complexity of longitudinal movement and recruitment patterns of facultative amphidromous fish. *Scientific Reports*, 12(1), 3164.
- Reid, A. J., Carlson, A. K., Creed, I. F., Eliason, E. J., Gell, P. A., Johnson, P. T., ... & Cooke, S. J. (2019). Emerging threats and persistent conservation challenges for freshwater biodiversity. *Biological Reviews*, 94(3), 849-873.
- Riordan, P. (2000). Population dynamics, habitat analysis and food assimilation in the freshwater crayfish *Paranephrops planifrons* in a North Island stream (Doctoral dissertation, University of Waikato).
- Rooney, N., McCann, K., Gellner, G., & Moore, J. C. (2006). Structural asymmetry and the stability of diverse food webs. *Nature*, 442(7100), 265-269.
- Rowe, D. K. (1993). Disappearance of koaro (*Galaxias brevipinnis*) from Lake Rotopounamu following the introduction of smelt (*Retropinna retropinna*). *Environmental Biology of Fishes*, 36, 329–336.
- Rowe, D. K. (1993). Identification of fish responsible for five layers of echoes recorded by high-frequency (200 kHz) echosounding in Lake Rotoiti, North Island, New Zealand. *New Zealand Journal of Marine and Freshwater Research*, 27(1), 87–100.
- Rowe, D., Graynoth, E., James, G., Taylor, M., & Hawke, L. (2003). Influence of turbidity and fluctuating water levels on the abundance and depth distribution of small, benthic fish in New Zealand alpine lakes. *Ecology of Freshwater Fish*, 12(3), 216–227.
- Rowe, D. K., Konui, G., & Christie, K. D. (2002). Population structure, distribution, reproduction, diet, and relative abundance of koaro (*Galaxias brevipinnis*) in a

- New Zealand lake. *Journal of the Royal Society of New Zealand*, 32(2), 275–291. <https://doi.org/10.1080/03014223.2002.9517695>
- Rowe, D. K., Smith, J. P., & Grayling, S. (2008). *Status of koaro (Galaxias brevipinnis) populations in the Te Arawa lakes and options for their restoration*. NIWA Client Report. Prepared for Te Arawa Lakes Trust. https://niwa.co.nz/sites/default/files/koaro_status_report_0.pdf
- Ruetz, C.R., III, Harris, B.S., McNair, J.N. and Homola, J.J. (2015), Removal and Mark–Recapture Methods for Estimating Abundance: Empirical and Simulation Results for Mottled Sculpin in Streams. *North American Journal of Fisheries Management*, 35: 62-74. <https://doi.org/10.1080/02755947.2014.970677>
- Schoener, T. W. (1974). Resource partitioning in ecological communities. *Science* 185: 27–39.
- Stevens G, McGlone M, McCulloch B. 1988. Prehistoric New Zealand. Auckland: Reed.
- Stewart, S. D., Holmes, R., Vadeboncoeur, Y., Bury, S. J., & Crump, S. (2022). Sea to the mountains: quantifying freshwater eel and trout diet reliance on marine subsidies from upstream migrating fish. *New Zealand Journal of Marine and Freshwater Research*, 56(3), 466–490.
- Stock, B.C., Jackson, A.L., Ward, E.J., Parnell, A.C., Phillips, D.L., Semmens, B.X. (2018). Analysing mixing systems using a new generation of Bayesian tracer mixing models. *PeerJ* 6:e5096 <https://doi.org/10.7717/peerj.5096>
- Stock, B.C. and B.X. Semmens (2016). MixSIAR GUI User Manual. Version 3.1. <https://github.com/brianstock/MixSIAR/>. doi:10.5281/zenodo.47719.
- Strayer, D. L., & Dudgeon, D. (2010). Freshwater biodiversity conservation: recent progress and future challenges. *Journal of the North American Benthological Society*, 29(1), 344-358.
- Stuart, R. E. (2021). The spatio-temporal dynamics of fish and invertebrate populations within coastal wetlands in Southland, New Zealand (Doctoral dissertation, University of Otago). Our Archive. <https://ourarchive.otago.ac.nz/handle/10523/9926>

- Stuart-Smith, R. D., Stuart-Smith, J. F., White, R. W. G., & Barmuta, L. A. (2007). Impact of an introduced predator on a threatened galaxiid fish is reduced by the availability of complex habitats. *Freshwater Biology*, 52(8), 1555–1563. <https://doi.org/10.1111/j.1365-2427.2007.01787.x>
- Takimoto, G., Iwata, T. & Murakami, M. Seasonal subsidy stabilizes food web dynamics: Balance in a heterogeneous landscape. *Ecological Research* 17, 433–439 (2002).
- Tickner, D., Opperman, J. J., Abell, R., Acreman, M., Arthington, A. H., Bunn, S. E., ... & Young, L. (2020). Bending the curve of global freshwater biodiversity loss: an emergency recovery plan. *BioScience*, 70(4), 330-342.
- Toorchi, M., Reid, M. R., & Closs, G. P. (2025). Contrasting Patterns of Larval Recruitment in River–Lake Systems in Migratory and Nonmigratory *Galaxias* Species. *Ecology of Freshwater Fish*, 34(2), Article e12829. <https://doi.org/10.1111/eff.12829>
- Vidal, J., Pasquaud, S., Lobry, J., & Lepage, M. (2020). Contribution of terrestrial organic matter to fish food webs in freshwater ecosystems: A stable isotope approach. *Freshwater Biology*, 65(3), 441–455. <https://doi.org/10.1111/fwb.13444>
- Wallis, G. P. (2021). Evolutionary Genetics and Biogeography of Galaxiid Fishes (Teleostei: Galaxiiformes: Galaxiidae). *Diversity (Basel)*, 13(4), 153.
- Waters, J. M., Burridge, C. P., & Craw, D. (2020). River Capture and Freshwater Biological Evolution: A Review of Galaxiid Fish Vicariance. *Diversity*, 12(6), 216.
- Waters, J.M. and Wallis, G.P. (2001), Mitochondrial DNA phylogenetics of the *Galaxias vulgaris* complex from South Island, New Zealand: rapid radiation of a species flock. *Journal of Fish Biology*, 58: 1166-1180.
- Wilhelm, F. M., Closs, G. P., & Burns, C. W. (2007). Seasonal diet and amphipod size selection of juvenile common bully, *Gobiomorphus cotidianus*, in a coastal nNw Zealand lake. *Hydrobiologia*, 586(1), 303-312. doi: <https://doi.org/10.1007/s10750-007-0703-9>
- Wilkinson, S. P., Gault, A. A., Welsh, S. A., Smith, J. P., David, B. O., Hicks, A. S., Fake, D. R., Suren, A. M., Shaffer, M. R., and Jarman, S. N. (2024). TICI: a taxon-

independent community index for eDNA-based ecological health assessment. *PeerJ* 12:e16963. doi: <https://doi.org/10.7717/peerj.16963>

Winterbourn, M. J., Gregson, K. L. D., & Dolphin, C. H. (2006). Guide to the Aquatic insects of New Zealand. 4th Edition, Bulletin Number 14 of the Entomological Society of New Zealand.

Woodford, D. J., & McIntosh, A. R. (2010). Evidence of source-sink metapopulations in a vulnerable native galaxiid fish driven by introduced trout. *Ecological Applications*, 20(4), 967–977. <https://doi.org/10.1890/08-1909.1>

Young, K. D. (2002). Life history of fluvial and lacustrine land-locked koaro (*Galaxias brevipinnis*) Günther (Pisces: Galaxiidae) in the Tarawera Lakes. Doctoral dissertation, The University of Waikato, Hamilton, New Zealand

Appendix

6.1 Appendix A All Traps

The patterns in kōaro body size, CPUE, and BPUE from all 20 traps sampled showed similar trends to those observed in the initial 12 traps (Figures 40-42).

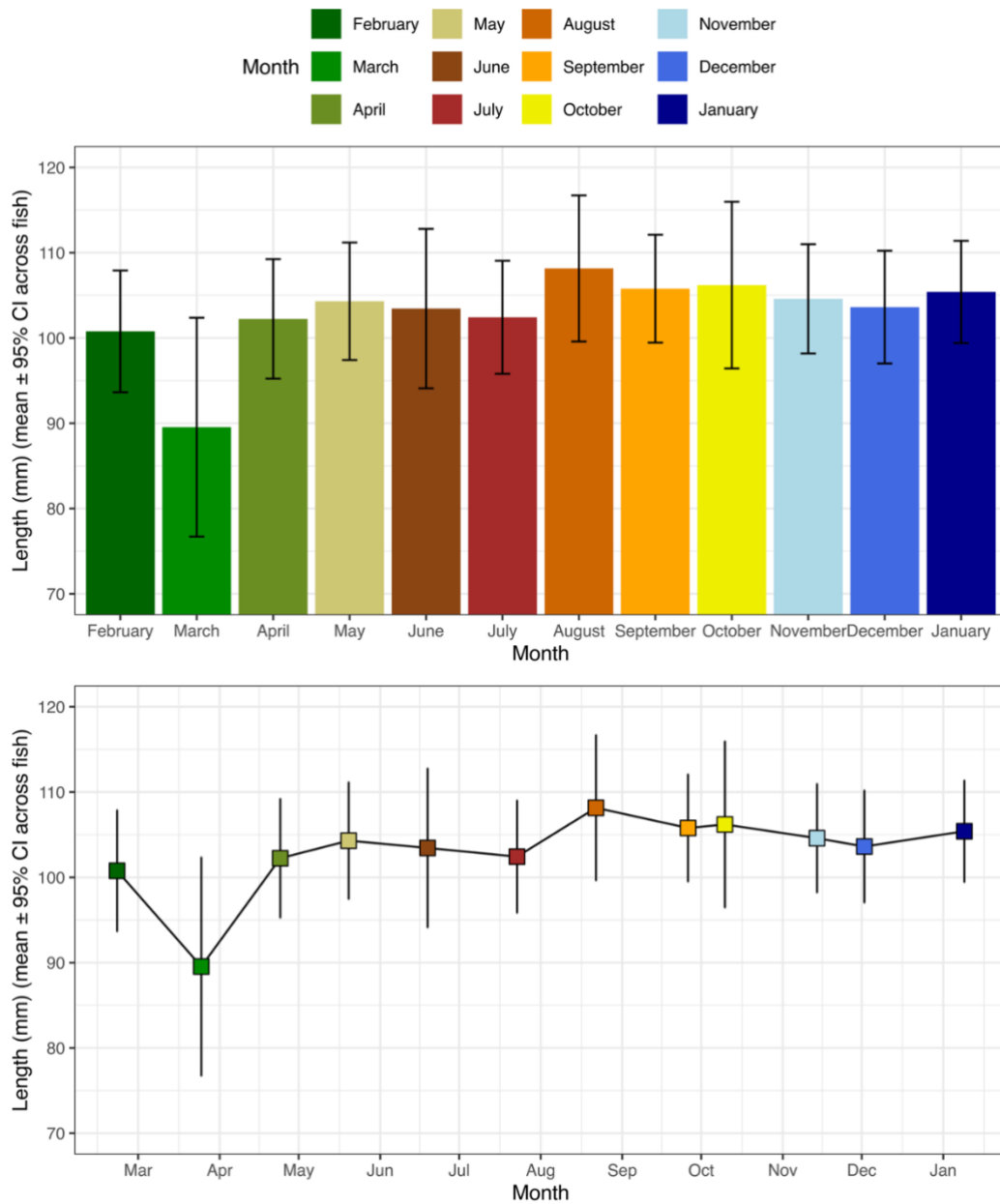


Figure 57: Monthly variation in mean kōaro (*Galaxias brevipinnis*) length (mm) in the Millar Road wetland. Data comes from all 20 Gee's minnow traps which were set monthly from February 2025 to January 2026. The error bars indicate the 95 % confidence interval (CI).

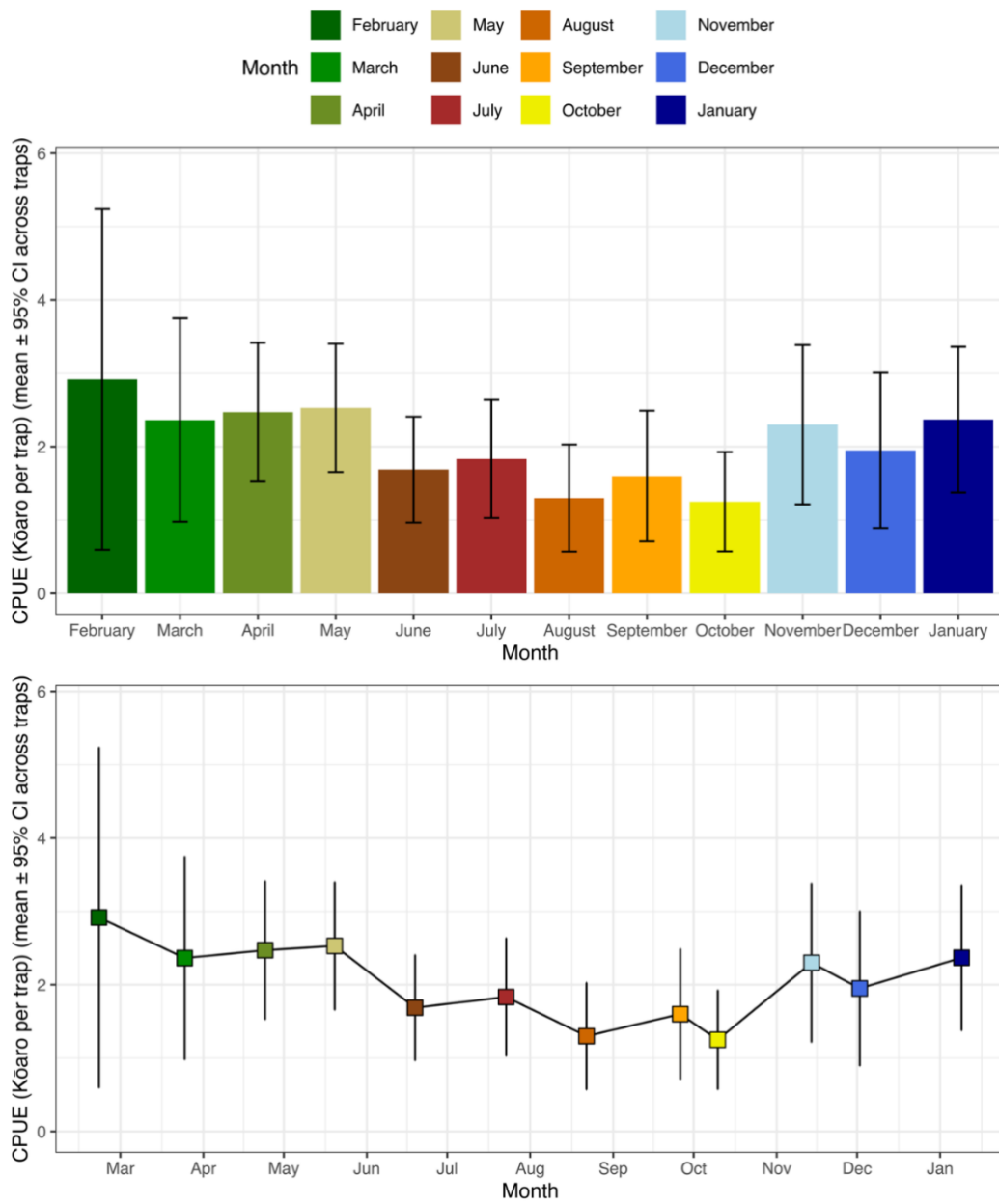


Figure 58: Monthly variation in mean kōaro (*Galaxias brevipinnis*) catch per unit effort (CPUE; mean kōaro per trap, per sampling occasion) in the Millar Road wetland. Data were derived from all 20 Gee's minnow traps sampled monthly from February 2025 to January 2026. Error bars indicate the 95 % confidence interval (CI).

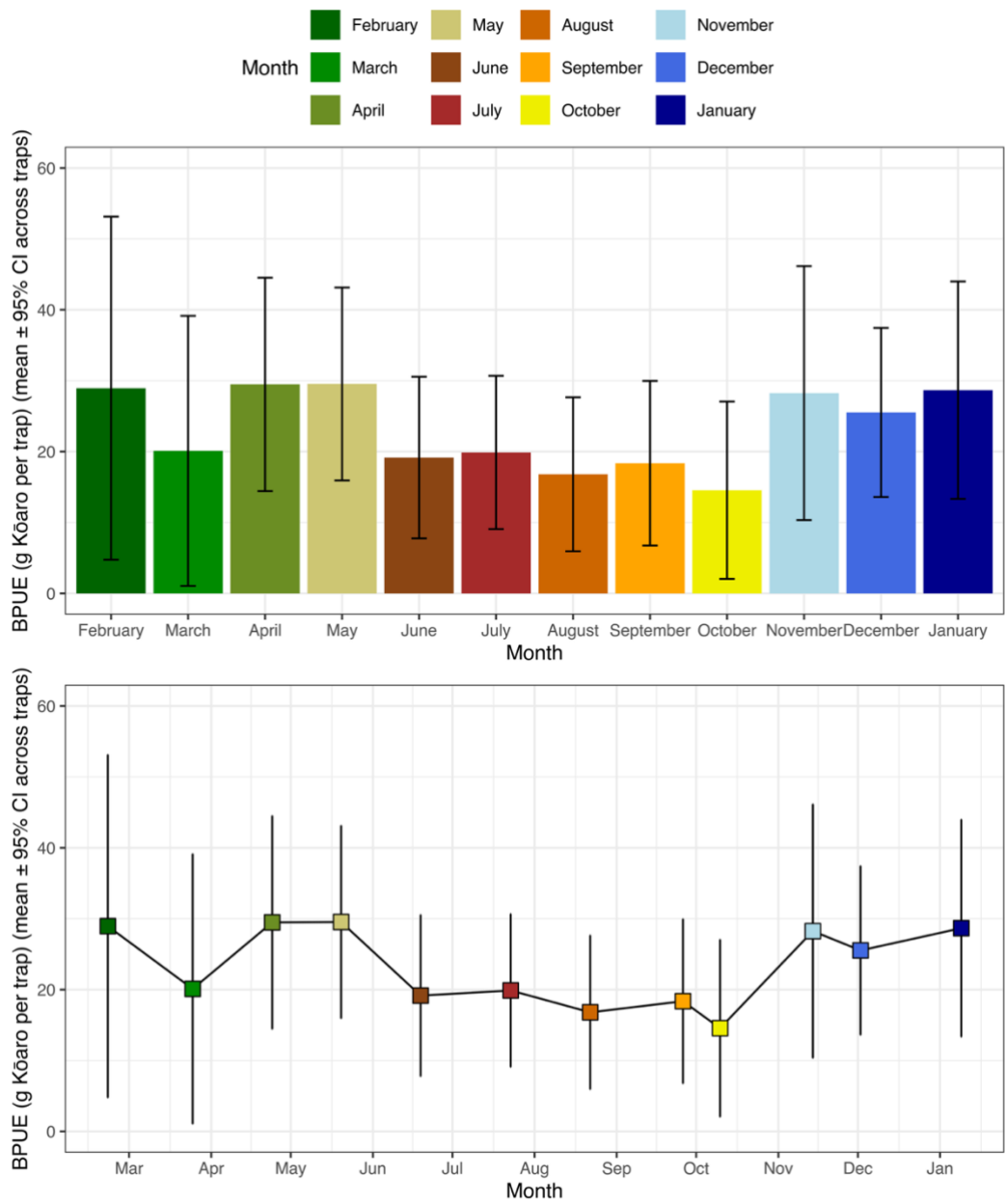






Figure 59: Monthly variation in mean kōaro (*Galaxias brevipinnis*) mass (g) in the Millar Road wetland. Data are from all 20 Gee's minnow traps which were set monthly from February 2025 to January 2026. Error bars indicate the 95 % confidence interval (CI).

6.2 Appendix B Habitat

		
Trap 1	Trap 2	Trap 3
		
Trap 4	Trap 5	Trap 6



Trap 7



Trap 8



Trap 9



Trap 10



Trap 11



Trap 12



Trap 13



Trap 14



Trap 15






		
<p><i>Trap 16</i></p>	<p><i>Trap17</i></p>	<p><i>Trap A</i></p>
		
<p><i>Trap B</i></p>	<p><i>Trap C</i></p>	

Figure 60: Trap locations (Trap 1–Trap 17 and Trap A–C) within the Millar Road wetland. Images show representative local habitat conditions used for qualitative and semi-quantitative habitat assessment in January 2026.

6.3 Appendix C Environmental DNA (eDNA)

Kōaro and common bully were consistently detected across all six replicates, with relative read proportions broadly reflecting patterns observed in trapping data, where bullies were numerically dominant but kōaro contributed substantial biomass. Rainbow trout were detected at low proportional read abundance in one replicate, consistent with their rare and episodic occurrence in physical trapping surveys. Kōura were also detected in the eDNA assay (data not shown), further supporting the presence of a native-dominated assemblage.

Read counts represent relative sequence abundance rather than absolute population size and should be interpreted cautiously; however, concordance between eDNA detections and trapping surveys increases confidence that trout detections were not false positives and that assemblage composition at the time of sampling was accurately characterised.

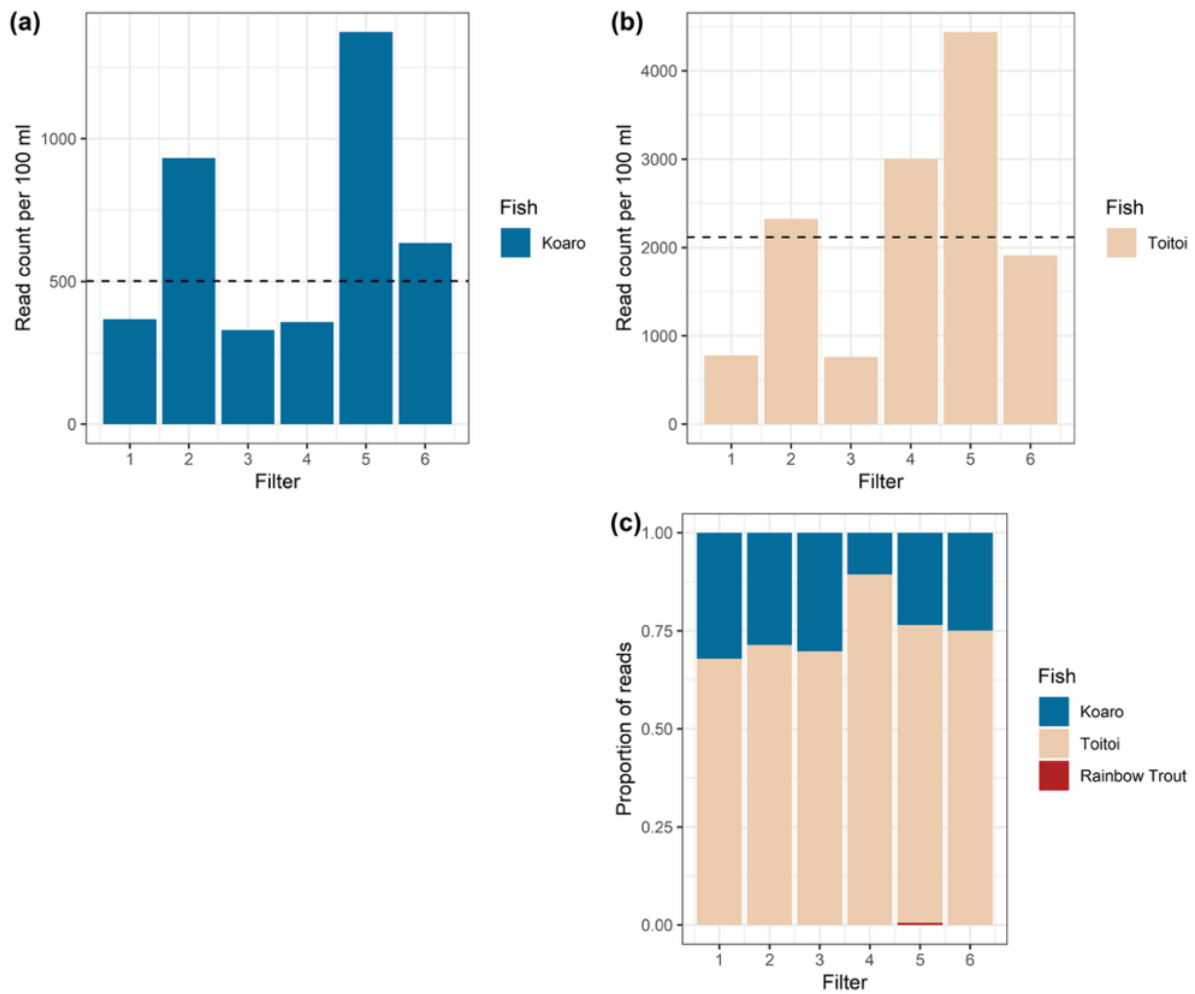


Figure 61: Environmental DNA (eDNA), collected at site T4 on 21 February 2025 in the Millar Road wetland using six replicate 1.2 μm cellulose acetate filters following Wilderlab protocols (Wilkinson et al., 2024). DNA was extracted, amplified, and sequenced using high-throughput metabarcoding targeting the 16S gene region for fish and the CO1 region for aquatic invertebrates. Panels (a) and (b) show read counts per 100 mL for kōaro (*Galaxias brevipinnis*) and common bully (“Toitoi”; *Gobiomorphus cotidianus*), respectively, across the six filter replicates. The dashed horizontal line indicates mean read count across replicates. Panel (c) shows proportional read composition of detected fish taxa per filter, including kōaro, common bully, and rainbow trout (*Oncorhynchus mykiss*).

6.4 Appendix D Stable Isotope Analysis

Table 9: Summary statistics for the Bayesian mixing model testing the contribution of four putative prey sources to the diet of kōaro (*Galaxias brevipinnis*) and common bully (*Gobiomorphus cotidianus*) in Millar Road Wetland. Statistics include mean, standard deviation (SD), median (50 %), and the 50 %, 90 % and 95 % credible intervals.

Fish	Source	Mean	SD	2.5 %	5 %	25 %	50 %	75 %	95 %	97.5 %
Kōaro	Moth	0.034	0.054	0	0	0	0.007	0.049	0.155	0.185
	Caddisfly	0.691	0.116	0.493	0.520	0.611	0.681	0.755	0.925	1
	Midge larvae	0.162	0.148	0	0	0.013	0.135	0.283	0.422	0.459
	Mud snail	0.113	0.108	0	0	0.004	0.086	0.203	0.304	0.333
Bully	Moth	0.107	0.109	0	0	0.001	0.079	0.190	0.308	0.337
	Caddisfly	0.069	0.096	0	0	0	0.019	0.109	0.278	0.338
	Midge larvae	0.750	0.215	0.255	0.352	0.612	0.776	0.948	1	1
	Mud snail	0.075	0.116	0	0	0	0.013	0.107	0.336	0.417

Table 10: Summary statistics for the Bayesian mixing model testing the contribution of autochthonous and allochthonous carbon to the diet of kōaro (*Galaxias brevipinnis*) and common bully (*Gobiomorphus cotidianus*) in Millar Road Wetland. Statistics include mean, standard deviation (SD), median (50 %), and the 50 %, 90 % and 95 % credible intervals.

Fish	Source	Mean	SD	2.5 %	5 %	25 %	50 %	75 %	95 %	97.5 %
Kōaro	Allochthonous	0.986	0.036	0.871	0.907	0.994	1	1	1	1
	Autochthonous	0.014	0.036	0	0	0	0	0.006	0.093	0.129
Bully	Allochthonous	0.071	0.116	0	0	0	0.002	0.111	0.338	0.395
	Autochthonous	0.929	0.116	0.605	0.662	0.889	0.998	1	1	1